Original research carried out in collaboration with: Jean Letessier (Paris), Michael Fromerth (Arizona/Cornell), Giorgio Torrieri (Arizona), Bob Thews (Arizona), supported by a grant from the U.S. Department of Energy, DE-FG03-95ER40937. Some reprints available. I thank CSSM for superb hospitality.

QUARK-GLUON PLASMA

Johann Rafelski

Department of Physics, University of ARIZONA, Tucson

NUPP, Victor Harbor, January 20-24, 2003

WHAT YOU NEED TO REVIEW

This is a very interdisciplinary subject matter:

attempt to answer the test questions quantitatively:

- Relativity: is Lorentz-contraction of space or body of matter; what is proper time, rapidity?
- Relativistic Statistical Physics: Is $3P \geq \varepsilon$ or $3P \leq \varepsilon$?
- Nuclear Physics: what is quark content of a hyperon?
- Particle Physics:
  what is evidence that gluons are charged, confined particles?
- Quantum Field Theory (for pedestrians):
  How strong is strong interaction α_s in quark-gluon plasma?
- Cosmology:
  when did quark Universe hadronize – what fixes the time scale!
- Astrophysics: why is not every neutron star a quark star, and conversely are any quark stars around?

IN FUTURE:

- Plasma Physics, Quantum Decoherence, Nonlinear Dynamics, . . . :

Short History of the Universe

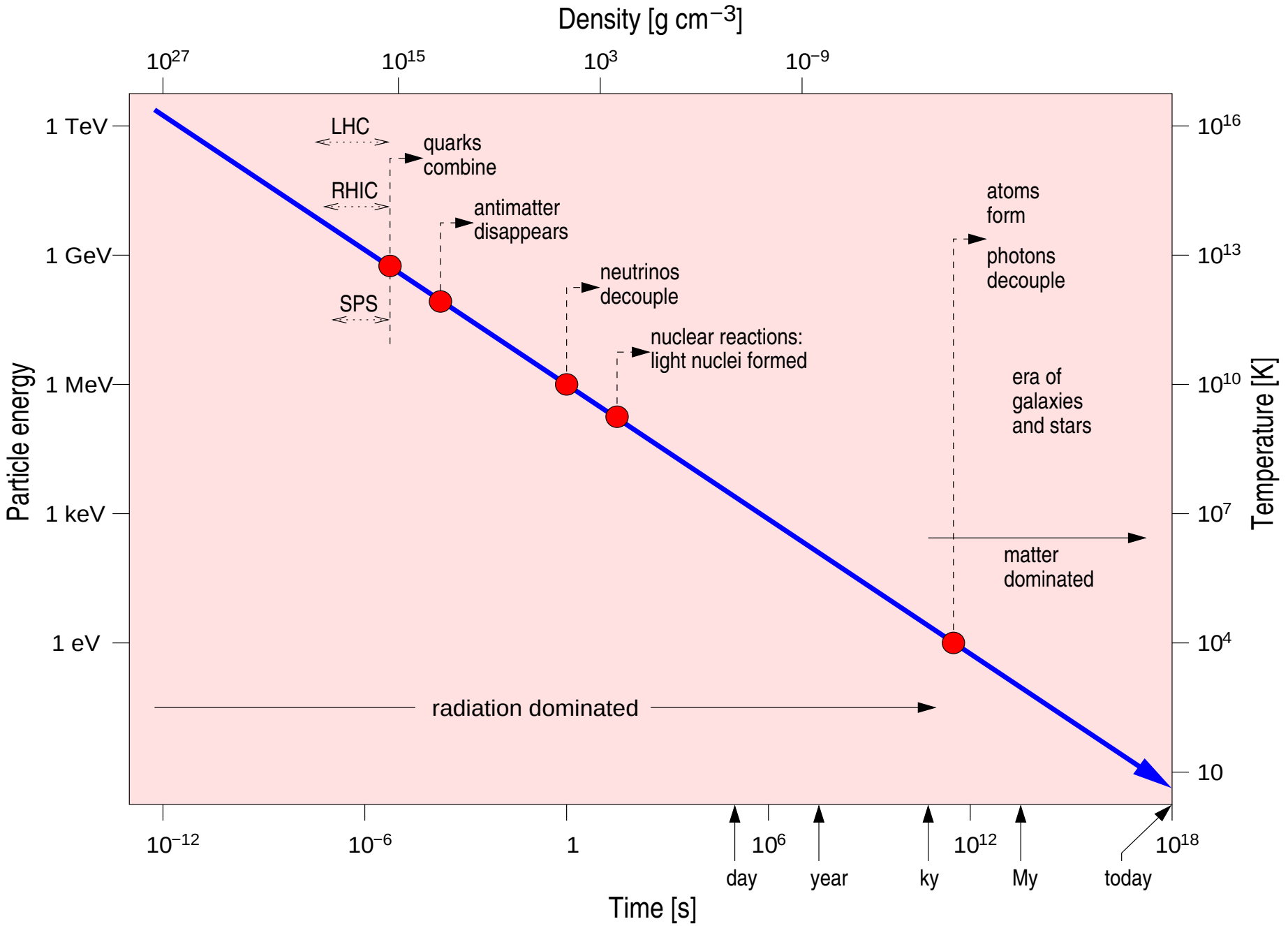

RECREATING THE EARLY UNIVERSE IN LABORATORY

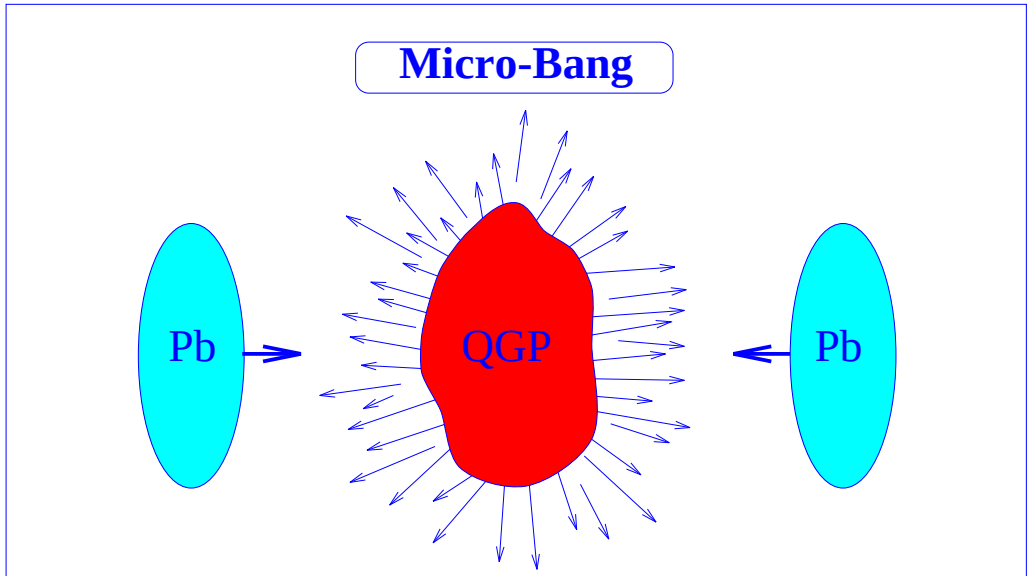

Big-Bang	Micro-Bang
$\tau \simeq 10\mu s$	$\tau \simeq 4\ 10^{-23} s$
$N_B / N \simeq 10^{-10}$	$N_B / N \simeq 0.1$

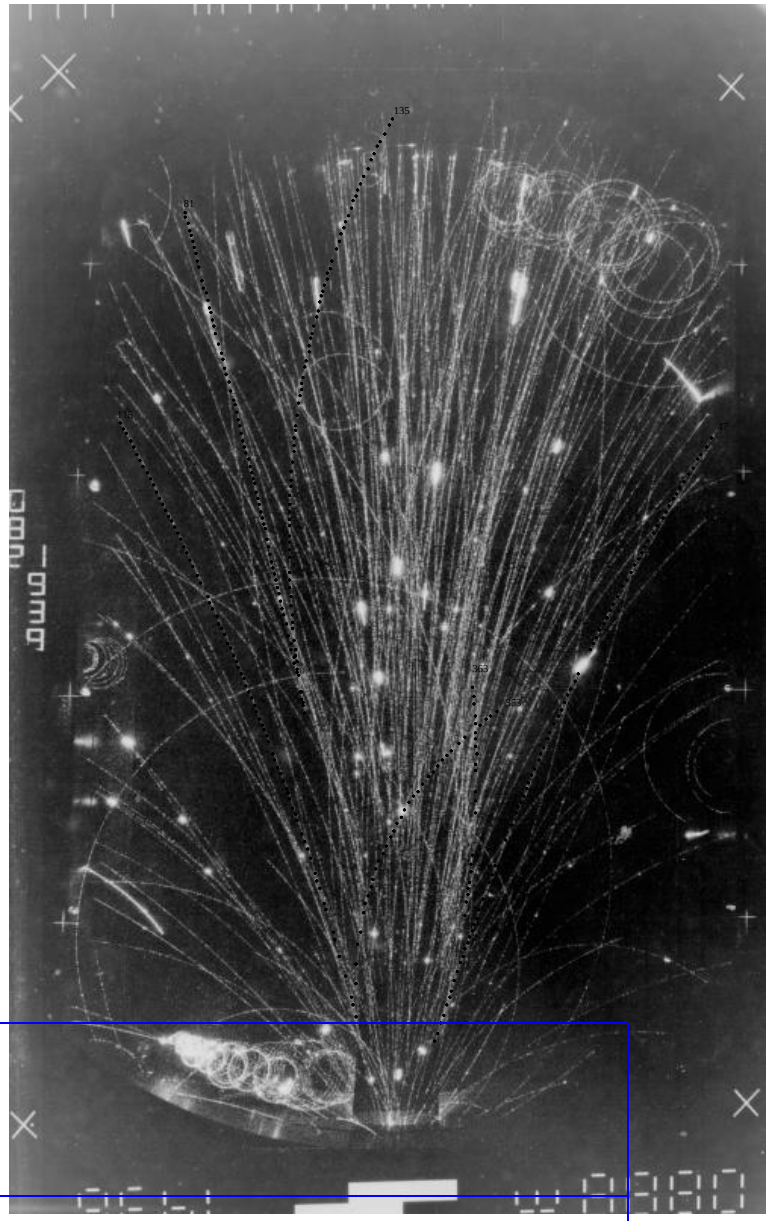

S–Ag Reaction at 200AGeV (by NA35)

Order of Magnitude

ENERGY density	ϵ	$\simeq$ 1–5GeV/fm^3 = 1.8–9 10^{15}g/cc
Latent vacuum heat	B	$\simeq$ 0.1–0.4GeV/fm^3 $\simeq$ (166–234MeV)^4
PRESSURE	P	$= \frac{1}{3}\epsilon = 0.52\ 10^{30}$ barn
TEMPERATURE	T_0, T_f	300–250, 175–145 MeV; 300MeV$\simeq$3.5 10^{12}K

Beyond Nuclear Matter: QGP

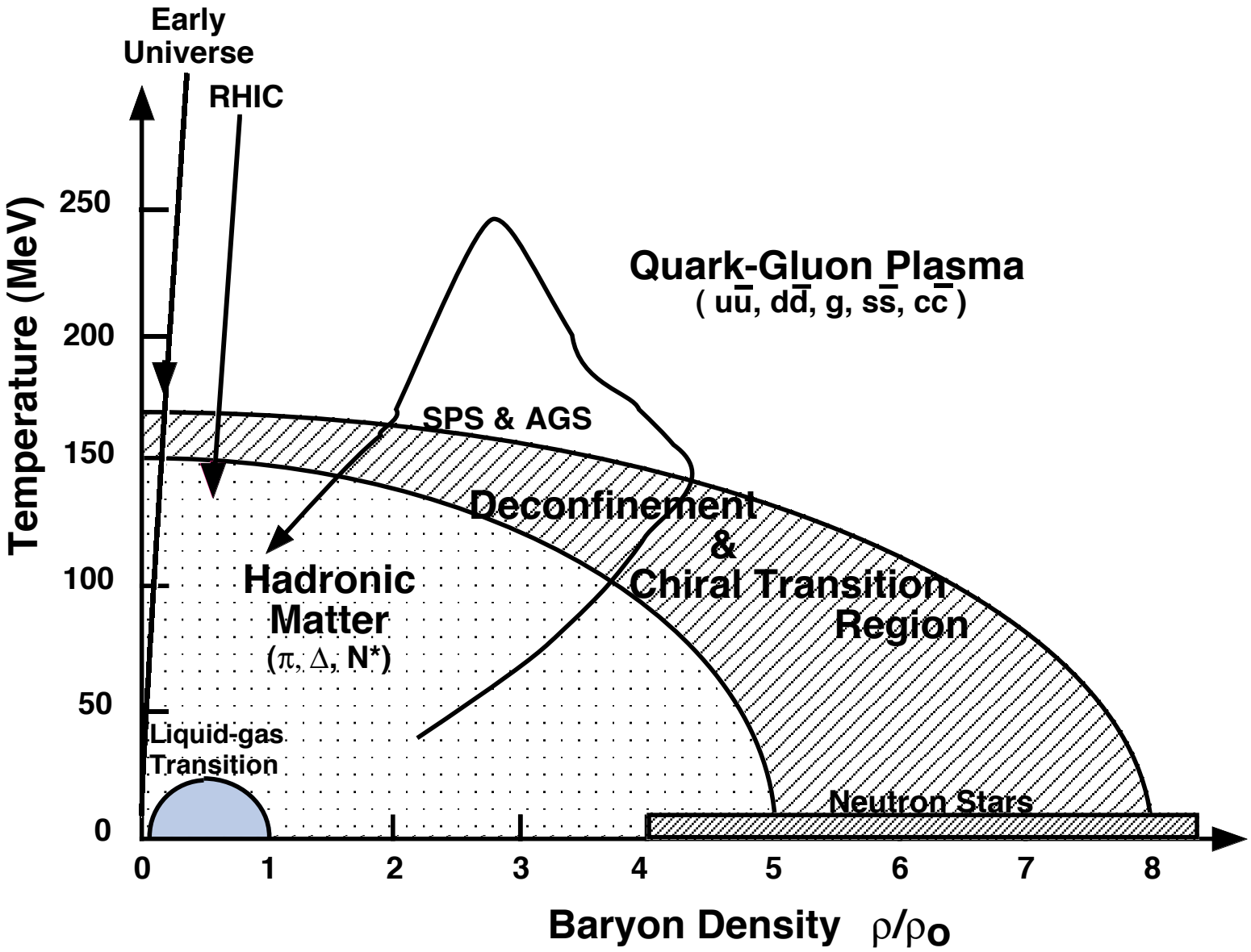

Time-paper-line: Hadronic Matter to QUARKS to QGP

- High Ener.Nuclear Events, E.Fermi Prog.Theor.Phys.5, 570 (1950)
- Statistical Thermodynamics of Strong Interactions at HE
  R. Hagedorn Nuovo Cim.Suppl. 3, 147-186 (1965)
- ...Quark Stars N. Itoh, Prog. Theor. Phys. 44, 291 (1970)
- Super-dense Matter: Neutrons or Free Quarks
  JC Collins and MJ Perry, PRL34: (21) 1353-1356 (1975)
- QGP and Hadronic Production of Leptons, Photons, and Psions
  EV Shuryak, PLB 78, 150 (1978)
- Strangeness Production in the QGP,
  (1979) $\rightarrow$ J. Rafelski, B Muller, PRL 48, 1066 (1982)
- Hydrodynamic Flow and Scaling High Energy Solution
  J. D. Bjorken, PRD27, 140 (1983)

- Experiments begin

Experimental Facilities

- Study of compressed nuclear matter:
  DUBNA, LBL-BEVELAC, GSI-SIS
- Study of hadronic matter: matter comprising a significant fraction of hadrons other than nucleons:
  BNL–AGS (Alternate Gradient Synchrotron)
- Beyond the threshold to quark matter:
  CERN-SPS (Super-Proton-Synchrotron)
  International Facility proposed at Darmstadt
- Study of quark-gluon matter:
  RHIC (Relativistic Heavy Ion Collider) at BNL
- Exploring conditions close to those seen in early Universe:
  CERN-LHC (Large Hadron Collider)

DUBNA, LBL and GSI: nuclear matter studies

DUBNA had capacity to accelerate only light ions. LBL-Berkeley closed the BEVELAC around the time GSI/Darmstadt turned on the SIS (SchwerIonenSynchrotron).

GSI A new international project is being proposed, with GSI-SIS being the injector. A double-ring synchrotron will provide ion beams of unprecedented intensities as well as of considerably increased energy, rivaling CERN SPS. Thereby intense beams of secondary beams – unstable nuclei or antiprotons – can also be produced. A total of 4 research programs is envisaged.

Construction of a Clinical Therapy Facility for Cancer Treatment with Ion Beams in progress in Heidelberg in partnership with Cancer Research Center and Uni Heidelberg

CERN

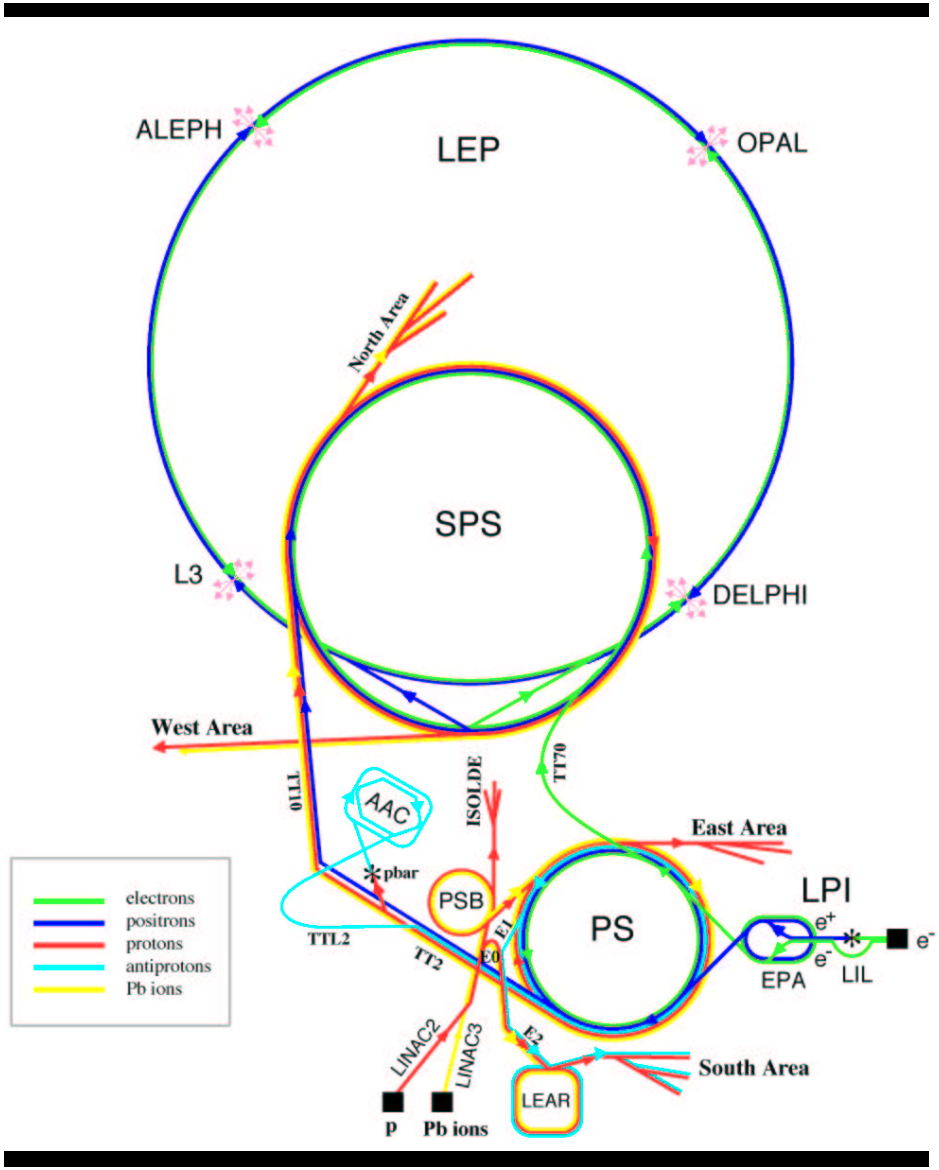

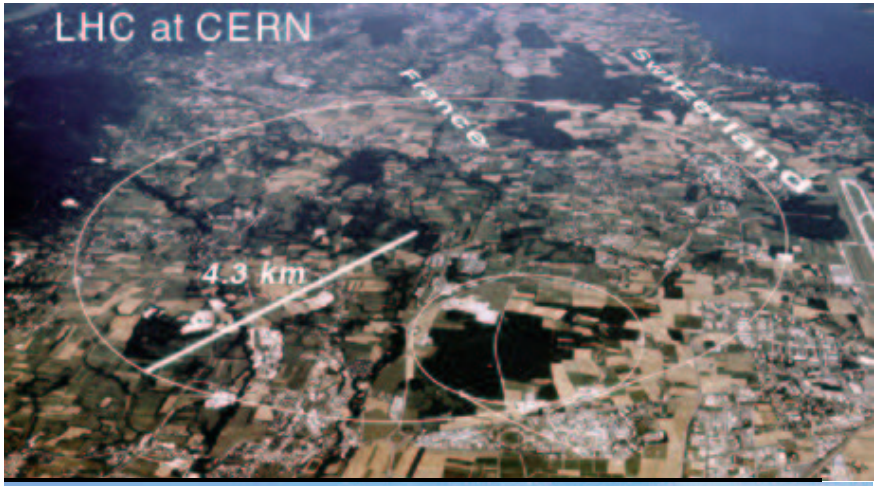

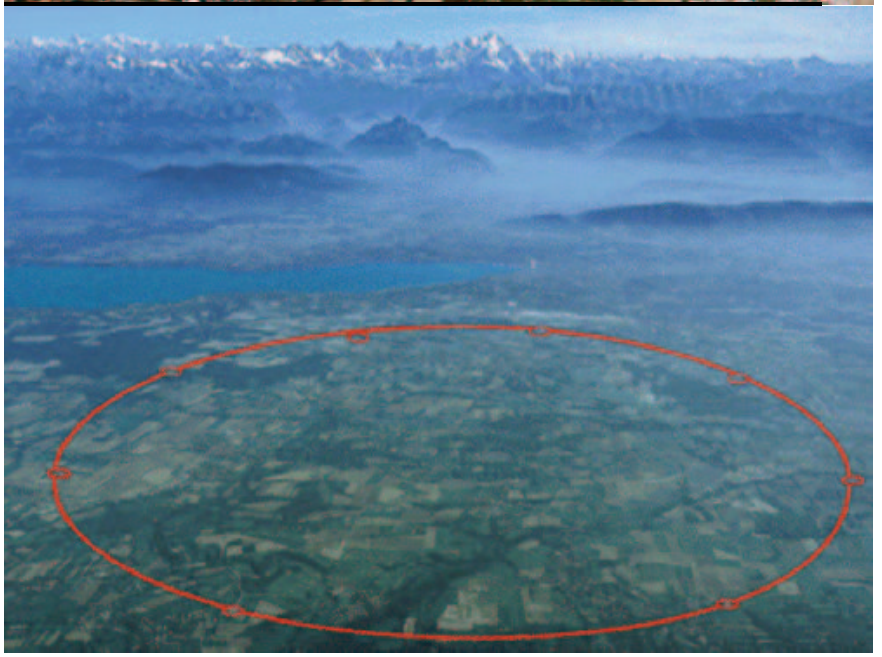

SPS and in future LHC

BROOKHAVEN NATIONAL LABORATORY

Relativistic Heavy Ion Collider

BROOKHAVEN NATIONAL LABORATORY

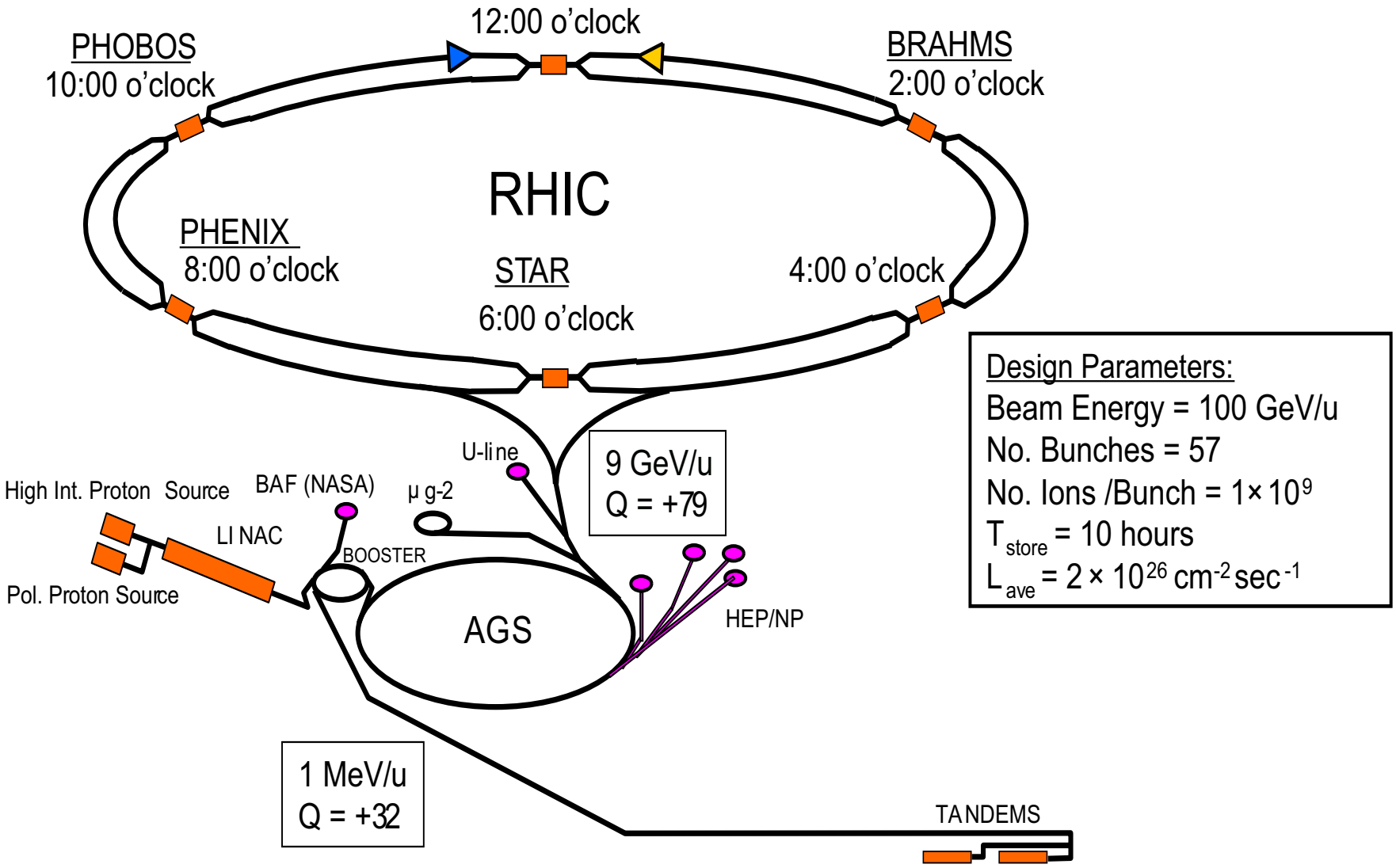

Design Parameters:
Beam Energy = 100 GeV/u
No. Bunches = 57
No. Ions /Bunch = 1×10^9
T_{store} = 10 hours
$L_{ave} = 2 \times 10^{26}\ cm^{-2} sec^{-1}$

Relativistic Heavy Ion Collider

RECREATING THE EARLY UNIVERSE AT RHIC

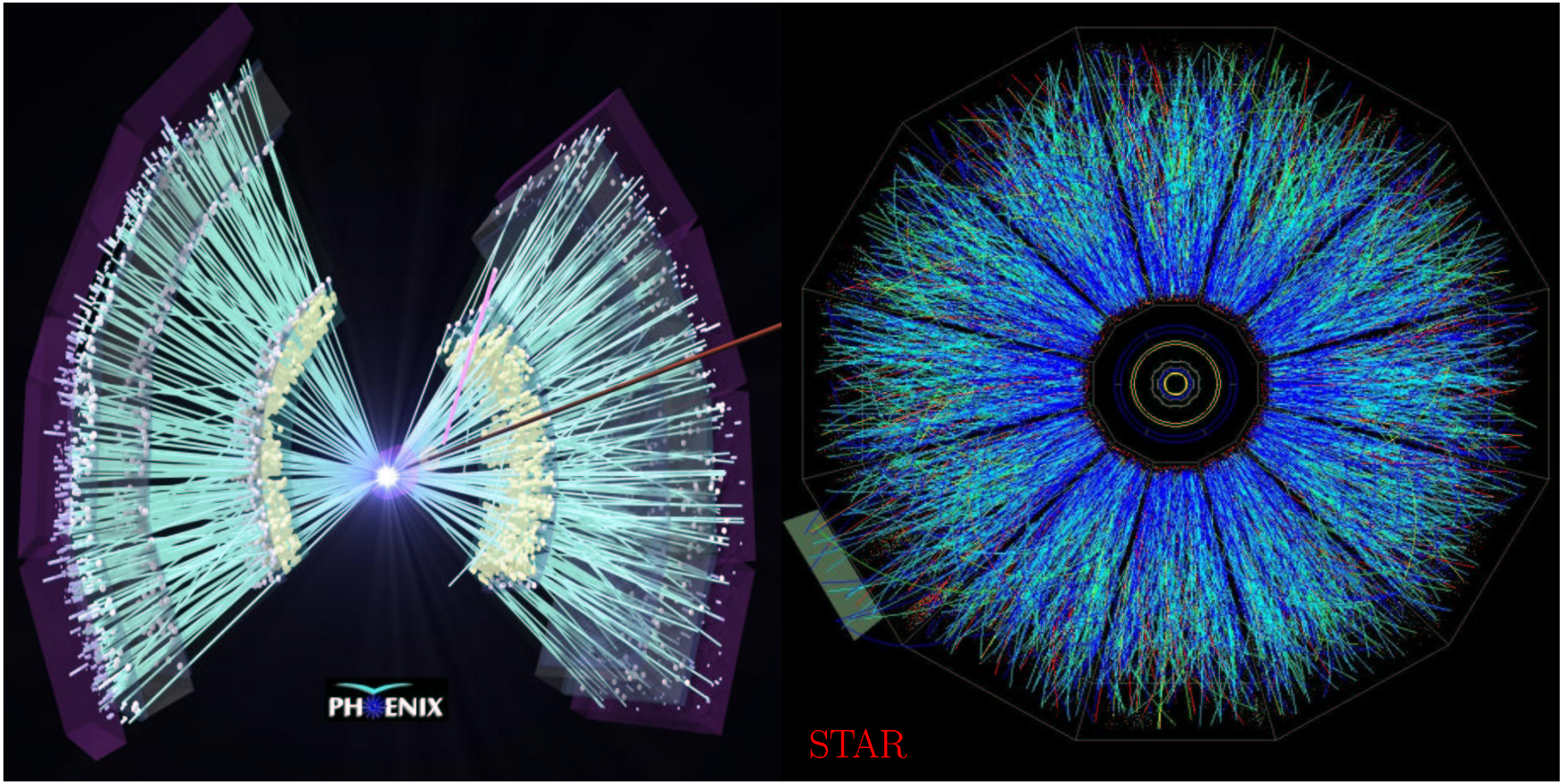

Is this maze of tracks of newly produced particles telling us anything we want to know about the early universe and its properties?

ABC of relativistic kinematics

$$E = \sqrt{m^2+\vec{p}_\perp^{\,2}+p_L^2} = \sqrt{m_\perp^2+p_L^2},$$

$$m_\perp = \sqrt{m^2+\vec{p}_\perp^{\,2}},$$

$$p_L \equiv m_\perp \sinh y, \rightarrow E = m_\perp \cosh y,$$

$$\rightarrow v_L \equiv \frac{cp_L}{E} = c\,\tanh y$$

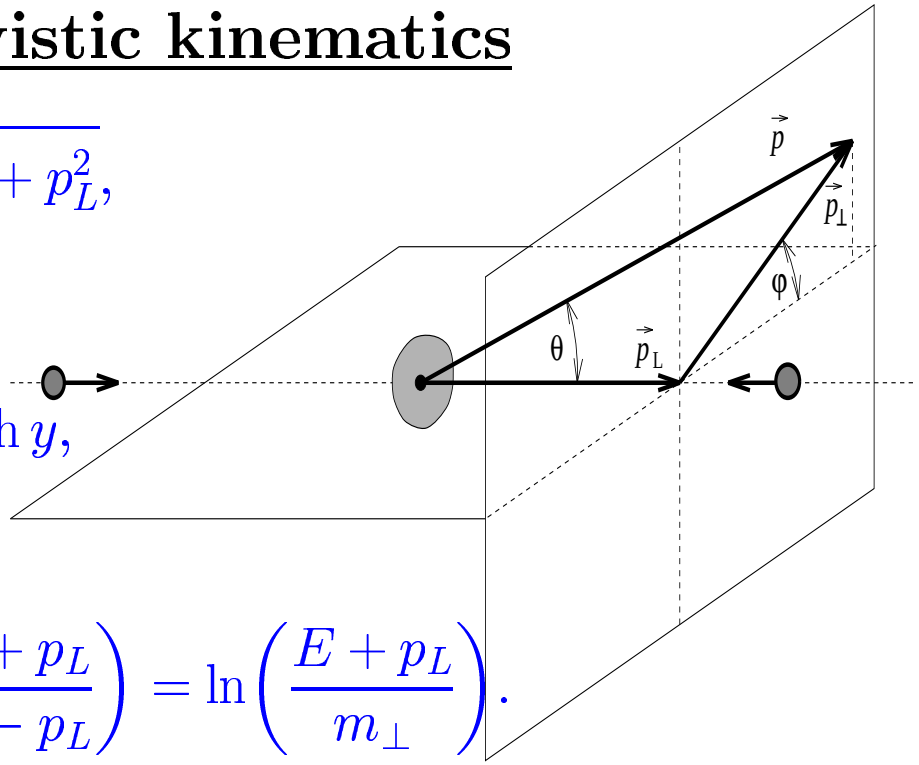

$$y = \frac{1}{2}\ln\left(\frac{1+v_L}{1-v_L}\right) = \frac{1}{2}\ln\left(\frac{E+p_L}{E-p_L}\right) = \ln\left(\frac{E+p_L}{m_\perp}\right).$$

$$\cosh y = \frac{1}{\sqrt{1-v_L^2}} \equiv \gamma_L, \qquad \sinh y = \gamma_L\, v_L$$

The longitudinal momentum p_L of a particle is an inconvenient variable, since it depends in a nonlinear way on the velocity of the CM frame with reference to the laboratory frame. The rapidity y is defined to be additive under successive Lorentz transformations along the same direction. It can be understood as the 'angle' of the (hyperbolic) rotation in (3 + 1)-dimensional space.

With $\cosh y_c = \gamma_c, \quad \sinh y_c = \gamma_c\, v_c$**,**

$$E' = \gamma_c(E + v_c\, p_L), \quad p'_L = \gamma_c(p_L + v_c\, E). \quad \rightarrow \quad E' = m_T\,\cosh(y+y_c), \quad p'_L = m_T\,\sinh(y+y_c).$$

Experimental Program: Energy – Rapidity Range

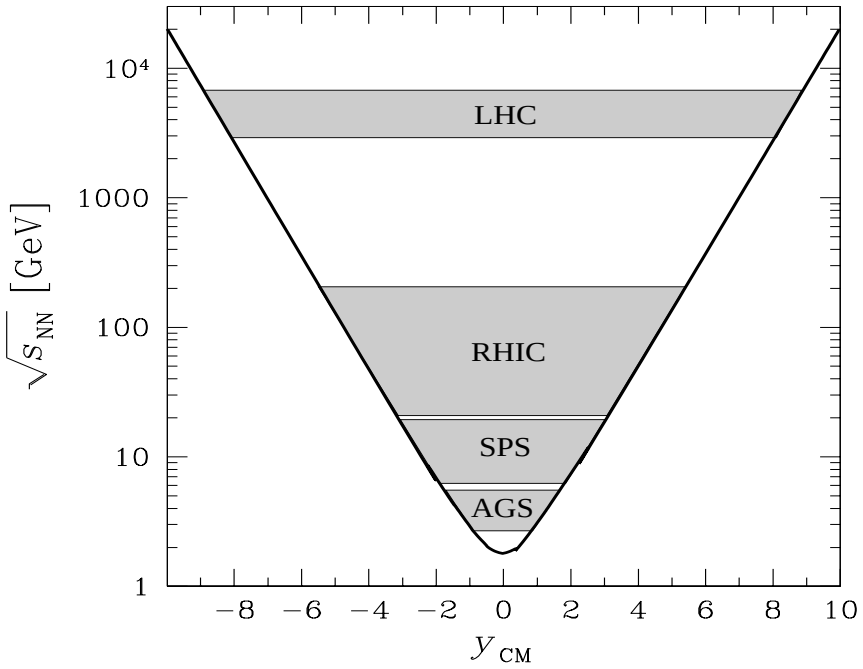

Rest energy content per PARTICIPATING nucleon pair :

$$\sqrt{s_{\rm NN}} = \frac{2}{A_p + A_t}\sqrt{(E_p + E_t)^2 - (p_p + p_t)^2}$$

just like

$$m = \sqrt{E^2 - p^2}$$

Why is high energy important?

	AGS	AGS	SPS	SPS	SPS	RHIC	RHIC	LHC
Start year	1986	1992	1986	1994	1999+	2000	2001+	2007
$A_{\rm max}$	^{28}Si	^{197}Au	^{32}S	^{208}Pb	^{208}Pb	^{197}Au	^{197}Au	^{208}Pb
$E_{\rm P}^{\rm max}[A$ GeV]	14.6	11	200	158	30–80	0.91×10^4	2.1×10^4	1.9×10^7
$\sqrt{s_{\rm NN}}$ [GeV]	5.4	4.7	19.2	17.2	7.5–12	130	200	6000
$\sqrt{s_{\rm AA}}$ [GeV]	151	934	614	3.6×10^3	1.5–2.5×10^3	2.6×10^4	4×10^4	1.2×10^6
$\Delta y/2$	1.72	1.58	2.96	2.91	2.08–2.57	4.94	5.37	8.77

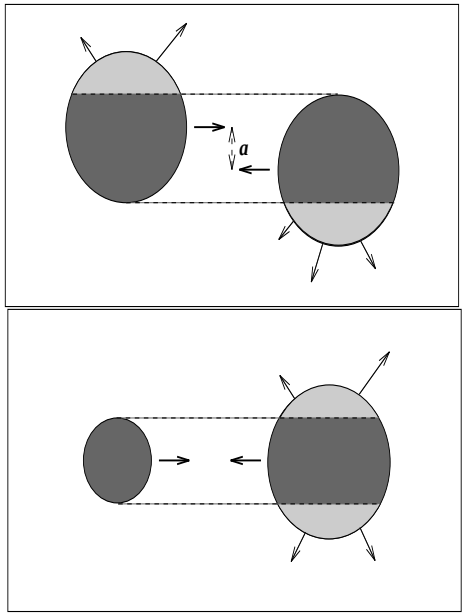

Two centralities

Geometrically central collisions: for symmetric systems rare but nearly all nucleons participate, asymmetric collisions have an edge but are more difficult to interpret.

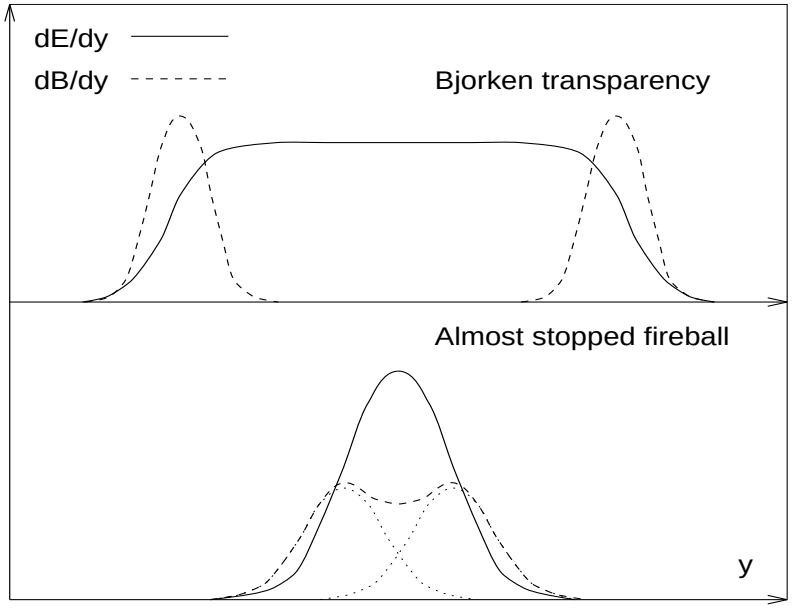

Central in rapidity particle spectra: those emitted near to the center of momentum condition, for collider, that is laboratory frame, for fixed target experiments shift by $y_{\rm CM}$.

Rapidity distributions of energy (solid lines) and baryon number (dashed lines) (in a qualitative representation): (a) for a 'Transparent' reaction mechanism; and (b) for full stopping in the collision

Non-identified particles and (π)-pseudorapidity

Often we do not know what is the mass of the particle observed. For relativistic particles $E = \sqrt{p^2 + m^2} \to p$, so often the value of m will not matter. When m is 'small' we introduce pseudorapidity η:

$$p = p_\perp \cosh\eta, \qquad p_L = p_T \sinh\eta,$$

$$y(m \to 0) \to \eta = \frac{1}{2}\ln\left(\frac{p + p_L}{p - p_L}\right) = \frac{1}{2}\ln\left(\frac{1 + \cos\theta}{1 - \cos\theta}\right) = \ln\left(\cot\frac{\theta}{2}\right).$$

θ is the particle-emission angle relative to the beam axis. Thus we obtain a remarkably simple way to measure pseudorapidity spectra: for charged particles in magnetic field we obtain momentum p from the curvature (rigidity) and angle of emission θ. Since most particles produced are pions it is customary to do as if this was the case for all charged particles, so $m \to m_\pi$. Errors are understood, not always negligible. From definition:

$$p_L = \sqrt{m^2 + p_\perp^2}\,\sinh y = \sqrt{m_\pi^2 + p_\perp^2}\,\sinh\eta_\pi,$$

we find for the true m (kaon, nucleon) what error we are making.

Experimental Output

Experiments deliver single particle SPECTRA of particles in rapidity y and $m_\perp$. Typically today these are spectra of HADRONS, spectra of photons, dileptons , are not yet accessible. We also study two particle correlations which offer through quantum interference opportunity to image the geometry of the particle source (HBT).

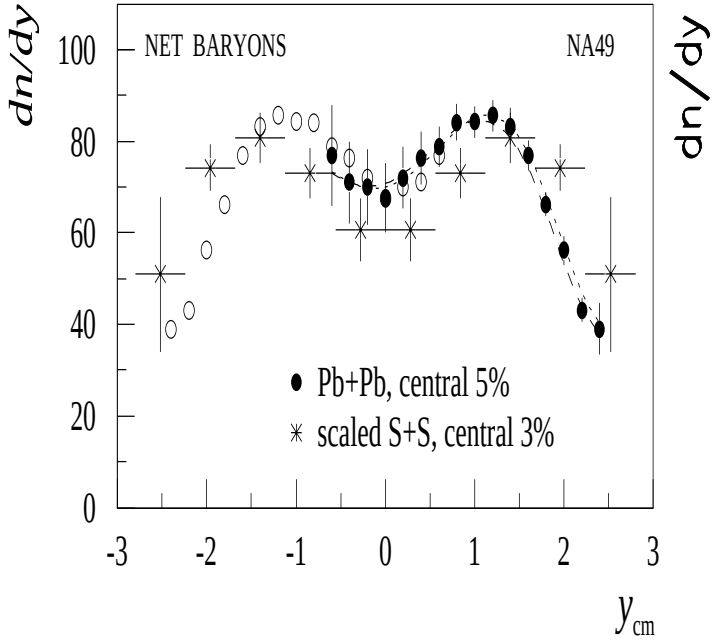

158 A GeV Pb on Pb
200 A GeV S on S
scaled with 352/52

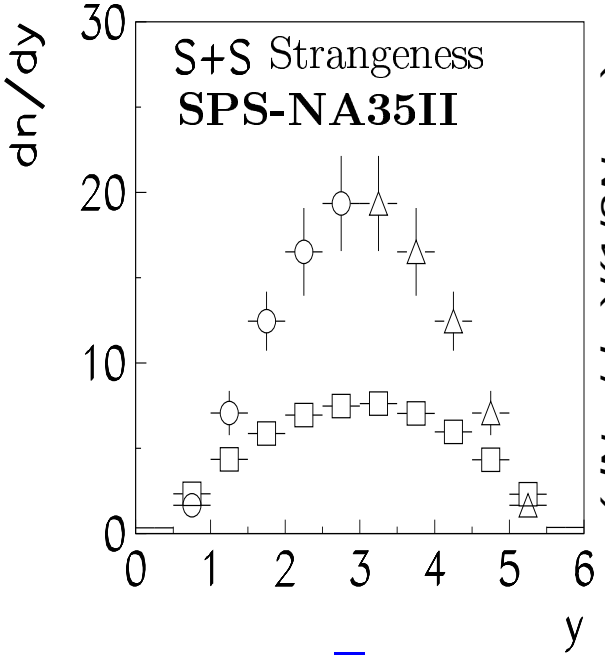

$1.6\Lambda + 1.6\overline{\Lambda} + 4\mathrm{K}s$
200 A GeV S on S
200 A GeV p on p
multiplicity scaled

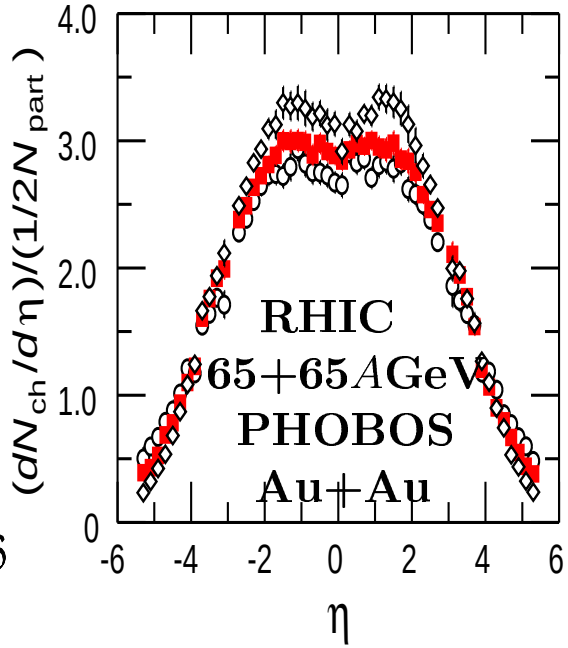

Centralities:
$\langle N \rangle = 102, 216, 354$

REACTION MECHANISMS LEADING TO MANY PARTICLES

- a series of individual nucleon-nucleon inelastic reactions
- a series of individual parton-parton inelastic reactions
- combination leading on to a high density of low energy confined soft hadrons

- all these leading on to a high density of SOFT DECONFINED quarks and gluons.

CENTRAL QUESTION IN SEARCH FOR THE DECONFINED PHASE OF MATTER:

ULTIMATELY the final state is made of free streaming hadrons. HOW can we tell, deconfinement had occurred?

PARADIGM SHIFT

Deconfinement requires a change of the vacuum state. Is this possible in a relatively small but microscopically large region of space time, or only accessible in the Universe as a whole?

Vacuum and Laws of Physics

- **Quantum fluctuations fill 'space devoid of matter'=VACUUM**
- **Quantum vacuum is polarizable: see atomic level shifts**
- **Quantum vacuum state has quantum structure:**
  GLUE condensate $|V\rangle$ = 'tru' and $|0\rangle$ = 'perturbative' vacuum:

$$\langle V|\frac{\alpha_s}{\pi}G^2|V\rangle - \langle 0|\frac{\alpha_s}{\pi}G^2|0\rangle \simeq (2.3\pm 0.3)10^{-2}\mathrm{GeV}^4 = [390\pm 12\,\mathrm{MeV}]^4 \quad ,$$

$$\langle V|G^a_{\mu\nu}|V\rangle = 0, \qquad G^2 \equiv \sum_a G^a_{\mu\nu}G^{\mu\nu}_a = 2\sum_a [\vec{B}^2_a - \vec{E}^2_a] \quad ,$$

  CHIRAL condensate

$$\frac{1}{2}\langle V|\bar{u}u + \bar{d}d|V\rangle - \frac{1}{2}\langle 0|\bar{u}u + \bar{d}d|0\rangle \equiv \frac{1}{2}\langle \bar{q}q\rangle \simeq -1.5\,\mathbf{fm}^{-3}$$

- **Vacuum determines inertial mass of all matter particles**

$$m_i\bar{\psi}_i\psi_i \to \frac{g_i}{\sqrt{2}}\psi_i\Phi\psi_i \quad m_i = g_i h, \quad h = \langle V|\Phi|V\rangle \quad g_{\mathrm{top}} = 1.00$$

For the Fermi coupling constant $G_F = 1.16639\,10^{-5}\,\mathbf{GeV}^{-2}$ the Higgs field expectation value $\langle\Phi\rangle = (\sqrt{2}G_F)^{-1/2} = 246.22\,\mathbf{GeV}$, and for unity Youkawa coupling $g_{\mathrm{top}} = 1.00$, $m_t^0 = 174.10\,\mathbf{GeV}$, which is the central value of the directly observed (pole) mass of the top quark.

Melting the Vacuum

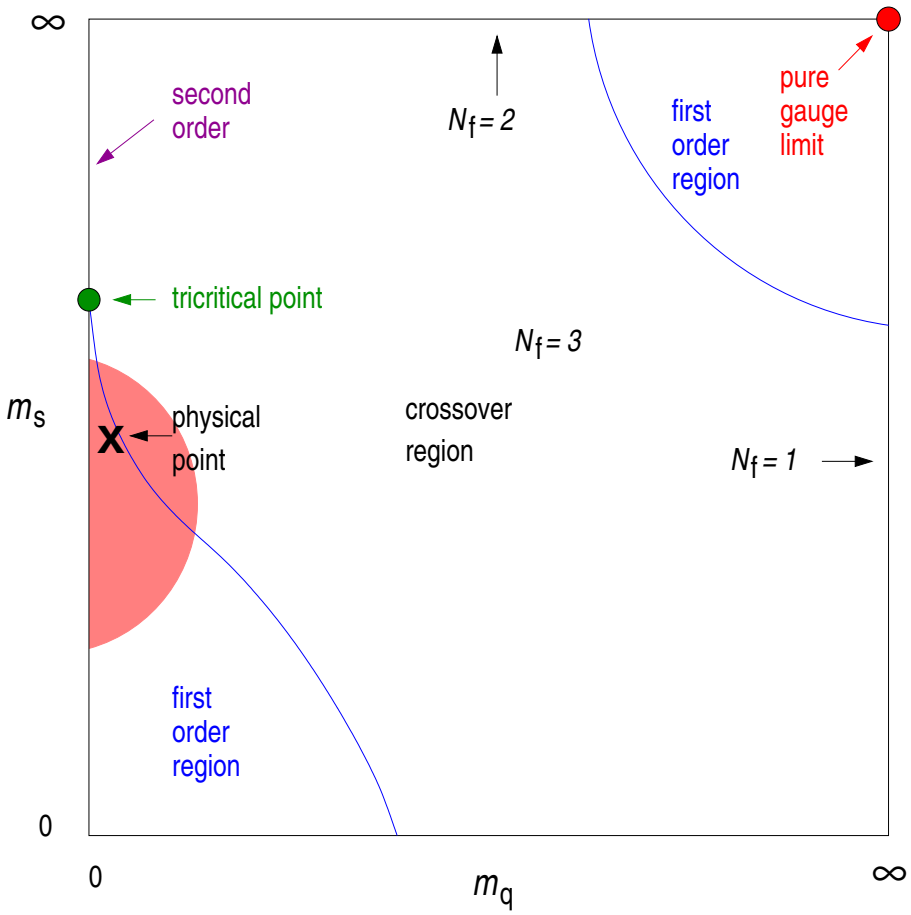

The high temperature vacuum state $|0\rangle$ in which the excitations are the quanta of perturbative quantum field theory, nearly free quarks and gluons. This is assured by the ideas of asymptotic freedom and has been a convincing result of lattice studies. An interesting question is if there is, or not an actual phase transition as the ground state changes. This question is not settled today, as it depends sensitively on quark masses.

Current lattice studies with $m_q = 35$ MeV and $m_s = 70$ MeV claim the physical point in the cross-over regime. Some of us (lecture by Tony Thomas) work hard to figure out how to extrapolate $m_q \to 0$ (chiral limit) and consider the matter, like me, still far from settled.

Phase Transition Tutorial

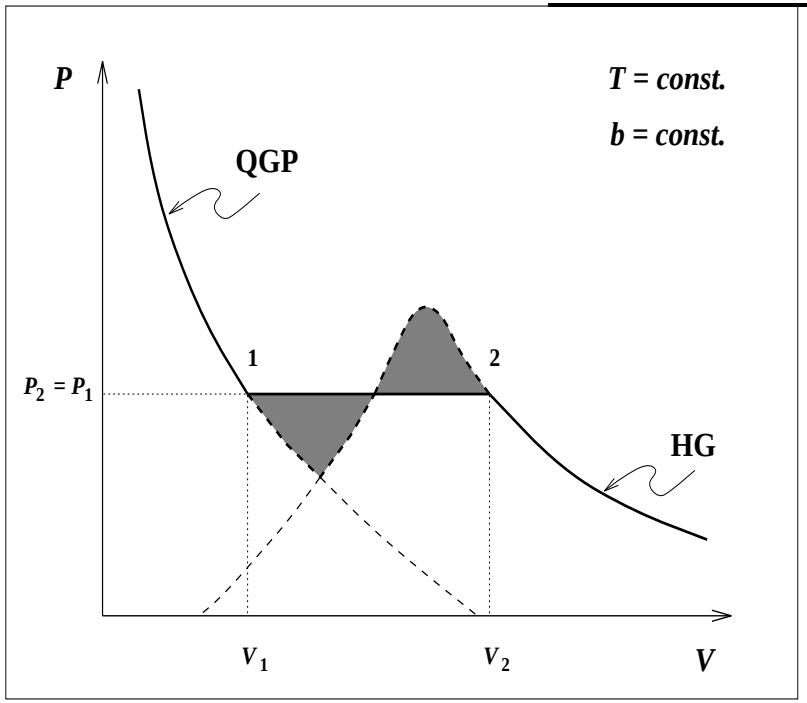

The P–V diagram for the QGP–HG system, shown at fixed temperature and baryon number; dashed lines indicate unstable domains of overheated and undercooled phases. Darkened area: Maxwell construction, connecting the volumes $V_1 = b/\rho_1$ and $V_2 = b/\rho_2$, such that work done along the metastable branches vanishes:

$$\int_{V_1}^{V_2} (P - P_{12})\, dV = 0.$$

Construction can be repeated for different values of b and T, the set of resulting points 1 and 2 forms then two phase-boundary lines.

Between V_1 and V_2 is the mixed phase comprising a mixture of hadrons and drops of QGP. Such a phase formed in early Universe but probably NOT in laboratory experiments.

In a second order phase transition, a discontinuity in e.g. energy density or baryon density is not present, higher order derivatives of partition function are discontinuous.

Statistical Physics Tutorial

The distribution $n = \{n_i\}$ having the same energy E_i can be achieved in many different ways. To find how many, consider the relation

$$K^N = (x_1 + x_2 + \cdots + \cdots x_K)^N|_{x_i=1} = \sum_n \frac{N!}{n_1! n_2! \cdots n_K!} x_1^{n_1} x_2^{n_2} \cdots x_K^{n_K}|_{x_i=1}.$$

The normalized coefficients are the relative probabilities of realizing each state in the ensemble n, with n_i equivalent elements. To find the most probable distribution $\overline{n}$ subject to the constraints of fixed total particle number and energy we introduce two Lagrange multipliers a and β and look for an extremum of:

$$A(n_1, n_2, \ldots, n_K) = \ln W(n) - a\sum_i n_i - \beta \sum_i n_i E_i,$$

$$\frac{\partial}{\partial n_i}[-\ln(n_i!) - n_i a - \beta n_i E_i]\Big|_{\bar{n}_m} = 0. \qquad \frac{d}{dk}[\ln(k!)] \approx \frac{\ln(k!) - \ln[(k-1)!]}{(k) - (k-1)} = \ln k.$$

We find the most probable distribution: $\bar{n}_i = \gamma e^{-\beta E_i}$, the inverse of the slope parameter β can be shown to be temperature. The particle number is $\sum_i \bar{n}_i = \gamma \sum_{i=1}^K e^{-\beta E_i} = N$. Thus $\gamma \equiv e^{-\mu/T}$ controls N, it is the chemical fugacity while μ is the chemical potential. The energy $E^{(N)} = \sum_i \bar{n}_i E_i = \gamma \sum_i E_i e^{-\beta E_i}$. divided by N,

$$\frac{E^{(N)}}{N} \equiv \overline{E^{(N)}} = \frac{\gamma \sum_i E_i\, e^{-\beta E_i}}{\gamma \sum_i e^{-\beta E_i}} \equiv -\frac{d}{d\beta} \ln Z; \qquad Z = \sum_i \gamma e^{-\beta E_i}.$$

motivates the introduction of the partition function$Z$. $\beta = 1/T$

Statistical and thermal physics relations

$$\beta P = \frac{\partial \ln \mathcal{Z}(V,\beta,\mu)}{\partial V}, \qquad E = -\frac{\partial \ln \mathcal{Z}(V,\beta,\mu)}{\partial \beta},$$

$$S = -\frac{d}{dT}\mathcal{F}(V,T,\mu) = \frac{d}{dT} T \ln \tilde{\mathcal{Z}}(V,T,\mu) = \frac{dP}{dT}\,|_{\mu}$$

$$\mathcal{F}(V,T,\mu)Z \equiv E - ST - \mu b = -P(T,\mu)V,$$

Statistical physics Gibbs–Duham relation

$$P = T\sigma + \mu\nu - \epsilon, \quad \sigma = \frac{S}{V}, \quad \nu = \frac{b}{V}, \quad \epsilon = \frac{E}{V},$$

is more powerful than the 1st law of thermodynamics:

$$dE(V,S,b) = -P\,dV + T\,dS + \mu\,db, \qquad d\mathcal{F} = -P\,dV - S\,dT - b\,d\mu,$$

Chemical Potentials Tutorial

particle fugacity: $\Upsilon_i \equiv e^{\sigma_i/T} \Longleftrightarrow \sigma_i$ **particle 'i' chemical potential**

Phase space density is:

$$\frac{d^6N_i}{d^3pd^3x} = g_i\frac{\Upsilon_i}{(2\pi)^3}e^{-E_i/T}, \qquad \frac{d^6N_i^{\rm F/B}}{d^3pd^3x} = \frac{g_i}{(2\pi)^3}\frac{1}{\Upsilon_i^{-1}e^{E_i/T}\pm 1}, \qquad \Upsilon_i^{\rm B} \leq e^{m_i/T},$$

each hadron comprise two chemical factors associated with the two different chemical equilibria, example of NUCLEONS:

$$\Upsilon_N = \gamma_N e^{\mu_b/T}, \qquad \Upsilon_{\overline{N}} = \gamma_N e^{-\mu_b/T};$$

$$\sigma_N \equiv \mu_b + T\ln\gamma_N, \qquad \sigma_{\overline{N}} \equiv -\mu_b + T\ln\gamma_N.$$

γ determines the number of nucleon-antinucleon pairs,

$\gamma_i(t)$ rises from 0 (initially absent) to 1 for chemical equilibrium.

The (baryo)chemical potential μ_b, controls the particle difference = baryon number.

This can be seen looking at the first law of thermodynamics:

$$dE + P\,dV - T\,dS = \sigma_N\,dN + \sigma_{\overline{N}}\,d\overline{N}$$

$$= \mu_b(dN - d\overline{N}) + T\ln\gamma_N(dN + d\overline{N}).$$

Valance quark content in a hadron is characterized by product of factors $\gamma_{u,d,s}$, and

$$\lambda_{u,d,s} = e^{\mu_{u,d,s}/T}, \qquad \mu_q = \frac{1}{2}(\mu_u + \mu_d), \quad \lambda_q^2 = \lambda_u\lambda_d \quad \lambda_b = \lambda_q^3.$$

NOTE relations between quark and hadron potential:

$\mu_b = 3\mu_q$ $\mu_s = \frac{1}{3}\mu_b - \mu_{\rm S}$, $\lambda_s = \frac{\lambda_q}{\lambda_{\rm S}}$,

NEGATIVE strangeness in s-hadrons. e.g.

$$\Upsilon_p = \gamma_u^2\gamma_d\,e^{2\mu_u+\mu_d}, \qquad \Upsilon_{\bar p} = \gamma_u^2\gamma_d\,e^{-2\mu_u-\mu_d},$$

$$\Upsilon_\Lambda = \gamma_u\gamma_d\gamma_s\,e^{\mu_u+\mu_d+\mu_s}, \qquad \Upsilon_{\overline{\Lambda}} = \gamma_u\gamma_d\gamma_s\,e^{-\mu_u-\mu_d-\mu_s},$$

Independent quantum (quasi)particles

$$\hat{H}|i\rangle = E_i|i\rangle; \qquad [\hat{b},\hat{H}] = 0; \qquad \hat{b}|i,b\rangle = b|i,b\rangle$$

The grand-canonical partition function, can be written as:

$$\mathcal{Z} \equiv \sum_{i,b}\langle i,b|\gamma e^{-\beta(\hat{H}-\mu\hat{b})}|i,b\rangle = \mathbf{Tr}\,\gamma\, e^{-\beta(\hat{H}-\mu\hat{b})} \equiv \sum_{n}\langle n|e^{-\beta(\hat{H}-\mu\hat{b}-\beta^{-1}\ln\gamma)}|n\rangle.$$

The trace of a quantum operator is representation-independent; that is, any complete set of microscopic basis states $|n\rangle$ may be used to find the (quantum) canonical or grand-canonical partition function. This allows us to obtain the physical properties of quantum gases in the, often useful, approximation that they consist of independent (quasi)particles, and, eventually, to incorporate any remaining interactions by means of a perturbative expansion.

$$\mathcal{Z} = \sum_{n} e^{-\sum_{i=1}^{\infty} n_i\beta(\varepsilon_i-\mu b_i-\beta^{-1}\ln\gamma)} = \sum_{n}\prod_{i} e^{-n_i\beta(\varepsilon_i-\mu b_i-\beta^{-1}\ln\gamma)} = \prod_{i}\sum_{n_i=0,1\ldots} e^{-n_i\beta(\varepsilon_i-\mu b_i-\beta^{-1}\ln\gamma)}.$$

To show last equality, one considers whether all the terms on the left-hand side are included on the right hand side, where the sum is not over all the sets of occupation numbers n, but over all the allowed values of occupation numbers n_i.For fermions (F,) we can have only $n_i = 0, 1$,whereas for bosons (Bs) $n_i = 0, 1, \ldots, \infty$. The resulting sums are easily carried out analytically:

$$\ln \mathcal{Z}_{\mathrm{F/B}} = \ln \prod_{i}\left(1 \pm \gamma e^{-\beta(\varepsilon_i-\mu b_i)}\right)^{\pm 1} = \pm\sum_{i}\ln(1 \pm \gamma\lambda_i^b e^{-\beta\varepsilon_i}).$$

- **For antiparticles, the eigenvalue of $\hat{b}$ is the negative of the particle value, the fugacity $\lambda_{\bar{\mathrm{f}}}$ for antiparticles $\lambda_{\bar{\mathrm{f}}} = \lambda_{\mathrm{f}}^{-1}$. This implies $\mu_{\mathrm{f}} = -\mu_{\bar{\mathrm{f}}}$.**
- **level sum $\sum_i$: If energy is the only controlling factor then we carry out this summation in terms of the single particle level density $\sigma_1(\varepsilon, V)$. Taking quantum levels in a box in the limit of infinite volume of the system we find the phase-space integral:**

$$\sum_i \to g \int \frac{d^3x\, d^3p}{(2\pi)^3}.$$

- **Independent particle energy $\varepsilon_i = \sqrt{m_i^2 + \vec{p}^2}$.**

$$\ln \mathcal{Z}_{\rm F/B}(V,\beta,\lambda,\gamma) = \pm gV \int \frac{d^3p}{(2\pi)^3} \left[\ln(1 \pm \gamma\lambda e^{-\beta\sqrt{p^2+m^2}}) + \ln(1 \pm \gamma\lambda^{-1} e^{-\beta\sqrt{p^2+m^2}})\right];$$

Boltzmann limit:

$$\ln \mathcal{Z}_{\rm cl}(V,\beta,\lambda,\gamma) = gV \int \frac{d^3p}{(2\pi)^3} \gamma(\lambda+\lambda^{-1}) e^{-\beta\sqrt{p^2+m^2}}.$$ **for Fermi and Bose**

Single particle phase space occupancy:

$$\begin{aligned}
\overline{w_i} \equiv \frac{\bar{n}_i}{N} &= \frac{e^{-\beta E_i}}{\sum_j e^{-\beta E_j}} \\
&= -\frac{1}{\beta}\frac{\partial}{\partial E_i}\left(\ln \sum_j \gamma e^{-\beta E_j}\right) = -\frac{1}{\beta}\frac{\partial}{\partial E_i}\ln Z \to \frac{1}{\gamma^{-1}\lambda^{-1}e^{\beta E_i} \pm 1} \\
&= \pm \sum_{n=1}^{\infty} \left(\pm\gamma\lambda e^{-\beta E_i}\right)^n \to \gamma\lambda e^{-\beta E_i},
\end{aligned}$$

we recognize FERMI, BOSE, BOLTZMANN distributions.
To evaluate a statistical physics property weight a distribution with suitable factor, for example, energy density results using as the weight single particle energy; particle density has weight 1 (integral of distribution).

Classical relativistic gas

Relativistic Boltzmann gas – a useful integral, for $\varepsilon = \sqrt{m^2+p^2}$:

$$W(\beta m) \equiv \beta^3 \int e^{-\beta\varepsilon} p^2\, dp = (\beta m)^2 K_2(\beta m), \quad \to 2, \ \text{for } m \to 0, \quad \to \sqrt{\frac{\pi m^3}{2T^3}} e^{-m/T}, \ \text{for } m \gg T$$

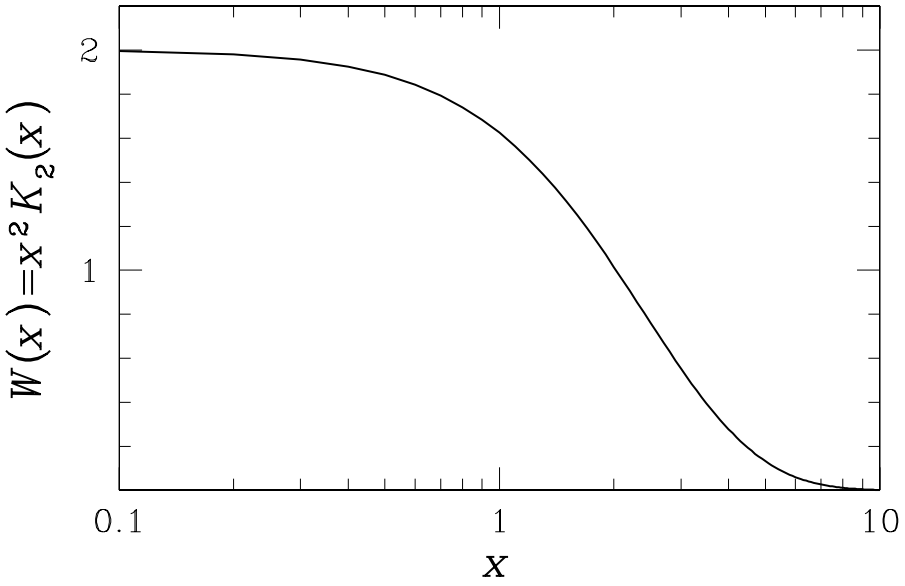

$$\ln \mathcal{Z}_{\rm cl} \equiv Z^{(1)} = \sum_i \gamma_i(\lambda_i + \lambda_i^{-1}) Z_i^{(1)},$$

$$Z_i^{(1)} = g_{\rm f} V \int \frac{d^3p}{(2\pi)^3} e^{-\beta\varepsilon(p)}$$

$$= g_i \frac{\beta^{-3} V}{2\pi^2} W(\beta m_i).$$

Relativistic Bose gas

Relativistic Bose gas, e.g. photon, gluons, pions: exploit the sum:

$$f(\varepsilon) = \frac{1}{\gamma^{-1}e^{\beta\varepsilon} - 1} = \sum_{n=1}^{\infty} \gamma^n e^{-n\beta\varepsilon}, \quad \gamma < e^{\beta m}.$$

or for the partition function

$$\ln \mathcal{Z} = -gV \int \frac{dp^3}{(2\pi)^3} \ln(1 - \gamma e^{-\beta\varepsilon}) = \frac{gV}{2\pi^2} \int_0^{\infty} dp p^2 \sum_{n=1}^{\infty} \frac{\gamma^n}{n} e^{-n\beta\varepsilon}, \quad \gamma < e^{\beta m}.$$

Exchange integral and sum! As we see, each term in the sum differs by $\beta \to n\beta$ and all we have to do it so make sure that we have the right power of $1/n$ in the final expression from substitution. Example: particle density:

$$\rho = \frac{g}{2\pi^2} T^3 \sum_{n=1}^{\infty} \frac{\gamma^n}{n^3} \int_0^{\infty} dx\, x^2 e^{-\sqrt{(nm/T)^2 + x^2}} = \frac{\beta^{-3} g}{2\pi^2} \sum_{n=1}^{\infty} \frac{\gamma^n}{n^3} (n\beta m)^2 K_2(n\beta m) \to \frac{gT^3}{\pi^2} \sum_{n=1}^{\infty} \frac{1}{n^3}.$$

Recall Riemann zeta function:

$$\zeta(k) = \sum_{n=1}^{\infty} \frac{1}{n^k}, \ \zeta(2) = \frac{\pi^2}{6}, \ \zeta(3) \simeq 1.202, \ \zeta(4) = \frac{\pi^4}{90}.$$

For a Fermi occupation function, the signs of the terms in the sums are alternating, which leads to the eta function

$$\eta(k) = \sum_{n=1}^{\infty} (-1)^{n-1} \frac{1}{n^k} = (1 - 2^{1-k})\zeta(k), \ \eta(3) = \frac{3}{4}\zeta(3) = 0.901\,5, \ \eta(4) = \frac{7}{8}\zeta(4) = \frac{7}{720}\pi^4.$$

Quark gas

Fermi gas, (note that we have assumed complete phase space occupancy $\gamma = 1$)

$$\ln \mathcal{Z}_{\rm F} \;=\; g_{\rm F} V \int \frac{d^3p}{(2\pi)^3}[\ln(1+e^{-\beta(\varepsilon-\mu)}) + \ln(1+e^{-\beta(\varepsilon+\mu)})],$$

integrate by parts: $d^3p \to 4\pi p^2 dp$

$$3\frac{T}{V}\ln \mathcal{Z}_{\rm F} \;=\; g_{\rm F}\frac{\beta}{3}\int \frac{d^3p}{(2\pi)^3}\frac{\vec{p}^{\,2}}{\varepsilon}\left(\frac{1}{e^{\beta(\varepsilon-\mu)}+1}+\frac{1}{e^{\beta(\varepsilon+\mu)}+1}\right).$$

Substitute the arguments of f and $\bar{f}$ with $x = \beta(\varepsilon \pm \mu)$:

$$3\frac{T}{V}\ln \mathcal{Z}_{\rm F} = \frac{g_{\rm F}}{2\pi^2}T^4\Big(\int_{\beta(m-\mu)}^{\infty} dx\,\frac{[(x+\mu/T)^2-(m/T)^2]^{3/2}}{e^x+1} + (\mu\to-\mu)\Big).$$

For $m \to 0$ $[(x \pm \mu/T)^2 - (m/T)^2]^{3/2} \to (|x \pm \beta\mu|)^3$, integrals split to be from $\pm\beta\mu \to 0$ and from $0 \to \infty$. The finite-range terms:

$$\int_{-\beta\mu}^{0} dx\,\frac{|x+\beta\mu|^3}{1+e^x} - \int_0^{\beta\mu} dx\frac{(x-\beta\mu)^3}{1+e^x} \;=\; \int_0^{\beta\mu} dx\,\frac{(\beta\mu-x)^3}{1+e^{-x}} + \int_0^{\beta\mu} dx\,\frac{(\beta\mu-x)^3}{1+e^x}$$

$$= \int_0^{\beta\mu} dx\,(\beta\mu-x)^3 = \frac{(\beta\mu)^4}{4},$$

The reminder evaluated expanding $(e^x+1)^{-1} = \sum_{n=1}^{\infty} e^{-nx}$.

$$\ln \mathcal{Z}_{\rm F}|_{m=0} = \frac{g_{\rm F} V \beta^{-3}}{6\pi^2}\left(\frac{7\pi^4}{60}+\frac{\pi^2}{2}\ln^2\lambda+\frac{1}{4}\ln^4\lambda\right).$$

s-QUARK PHASE-SPACE in QGP with Coulomb

For quarks chemical fugacity λ_s;

For antiquarks chemical fugacity λ_s^{-1};

Both quarks and antiquarks subject to pair-abundance factor γ_s

$$\langle s-\bar{s}\rangle = \int g_s \frac{d^3p d^3x}{(2\pi)^3} \frac{1}{1+\gamma_s\lambda_s e^{-(E-\frac{1}{3}V_c)/T}} - \frac{1}{1+\gamma_s\lambda_s^{-1} e^{-(E+\frac{1}{3}V_c)/T}}$$

When Coulomb field is negligible:

deconfinement and $\langle s-\bar{s}\rangle = 0 \Rightarrow \boxed{\lambda_s = 1}$

COULOMB EFFECT on s-QUARK PHASE-SPACE in QGP

Relevant only for CERN Pb–Pb. In Boltzmann approximation:

$$\langle s-\bar{s}\rangle = \int g_s \frac{d^3p}{(2\pi)^3}\gamma_s e^{-E/T} \int_{R_{\rm f}} \frac{d^3r}{V_{R_{\rm f}}} \left[\lambda_s e^{\frac{V_c}{3T}} - \lambda_s^{-1} e^{-\frac{V_c}{3T}}\right] .$$

for $R_{\rm f} = 8\,$**fm,** $T = 140\,$**MeV,** $m_s = 200\,$**MeV and** $Z_{\rm f} = 150 \Rightarrow \boxed{\lambda_s = 1.1}$

PERTURBATIVE EFFECTS

an essential prerequirement for the perturbative theory to be applicable in domain of interest to us, is the relatively small experimental value $\alpha_{\rm s}(M_Z) \simeq 0.118$, experimentally established in recent years.

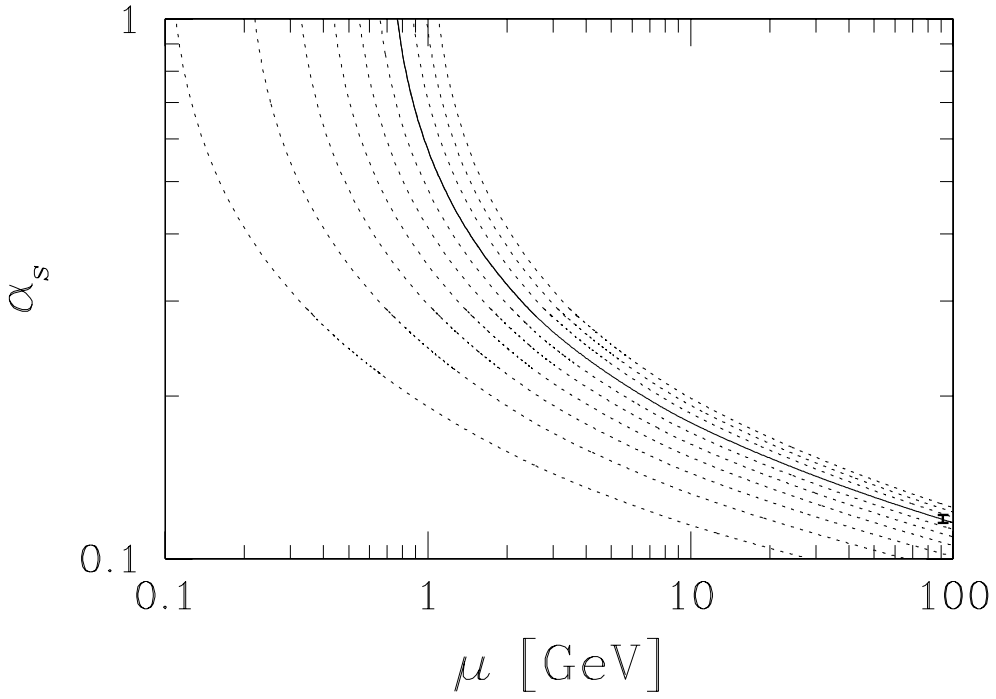

$\alpha_{\rm s}^{(4)}(\mu)$ as function of energy scale μ for a variety of initial conditions. Solid line: $\alpha_{\rm s}(M_Z) = 0.1182$ (experimental point, includes the error bar at $\mu = M_Z$). Result of integration of renormalization group equation.

$$\mu\frac{\partial\alpha_s}{\partial\mu} = -b_0\alpha_s^2 - b_1\alpha_s^3 + \ldots \equiv \beta_2^{\rm pert}\,,$$

note that above μ is scale of energy NOT chemical potential

$$b_0 = \frac{11 - 2n_{\rm f}/3}{2\pi}\,, \qquad b_1 = \frac{51 - 19n_{\rm f}/3}{4\pi^2}\,.$$

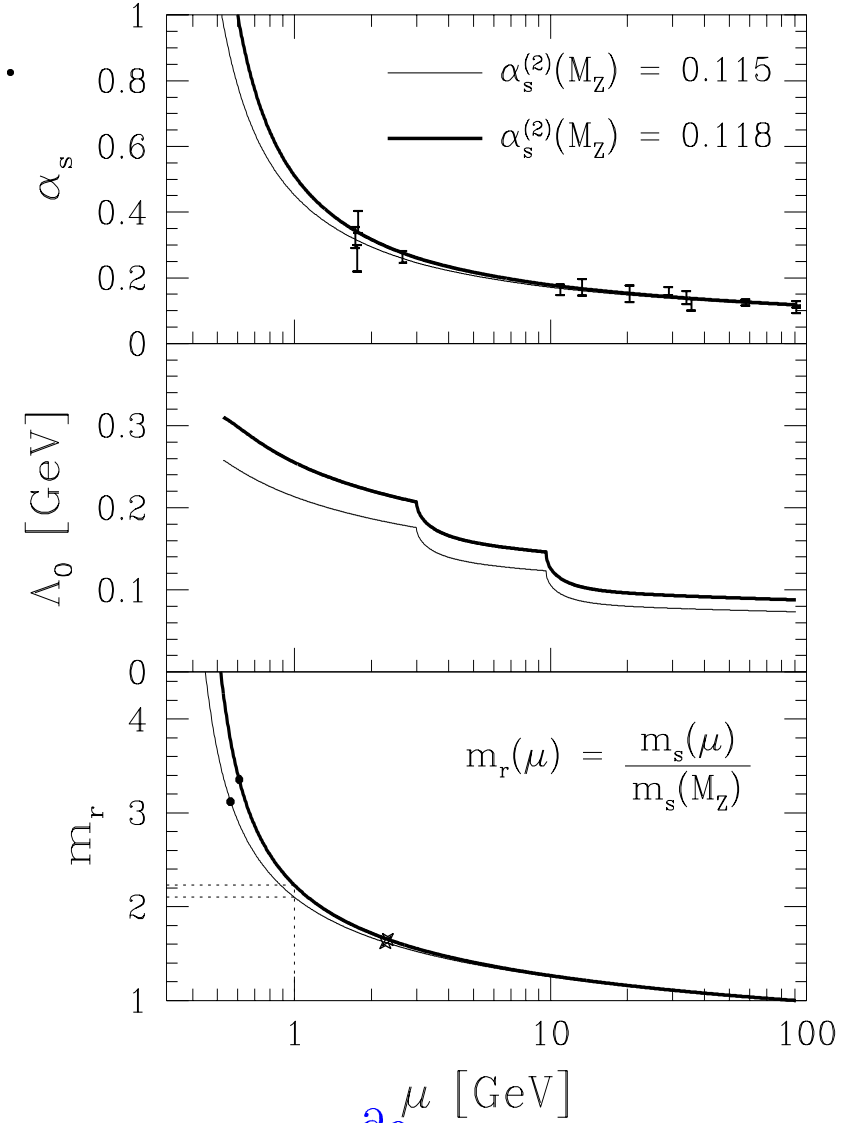

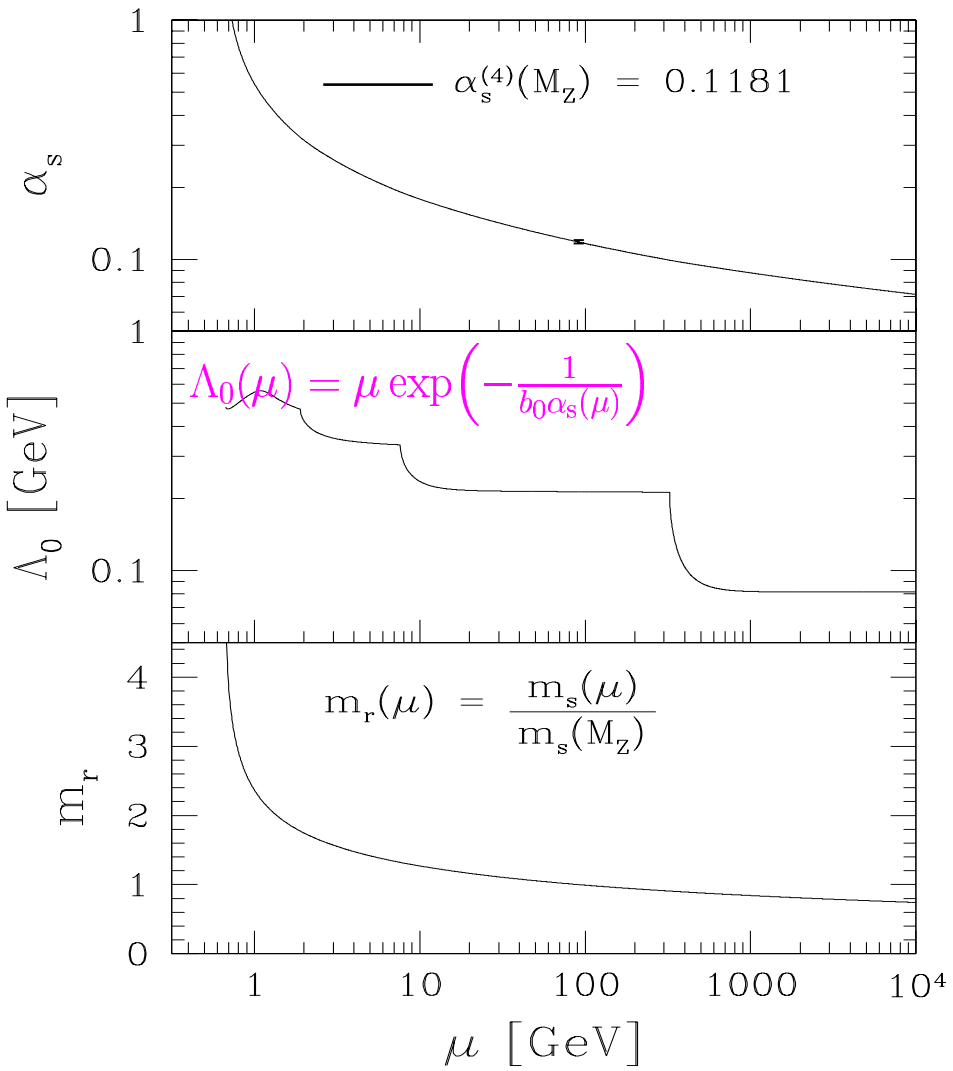

$$\mu \frac{\partial \alpha}{\partial \mu} \equiv \beta(\alpha_s) \qquad \beta^{\rm pert} = -\alpha_s^2 \left[\, b_0 + b_1 \alpha_s + b_2 \alpha_s^2 + \cdots \,\right]$$

$$-\frac{\mu}{m}\frac{\partial m}{\partial \mu} \equiv \gamma(\alpha_s), \qquad \gamma_m^{\rm pert} = \alpha_s \left[\, w_0 + w_1 \alpha_s + w_2 \alpha_s^2 + \cdots \,\right]$$

see Rod Cruthers lecture

QCD perturbative interaction

QCD perturbative interaction reduce effective degeneracy: for each flavor of quarks (u, d, s) we have 2-spins, 3-colors, so $g_{u,d,s} = 6$, and need to keep in mind the doubling due to particle-antiparticle symmetry. Evaluation in thermal field theory of the Feynman diagrams in order α_s shows that on average this interaction is ATTRACTIVE and some of the many degrees of freedom freeze. Feynman diagrams contributing are of the type:

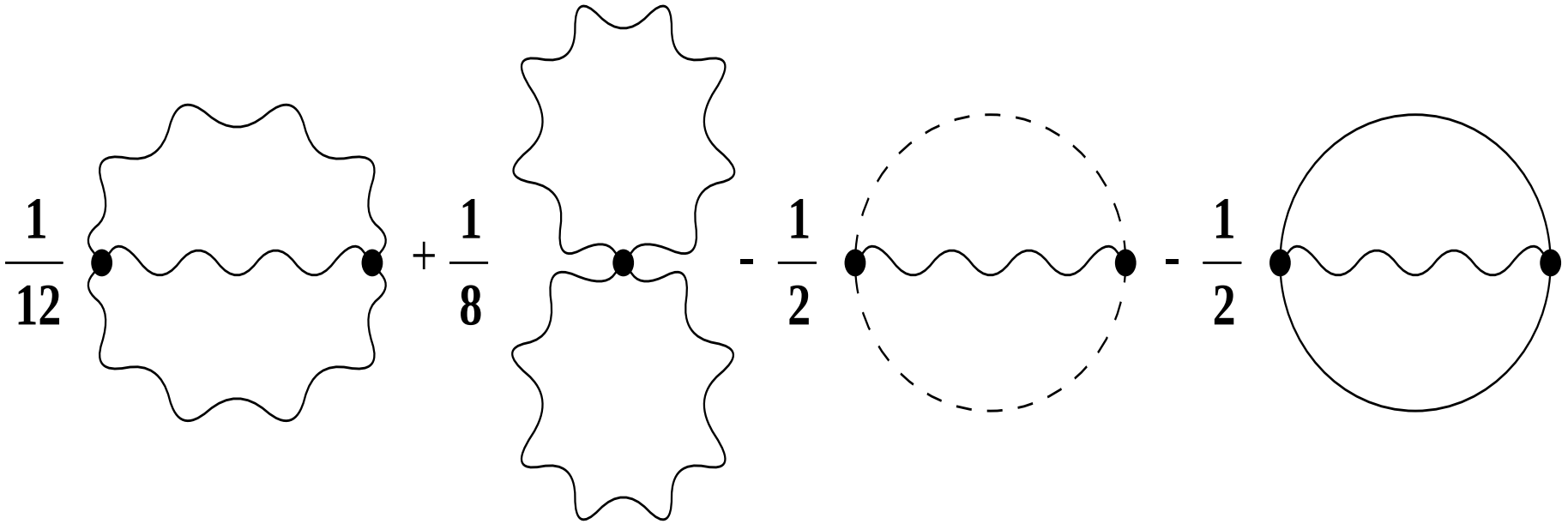

Wavy lines represent gluons, solid lines represent quarks, and dashed lines denote the ghost subtractions of non-physical degrees of freedom.

Perturbative QCD and QGP

$$\frac{T}{V}\ln\mathcal{Z}_{QGP}=-\mathcal{B}+\frac{8}{45\pi^2}c_1(\pi T)^4+\sum_{i=u,d,s}\frac{n_i}{15\pi^2}\left[\frac{7}{4}c_2(\pi T)^4+\frac{15}{2}c_3\left(\mu_i^2(\pi T)^2+\frac{1}{2}\mu_i^4\right)\right]$$

$$c_1=1-\frac{15\alpha_s}{4\pi}\,,\quad c_2=1-\frac{50\alpha_s}{21\pi}\,,\quad c_3=1-\frac{2\alpha_s}{\pi}\,.$$

We recall that $\mu_b=3\mu_q$ and $\lambda_q=e^{\mu_q/T}$. The temperature dependence $\alpha_s(T)$ is obtained from $\alpha_s(\mu)$ setting the energy scale $\mu=2\pi T$. $\alpha_s(\mu)$ is obtained integrating the renormalization group equation, where $\alpha_s(\mu=M_Z)=0.1182+0.001-0.0016$. in the domain of relevance $\alpha_s/\pi<0.22$ We cross several flavor mass thresholds, $n_{\rm f}(\mu)\neq$ Const. Error of solution with $n_{\rm f}(\mu)=$ Const. accumulates,

$$\alpha_s^2(\mu)\simeq\frac{2}{b_0\bar{L}}\left[1-\frac{2b_1}{b_0^2}\frac{\ln\bar{L}}{\bar{L}}\right],\quad \bar{L}\equiv\ln(\mu^2/\Lambda^2)\,,$$

with $\Lambda=0.15\,$GeV is not precise enough at scale to interest compared to exact 2-loop numerical solution. This form suitable for $\mu>10\,$GeV.

$\alpha_s(T)$ and Pressure of QGP-Liquid

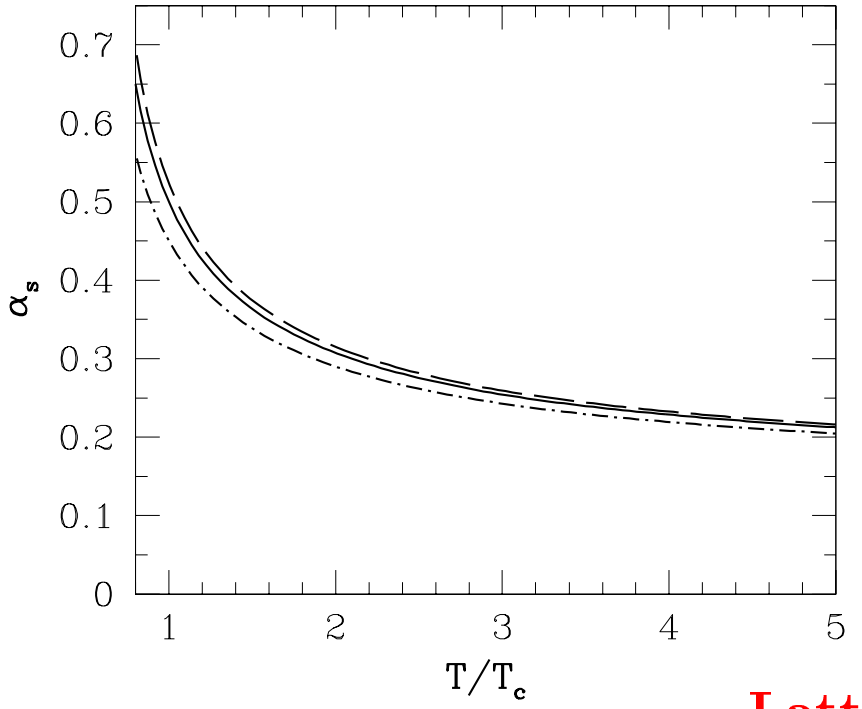

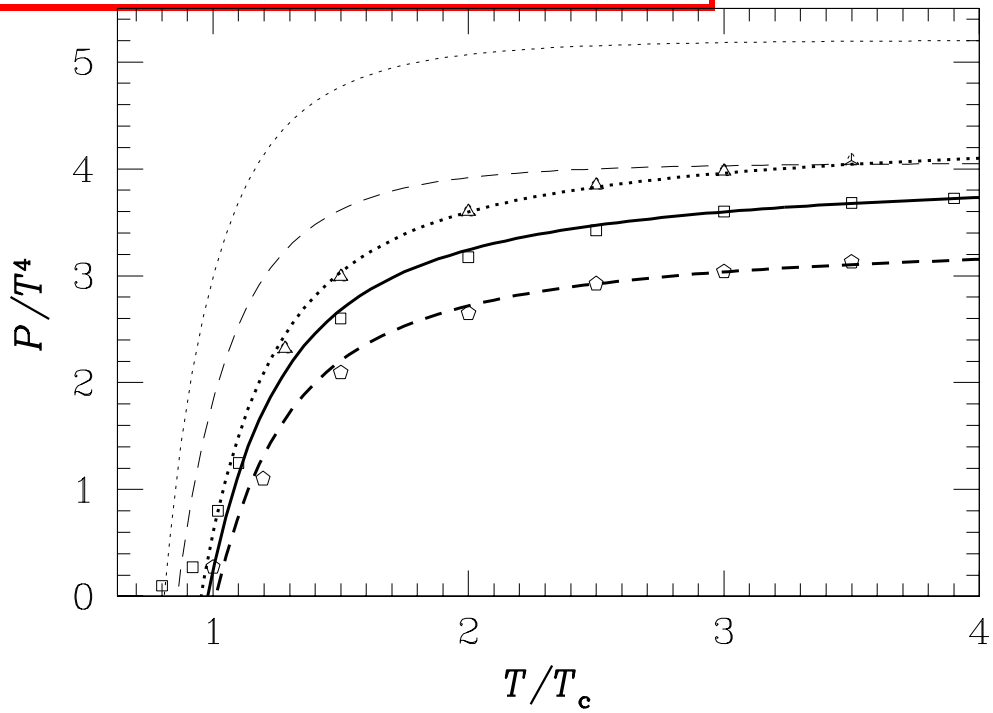

$\alpha_s(2\pi T)$ **for** $T_c = 0.16$ **GeV.**
$\mu = 2\pi T = T/T_c$ **[GeV]**
Dashed line:
$\alpha_s(M_Z) = 0.119$**;**
solid line $= 0.118$**;**
dot-dashed $= 0.1156$**.**
For $T < 5T_c$**:**

$$\alpha_{\rm s}(T) \simeq \frac{\alpha_{\rm s}(T_{\rm c})}{1+C\ln(T/T_{\rm c})}$$

$$\alpha_{\rm s}(T_{\rm c}) = 0.50^{-0.05}_{+0.03}$$

$$C = 0.760 \pm 0.002.$$

Lattice-QCD results F. Karsch, E. Laermann and A. Peikert *Phys. Lett.* **B 478, 447-455, (2000); Quark-gluon liquid model at** $\lambda_q = 1$ **(thick lines) and with** $\mu = 2\pi T = \kappa T/T_c, \kappa = 1$ **GeV.** $\mathcal{B} = 0.19\,\mathbf{GeV/fm^3}$**. Solid line 2+1 flavors** ($m_s/T = 1.7$)
dotted: 3 flavors, dashed: 2 flavors.
Thin lines: without perturbative α_s **effects,which is just the bag model.**

What do Interactions, What does $\mathcal{B}$

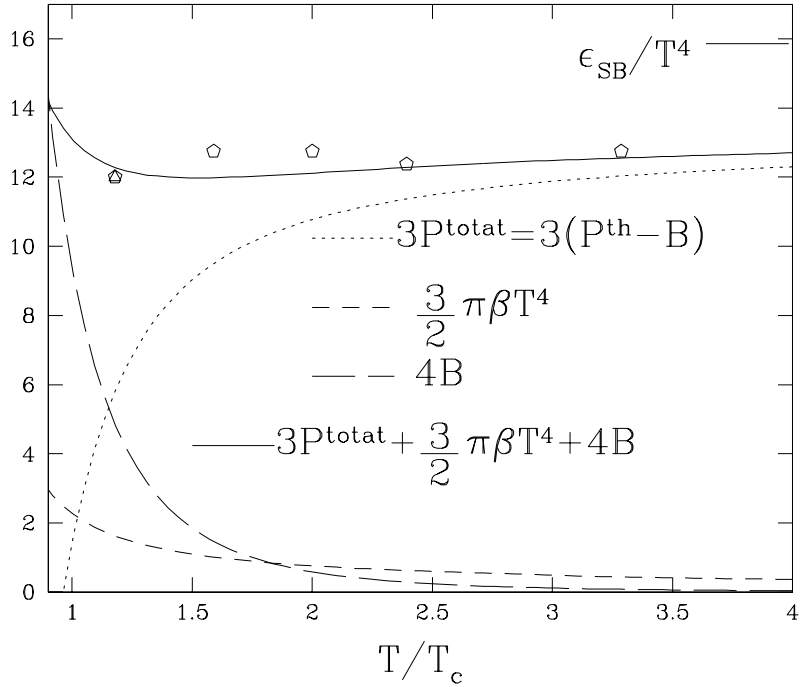

$\kappa=1,\ B=2$

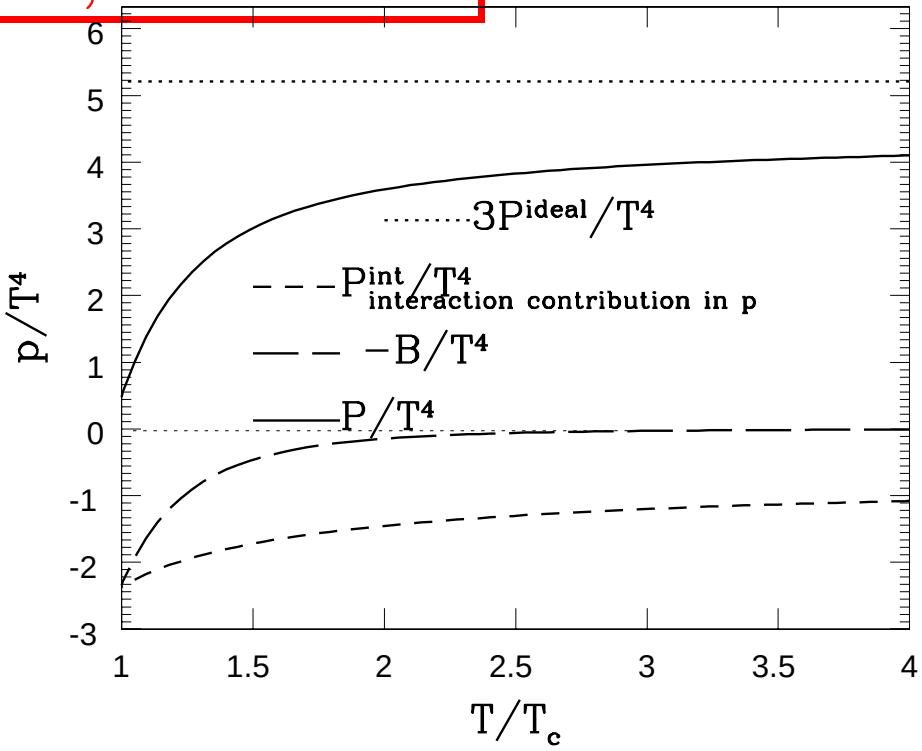

$\kappa=1,\ B=0.2, N_f=3, m/T=0$

$$\epsilon_{\rm QGP} = -\frac{\partial \ln \mathcal{Z}_{QGP}(\beta,\lambda)}{V\partial\beta} = 4\mathcal{B} + 3P_{QGP} + A\,,$$

$$A = (b_0\alpha_s^2 + b_1\alpha_s^3)\left[\frac{2\pi}{3}T^4 + \frac{n_{\rm f}5\pi}{18}T^4 + \frac{n_{\rm f}}{\pi}\left\{\mu_{\rm q}^2T^2 + \frac{1}{2\pi^2}\mu_{\rm q}^4\right\}\right]\,.$$

Extension to finite baryon density

To relate the QCD scale to the temperature $T = 1/\beta$ we use

$$\mu = 2\sqrt{(\pi T)^2 + \mu_q^2} = 2\pi\beta^{-1}\sqrt{1 + \frac{1}{\pi^2}\ln^2\lambda_q}\,.$$

A convenient way to obtain entropy and baryon density uses the thermodynamic potential $\mathcal{F}$:

$$\frac{\mathcal{F}(T,\mu_q,V)}{V} = -\frac{T}{V}\ln\mathcal{Z}(\beta,\lambda_q,V)_{QGP} = -P_{QGP}\,.$$

The entropy density is:

$$s_{QGP} = -\frac{d\mathcal{F}}{V\,dT} = \frac{32\pi^2}{45}c_1T^3 + \frac{n_{\rm f}7\pi^2}{15}c_2T^3 + n_{\rm f}c_3\mu_{\rm q}^2T + A\frac{\pi^2T}{\pi^2T^2+\mu_{\rm q}^2}\,.$$

Noting that baryon density is 1/3 of quark density, we have:

$$\rho_{\rm B} = -\frac{1}{3}\frac{d\mathcal{F}}{V\,d\mu_{\rm q}} = \frac{n_{\rm f}}{3}c_3\left\{\mu_{\rm q}T^2 + \frac{1}{\pi^2}\mu_{\rm q}^3\right\} + \frac{1}{3}A\frac{\mu_{\rm q}}{\pi^2T^2+\mu_{\rm q}^2}\,.$$

$$A = A_g + A_q + A_s; \qquad A_g = (b_0\alpha_s^2 + b_1\alpha_s^3)\frac{2\pi}{3}T^4$$

$$A_{i=q,s} = (b_0\alpha_s^2 + b_1\alpha_s^3)\left[\frac{n_{\rm i}5\pi}{18}T^4 + \frac{n_{\rm i}}{\pi}\left\{\mu_{\rm i}^2T^2 + \frac{1}{2\pi^2}\mu_{\rm i}^4\right\}\right]\,.$$

Extension to finite baryon density works

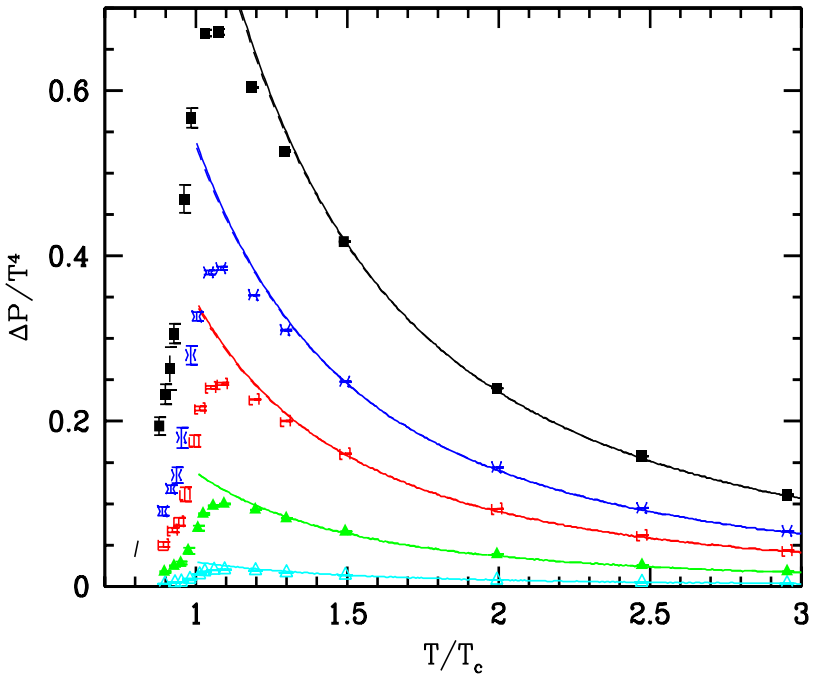

$\Delta P \equiv P(T,\mu_b) - P(T,\mu_b = 0)$ **normalized by** T^4 **as function of** T/T_c **for** $\mu_b =$**, 100, 210, 330, 410 and 530 MeV from bottom to top. Data points from Z. Fodor et al lattice work, solid lines massless liquid of quarks. Dashed (and mostly invisible) results with finite mass correction applied for** $m_q = 65$ **MeV as used in lattice data.**

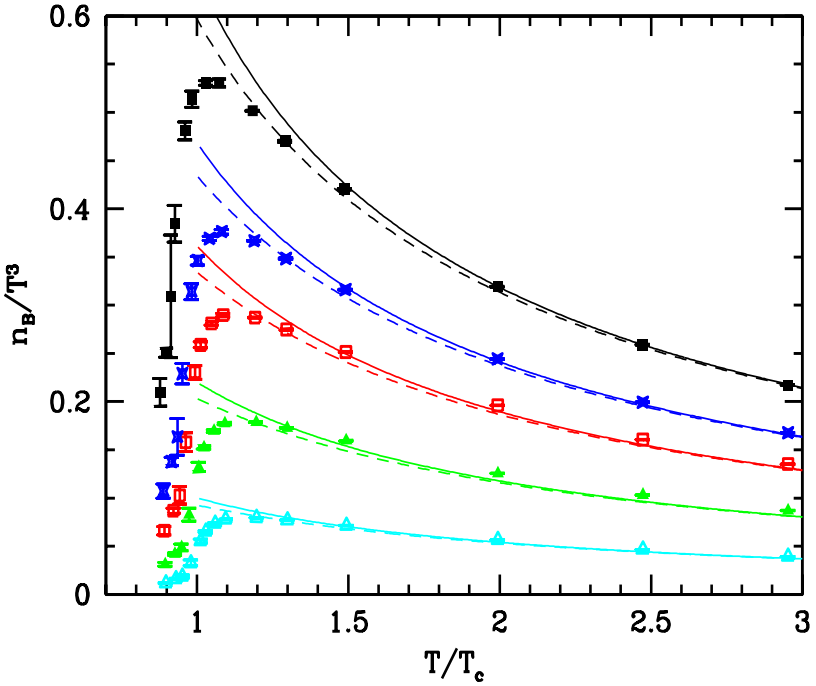

Baryon density $n_{\rm B}$ **normalized by** T^3 **as function of** T/T_c **for** $\mu_b = 100$**, 210, 330, 410 and 530 MeV from bottom to top. Solid lines massless liquid of quarks. Dashed lines: allowance is made for** $m_q = 65$ **MeV as is used to obtain the lattice data.**

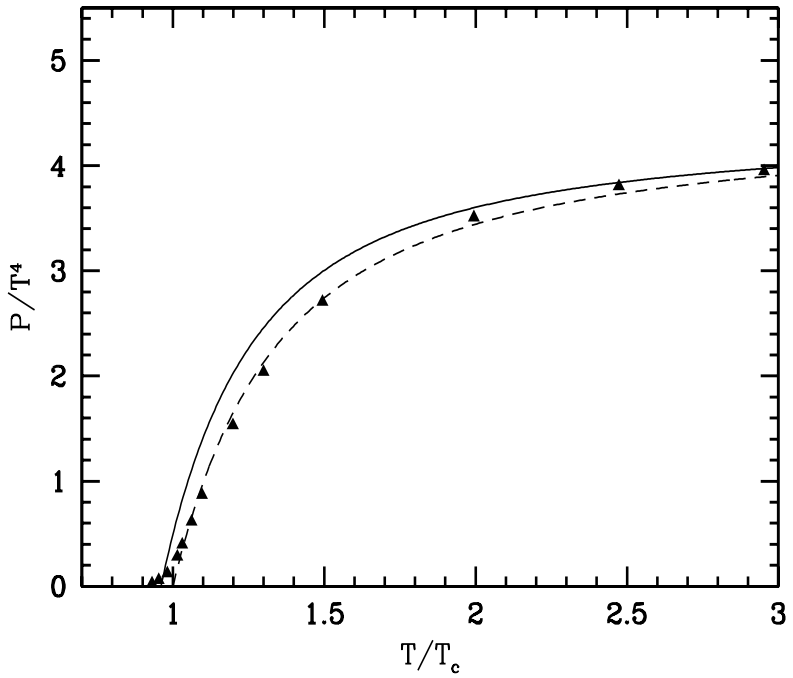

The pressure $P(T, \mu_b = 0)$ normalized by T^4 as function of T/T_c. Data points from Z. Fodor et al lattice work. Solid lines: massless gluons with $\mathcal{B} = (0.211\,\mathrm{GeV})^4$. Dashed line allows for a finite mass $m_G = 200$ MeV.

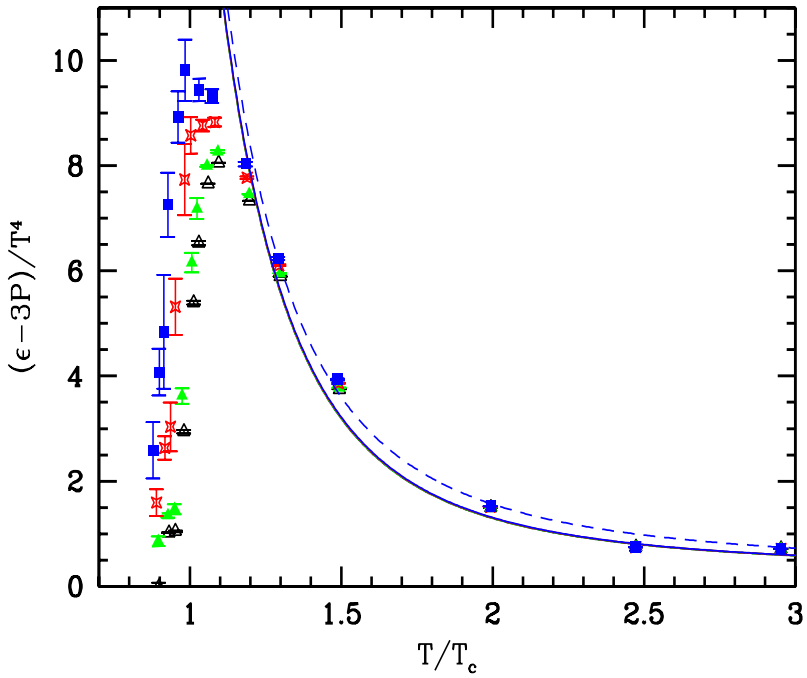

$(\epsilon - 3P)/T^4$ as function of T/T_c for $\mu_b = 0$, 210, 410 and 530 MeV, for $\mathcal{B} = (0.211\,\mathrm{GeV})^4$ and $T_c = 173\,\mathrm{MeV}$. Solid lines: massless gluons. Dashed lines: allowance is made for $m_G = 200$ MeV. All chemical potential lines coincide within line-width.

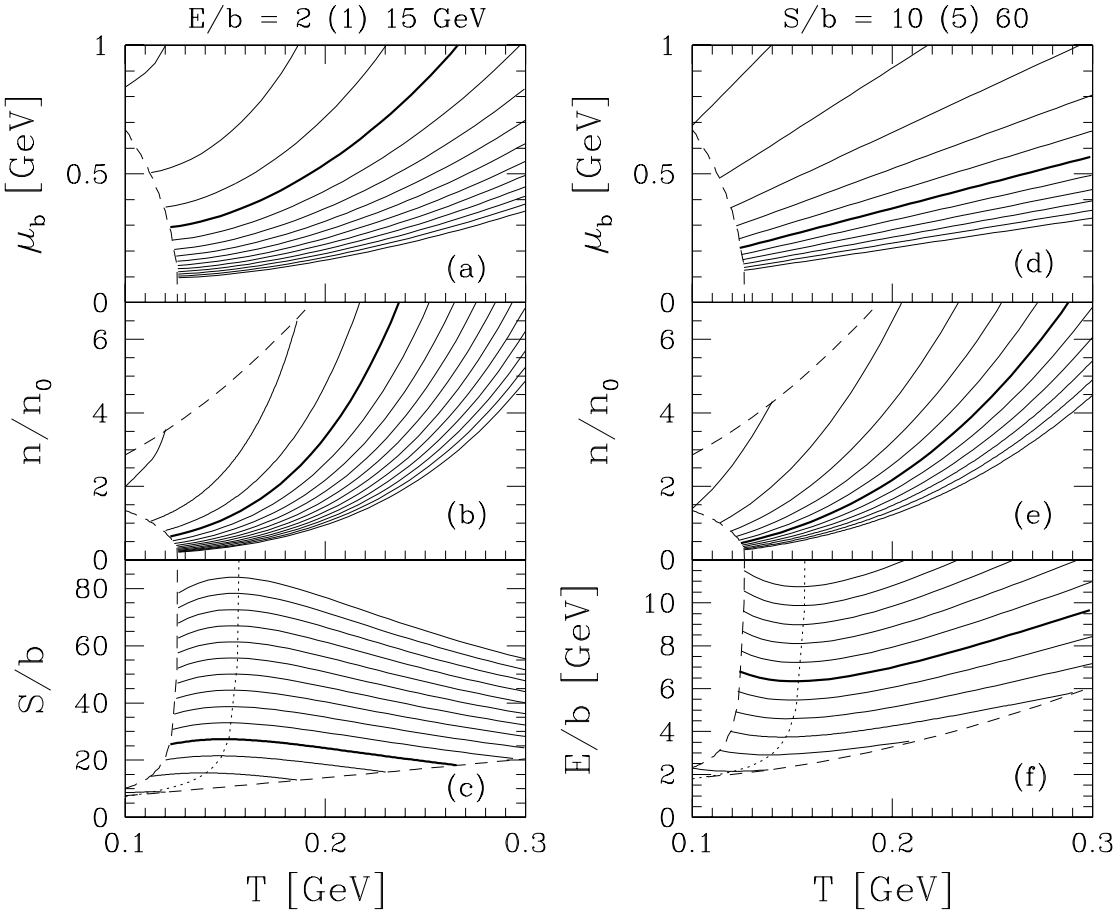

Left: lines corresponding to fixed energy per baryon $E/b = 2$ to 15 GeV in steps of 1 GeV, with $E/b = 5$ highlighted. Right: E/b lines corresponding to fixed entropy per baryon $S/b = 10$ to 60 in steps of 5, with $S/b = 35$ highlighted. (a) and (d) (top section), baryo-chemical potential μ_b , (b) and (e) (middle section), baryon density n/n_0 in units of equilibrium nuclear density, and (c) bottom portion: on left S/b, the entropy per baryon (highest E/b at the top), and (f) on right E/b, (highest S/b at the bottom).

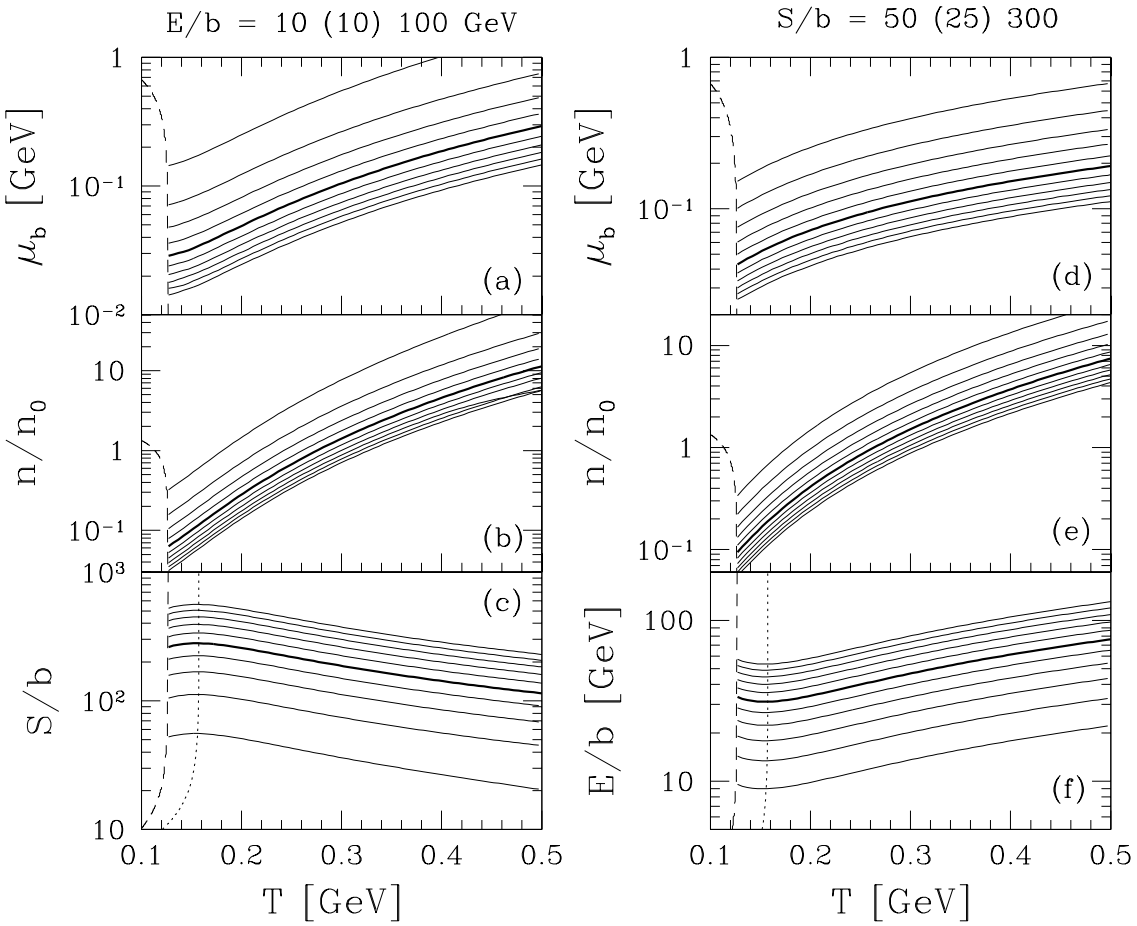

Now for the RHIC energy domain. Left, lines at fixed energy per baryon $E/b = 10$ to 100 GeV in steps of 10 GeV, with $E/b = 50$ GeV highlighted. Right, lines at fixed entropy per baryon $S/b = 50$ to 300 in steps of 25, with $S/b = 175$ hilighted.

Other way: massive quasi-particles

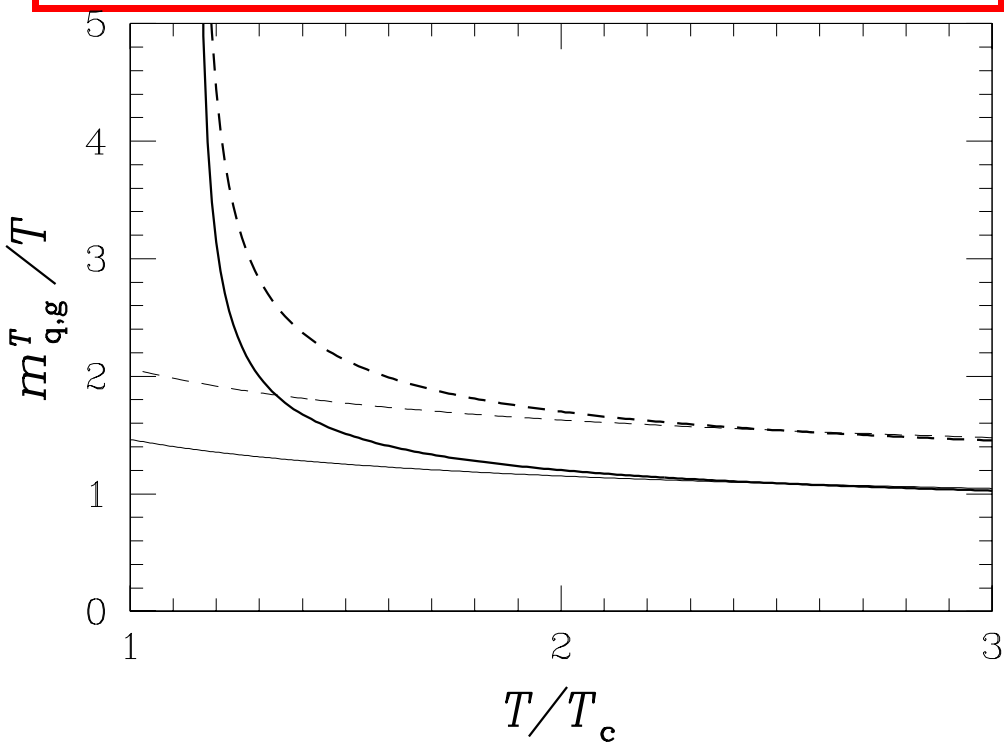

Thermal masses fitted to reproduce Lattice-QCD results
Thick solid line for quarks, and thick dashed line for gluons. Thin lines, perturbative QCD masses for $\alpha_s(\mu = 2\pi T)$.

$$(m_{\rm q}^{\rm T})^2 = \frac{4\pi}{3}\alpha_s T^2\,, \qquad (m_{\rm g}^{\rm T})^2 = 2\pi\alpha_s T^2\left(1+\frac{n_{\rm f}}{6}\right)\,,$$

The thermal masses required to describe the reduction of the number of degrees of freedom for $T > 2T_{\rm c}$ are outside of the range of the vacuum structure influence ($\mathcal{B}$) the perturbative QCD result. This means that thermal masses express, in a different way, the effect of perturbative QCD

Hadron Gas Phase

We can use the methods we proposed for quarks and gluons to describe the gas of pions, nucleons and all the rest! To be precise many thousand hadronic particles. Hadron Gas phase. A topic in itself, so I will just glance at it and its properties.

MISSING HADRON RESONANCES

Hagedorn mass spectrum is exponential, experimentally known resonances are exponential, within experimental limits:

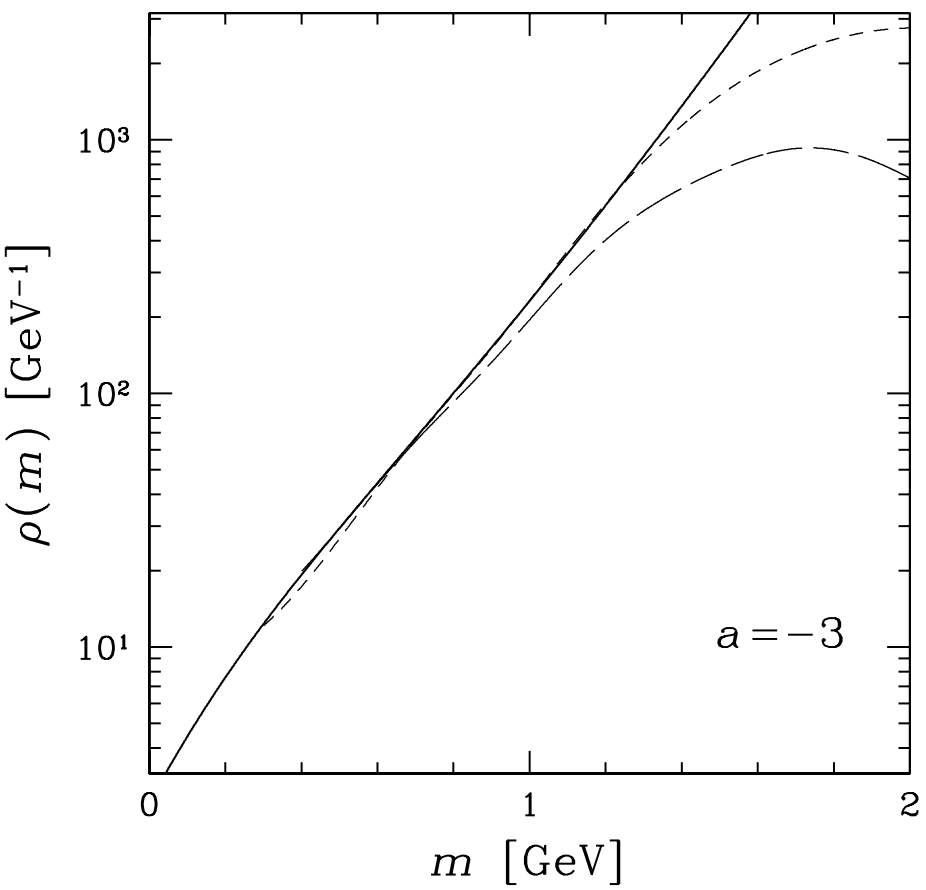

Dashed lines are the (smoothed) hadronic mass spectrum. The solid line represents the fit

$$\rho(m) \approx c(m_0^2 + m^2)^{a/2} \exp(m/T_0)$$

$T_0 = 0.158$ **GeV,** ($a = -3$ **preferred in the statistical bootstrap model,** $m_0 = 0.66$ **GeV).**

Long-dashed line:
1411 states of 1967.

Short-dashed line:
4627 states of 1996.

Exponential behavior related to critical behavior.

Lots of resonances missing above 1.4 GeV (log scale!)

How relevant an effect

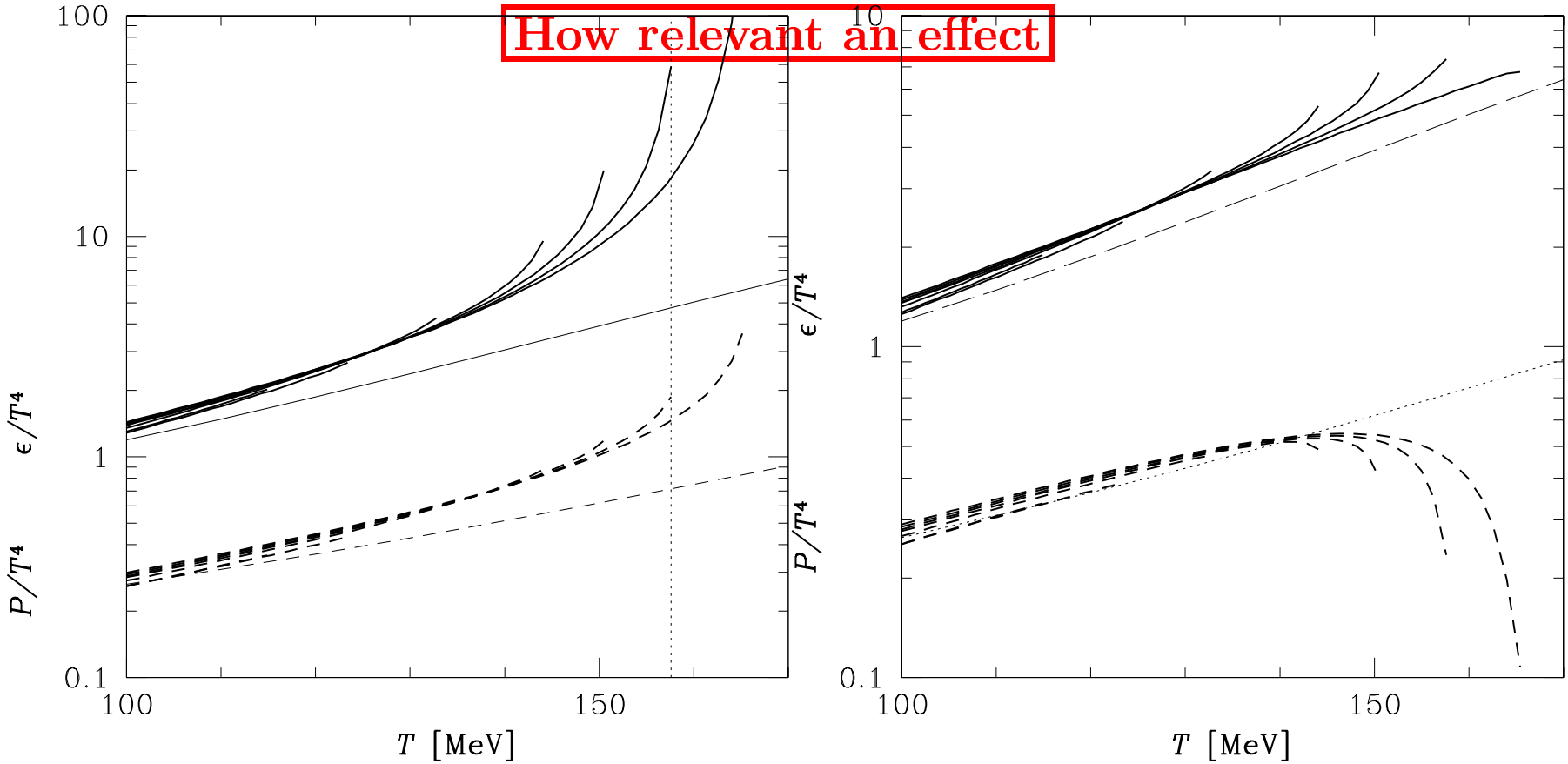

Point hadron gas **Hadrons of finite volume**

Thin lines from currently known experimental mass spectrum. All fugacities= 1. Thick: exponential mass spectrum with values of $a \in (-2.5, -7)$. Despite cancellation between two omissions hadron multiplicity e.g. π, h^- certainly 10–30% too low (fit 6%, if you believe fits). FUDGE FACTORS ARE NEEDED

Inertia to Force Ratio

For study of flow of matter one of most relevant quantities is the rigidity of the matter. Hadrons are heavy thus their pressure is less, hence unlike for relativistic matter, $\epsilon/P > 3$ But there is a 'soft' point.

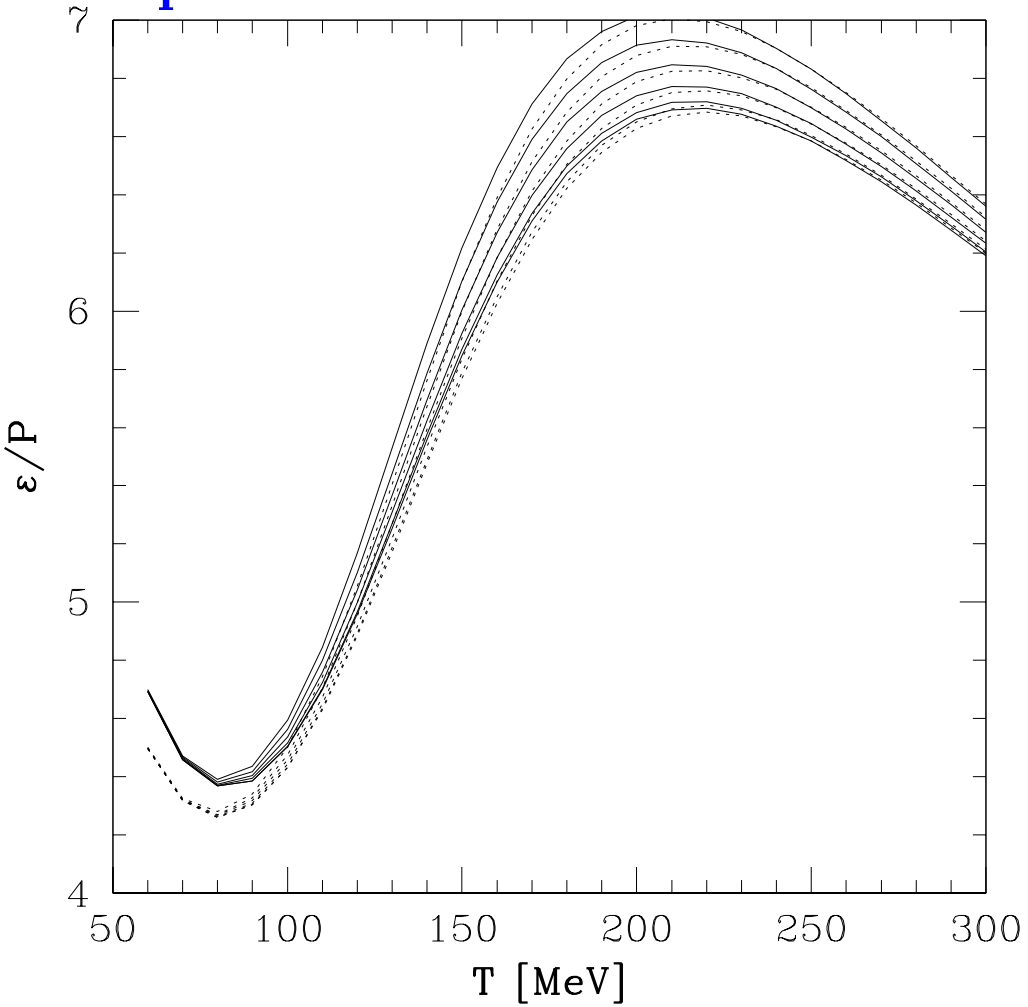

The energy density over pressure for a hadronic gas with statistical parameters $\lambda_s = 1.1$ and $\gamma_s/\gamma_q = 0.8$, with $\lambda_q = 1$ to 2 in steps of 0.2 from bottom to top and $\gamma_q = 1$ (dashed lines), or $\gamma_q = e^{m_\pi/(2T)}$ (full lines).

Hadronic gas flows very different from quark-gluon plasma.

Relativistic FLOW

Flow of matter in presence of two conservation laws: the flow of baryon number is conserved, and the flow of energy-momentum is conserved. In the hydrodynamic description of the evolution of matter, rather than individual particles, is considered. These flows are described in terms of the local flow field $\vec{v}(\vec{x},t)$, or equivalently in terms of the 4-velocity vector of the flow u^μ:

$$u^\mu(x)=\gamma(1,\vec{v}),\qquad \frac{dt}{d\tau}\equiv\gamma=\frac{1}{\sqrt{1-\vec{v}^2}};\qquad u_\mu u^\mu\equiv u^2=1,\quad u_\mu=g_{\mu\nu}u^\nu.$$

The proper time τ coordinate of the local volume element and laboratory frame coordinates are related by the Euler relation:

$$\frac{d}{d\tau}=u^\mu\partial_\mu=\gamma\left(\frac{\partial}{\partial t}+\vec{v}\cdot\vec{\nabla}\right),\ \partial_\mu=\frac{\partial}{\partial x^\mu}=\left\{\frac{\partial}{\partial_t},\vec{\nabla}\right\},\ g^{\mu\nu}\equiv\mathrm{diag}(1,-1,-1,-1)$$

We write a conserved current j_μ in terms of the local density ρ:

$$\partial_\mu(\rho u^\mu)=\rho\partial_\mu u^\mu+u^\mu\partial_\mu\rho=0,\qquad \partial_\mu u^\mu=-\frac{1}{\rho_i}\frac{d\rho_i}{d\tau}\equiv\frac{1}{\tau^{\rm exp}}.$$

Relativistic Hydrodynamics Tutorial

The hydrodynamic energy–momentum-flow equation, is

$$f^\nu \equiv \frac{\partial T^{\mu\nu}}{\partial x^\mu}, \qquad T^{\mu\nu} = (\epsilon + P)u^\mu u^\nu - g^{\mu\nu}P.$$

when the external force density vanishes, $f^\nu \to 0$, multiplication by u^ν yields,

$$u^\mu \partial_\mu \epsilon + (\epsilon + P)\partial_\mu u^\mu = 0, \quad \frac{\epsilon + P}{\epsilon}\partial_\mu u^\mu = -\frac{1}{\epsilon}\frac{d\epsilon}{d\tau}.$$

For $P \neq 0$, the energy flow $(u^\mu \epsilon)$ is not conserved. For $P > 0$, there is a transfer of the energy content of matter to the kinetic energy of the flow of matter. The expanding matter cools. In the rare situation that $P < 0$ the transfer of energy goes from kinetic energy of flow back to the intrinsic energy density ϵ.

The other three equations determine the velocity field $\vec{v}(\vec{x}, t)$,

$$\frac{\partial \vec{v}}{\partial t} + (\vec{v}\cdot\vec{\nabla})\vec{v} = -\frac{1 - v^2}{\epsilon + P}\left(\vec{\nabla}P + \vec{v}\frac{\partial P}{\partial t}\right),$$

One dimensional relativistic coordinates

Introduce "space-time rapidity" also called y as a second space-time coordinate aside of proper time τ of a volume element:

$$\tau = (t^2 - z^2)^{1/2},\ y = \frac{1}{2}\ln\left(\frac{t+z}{t-z}\right), \quad t = \tau\,\cosh y,\ z = \tau\,\sinh y,\ dt\,dz = \tau\,d\tau\,dy.$$

$$\frac{\partial y}{\partial t} = -\frac{z}{t^2 - z^2}, \quad \frac{\partial y}{\partial z} = \frac{t}{t^2 - z^2}, \quad \frac{\partial \tau}{\partial t} = \frac{t}{(t^2 - z^2)^{1/2}}, \quad \frac{\partial \tau}{\partial z} = \frac{-z}{(t^2 - z^2)^{1/2}},$$

$$\frac{\partial t}{\partial y} = \tau\sinh y, \quad \frac{\partial t}{\partial \tau} = \cosh y, \quad \frac{\partial z}{\partial y} = \tau\cosh y, \quad \frac{\partial z}{\partial \tau} = \sinh y.$$

The 4-velocity field of some volume element at proper time τ is only dependent on y, independent of τ

$$u^\mu \equiv \frac{dx^\mu}{d\tau} = (\cosh y, 0, 0, \sinh y), \quad u^2 = 1$$

$$\partial_\mu u^\mu = \frac{\partial u^0}{\partial t} + \frac{\partial u^3}{\partial z} = \frac{\partial y}{\partial t}\frac{\partial \cosh y}{\partial y} + \frac{\partial y}{\partial z}\frac{\partial \sinh y}{\partial y} = \frac{1}{\tau}.$$

One dimensional Bjorken solution

We recall

$$\frac{\epsilon+P}{\epsilon}\partial_\mu u^\mu = -\frac{1}{\epsilon}\frac{d\epsilon}{d\tau} \to \frac{\epsilon+P}{\tau}+\frac{d\epsilon}{d\tau}=0.$$

With velocity of sound:

$$\frac{1}{v_{\rm s}^2} \equiv \left.\frac{d\epsilon}{dP}\right|_{S=\textbf{constant}},$$

we can express

$$\frac{d\epsilon}{d\tau}=\frac{d\epsilon}{dP}\frac{dP}{dT}\frac{dT}{d\tau}=\frac{1}{v_{\rm s}^2}\sigma\frac{dT}{d\tau}, \qquad \sigma\equiv\frac{S}{V}=\frac{dP}{dT},$$

$$\partial_\mu u^\mu = -\frac{T\sigma}{\epsilon+P}\frac{1}{v_{\rm s}^2}\frac{1}{T}\frac{dT}{d\tau} \to \frac{v_{\rm s}^2}{\tau}=-\frac{1}{T}\frac{dT}{d\tau}.$$

For a (nearly) relativistic gas $v_{\rm s}^2 \lesssim \frac{1}{3}$, and the decrease of the temperature is slow. Explicitly, assuming that the velocity of sound changes slowly,

$$T=T_0\left(\frac{\tau_0}{\tau}\right)^{v_{\rm s}^2},$$

In a more realistic evolution of a fireball, which allows for transverse expansion, the expansion cooling is faster. On the other hand, there is less than fully relativistic sound velocity. A small change in $v_{\rm s}$ matters.

Entropy conservation and Bjorken solution

In general hydrodynamic flow without viscosity does not produce entropy.

For Bjorken solution

$$0 = \frac{\partial \sigma_\mu}{\partial x_\mu} = \frac{\sigma}{\tau} + \frac{d\sigma}{d\tau} = \frac{1}{\tau}\frac{d(\tau\sigma)}{d\tau}, \qquad \tau\sigma(\tau) = \sigma(\tau_0)\tau_0 = \sigma(\tau_f)\tau_f = \textbf{Const.},$$

In the locally at rest frame of the fluid (the comoving frame) we have $\Delta S = \sigma\, dz\, dt = \sigma\tau\, dy\, d\tau$.

$$\frac{d}{d\tau}\left(\frac{dS}{dy}\right) = \frac{d}{d\tau}(\tau\sigma) = 0, \qquad \frac{dS}{dy} = \textbf{Const.},$$

dS/dy **is independent of** y **(scaling) and not a function of** τ**, it is independent of when freeze-out occurs. Entropy is characteristic of the particle yield, thus particle multiplicity is flat in rapidity, and is not sensitive to freeze-out condition.**

SPACE-TIME PICTURE

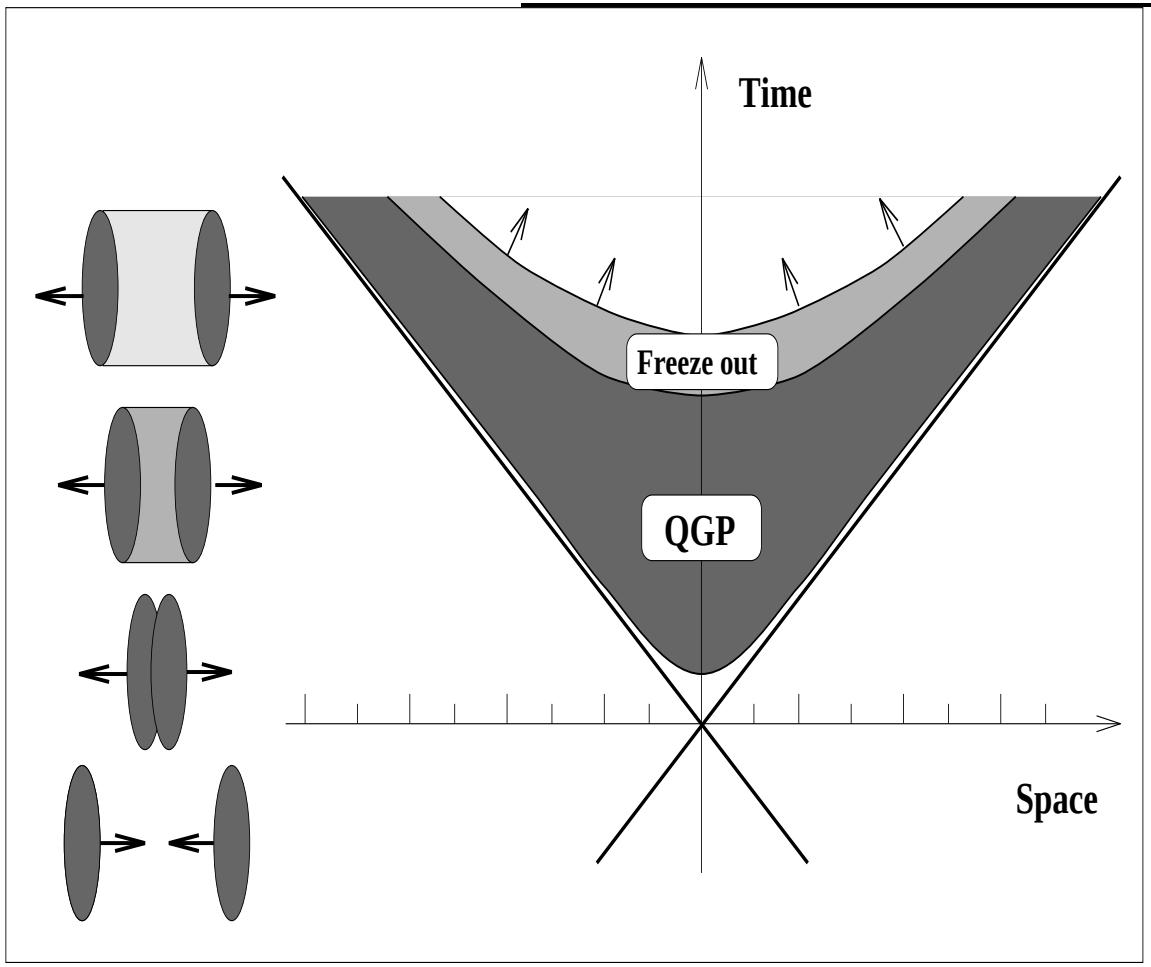

Illustration of a heavy-ion collision in the ultra-relativistic (Bjørken) collision limit. Left: Lorentz-contracted nuclei collide and separate as a function of the laboratory time (vertical axis). Right: the light cone establishes the causality limit for the flow of energy, which fills the space–time domain between the separating nuclei.

HBT view of hadronization

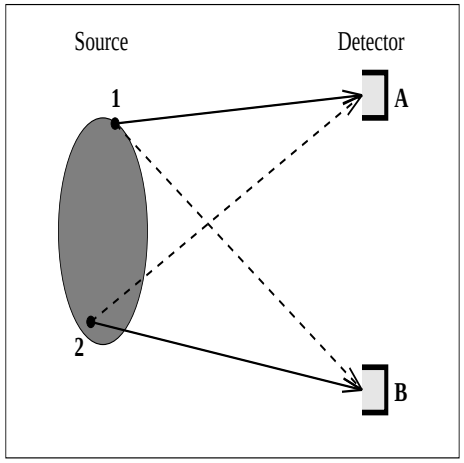

HBT Correlation method allows to evaluate space-time geometry from which correlated particles (typically pions are emitted).

$$C_2(p_{\rm A}, p_{\rm B}) = \frac{\rho({\rm A},{\rm B})}{\rho({\rm A}) * \rho({\rm B})},$$

If no correlation in particle intensity exists, the counts in both detectors are independent, $C_2 \to 1$. Analysis in highly granular detectors is now truly multi-dimensional, e.g

$$C_2 = D\left(1 + \lambda e^{-(q_{\rm o}^2 R_{\rm o}^2 + q_{\rm s}^2 R_{\rm s}^2 + q_{\rm l}^2 R_{\rm l}^2)}\right).$$

Though interpretation somewhat model dependent, there is abundant evidence that the size of emitter does not grow with energy and its lifespan is unexpectedly short.

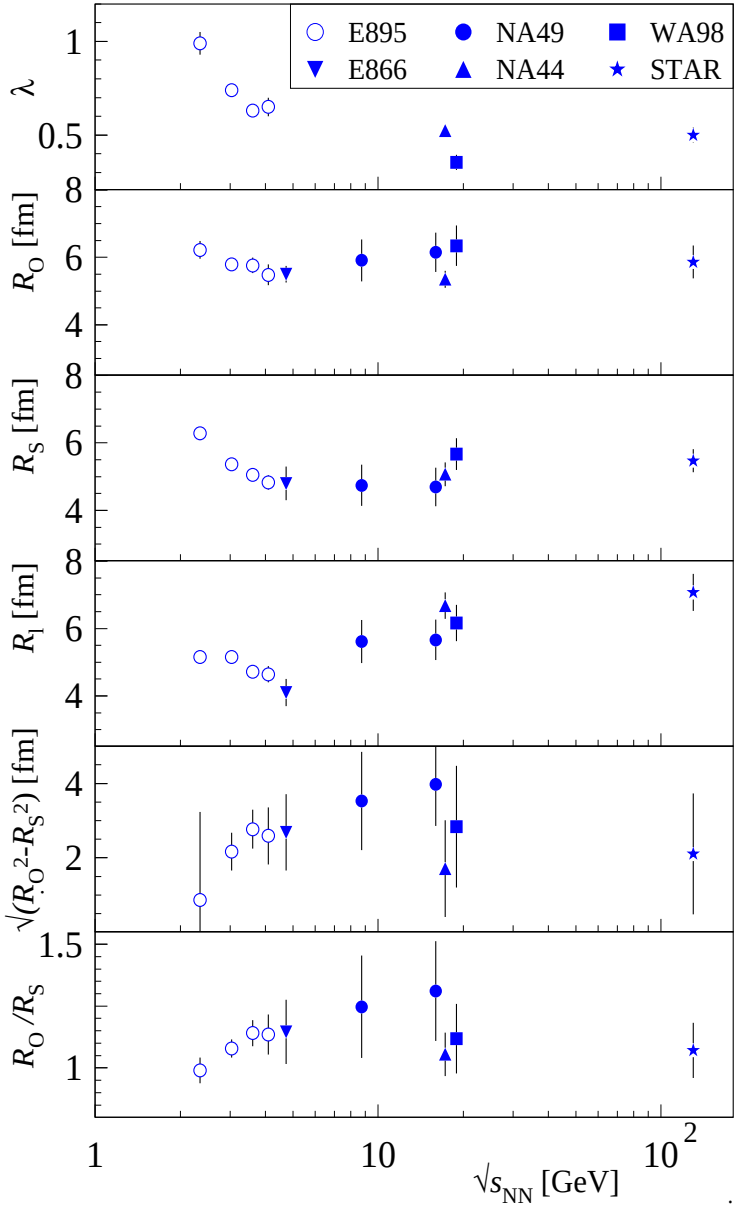

Super-cooling of a fast expanding fireball

P and ε: local in QGP particle pressure, energy density, $\vec{v}$ local flow velocity. The pressure component in the energy-momentum tensor:

$$T^{ij} = P\delta_{ij} + (P+\varepsilon)\frac{v_i v_j}{1-\vec{v}^2}\,.$$

The rate of momentum flow vector $\vec{\mathcal{P}}$ at the surface of the fireball is obtained from the energy-stress tensor T_{kl} :

$$\vec{\mathcal{P}} \equiv \widehat{\mathcal{T}}\cdot\vec{n} = P\vec{n} + (P+\varepsilon)\frac{\vec{v}_{\rm c}\,\vec{v}_{\rm c}\cdot\vec{n}}{1-\vec{v}_{\rm c}^{\,2}}\,.$$

The pressure and energy comprise particle and the vacuum properties: $P = P_{\rm p} - \mathcal{B}$, $\varepsilon = \varepsilon_{\rm p} + \mathcal{B}$. Condition $\vec{\mathcal{P}} = 0$ reads:

$$\mathcal{B}\vec{n} = P_{\rm p}\vec{n} + (P_{\rm p}+\varepsilon_{\rm p})\frac{\vec{v}_{\rm c}\,\vec{v}_{\rm c}\cdot\vec{n}}{1-v_{\rm c}^2}\,,$$

Multiplying with $\vec{n}$, we find,

$$\mathcal{B} = P_{\rm p} + (P_{\rm p}+\varepsilon_{\rm p})\frac{\kappa v_{\rm c}^2}{1-v_{\rm c}^2}\,, \qquad \kappa = \frac{(\vec{v}_{\rm c}\cdot\vec{n})^2}{v_{\rm c}^2}\,.$$

This requires $P_{\rm p} < \mathcal{B}$: QGP phase pressure P must be NEGATIVE. A fireball surface region which reaches $\mathcal{P}\to 0$ and continues to flow outward is torn apart in a rapid instability. This can ONLY arise since matter presses again the vacuum which is not subject to collective dynamics.

Phase boundary and mechanical instability

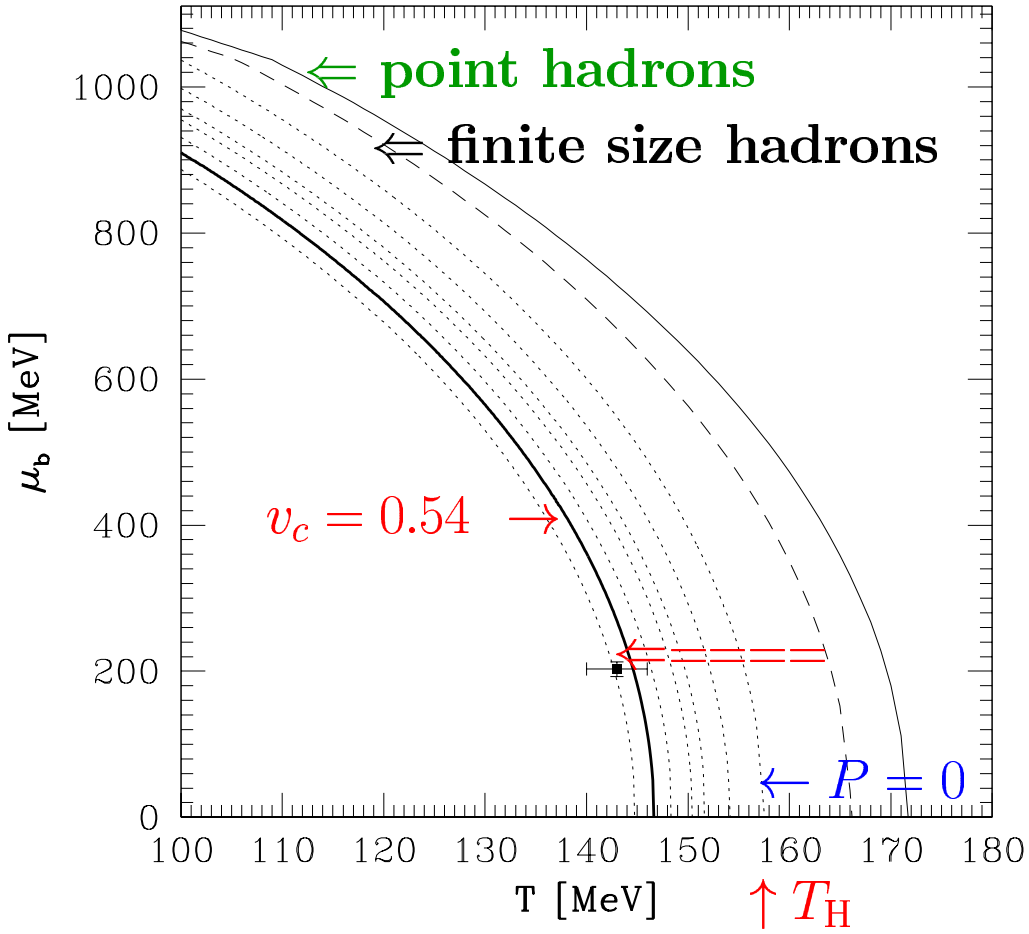

Solid: point hadrons T_p

Dashed: finite size

Dotted: $T_c(\mu_b)|_{P_{eff}-\mathcal{B}=0}$ for $v^2 = 0, 1/10, 1/6, 1/5, 1/4, 1/3$.

Thick solid: breakup with $v = 0.54$ ($\kappa = 0.6$)

PRL 85 (2000) 4695

DEEP SUPERCOOLING by 20 MeV

$T_H = 158$ **MeV Hagedorn temperature where $P = 0$, no hadron P**

$T_f \simeq 0.9 T_H \simeq 143$ **MeV is where supercooled QGP fireball breaks up**

equilibrium phase transformation is at $\simeq 166$.

Deconfinement Signatures

PROBLEM: when all is over, we have just many hadrons, some rare direct photons, some rare direct 'dileptons'. How can we tell there was deconfinement? Early ideas about direct γ, e^+e^-, $\mu^+\mu^-$ not yet practical (maybe never). Two hadronic observables are well studied, the J/Ψ suppression (mention), and strangeness next topic.

Illustration of suppression idea.

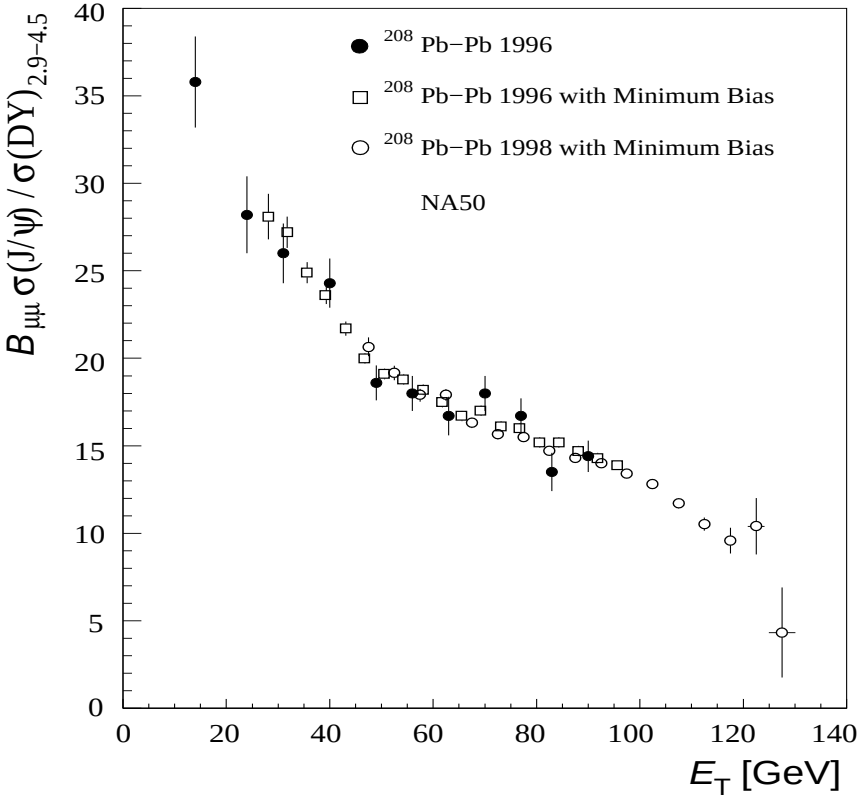

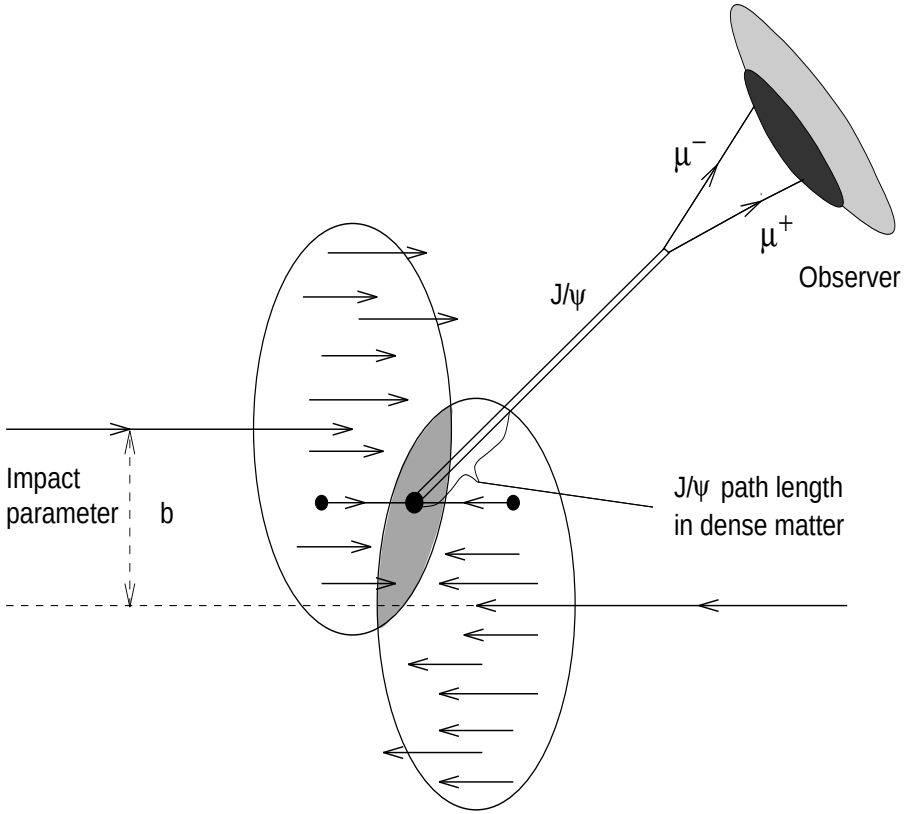

Suppression of production of J/Ψ as a function of AA-collision centrality, characterized in terms of the transverse energy $E_{\rm T}$ produced in the reaction. Results of experiment NA50.

Strangeness – a popular QGP diagnostic tool

EXPERIMENTAL REASONS

- **There are many strange particles allowing to study different physics questions** $(q = u, d)$**:**

$$\phi(s\bar{s}), \quad K(q\bar{s}), \quad \overline{K}(\bar{q}s), \quad \Lambda(qqs), \quad \overline{\Lambda}(\bar{q}\bar{q}\bar{s}),$$

$$\Xi(qss), \quad \overline{\Xi}(\bar{q}\bar{s}\bar{s}), \quad \Omega(sss), \quad \overline{\Omega}(\bar{s}\bar{s}\bar{s})$$

- **Strange hadrons are subject to a self analyzing decay within a few cm from the point of production;**

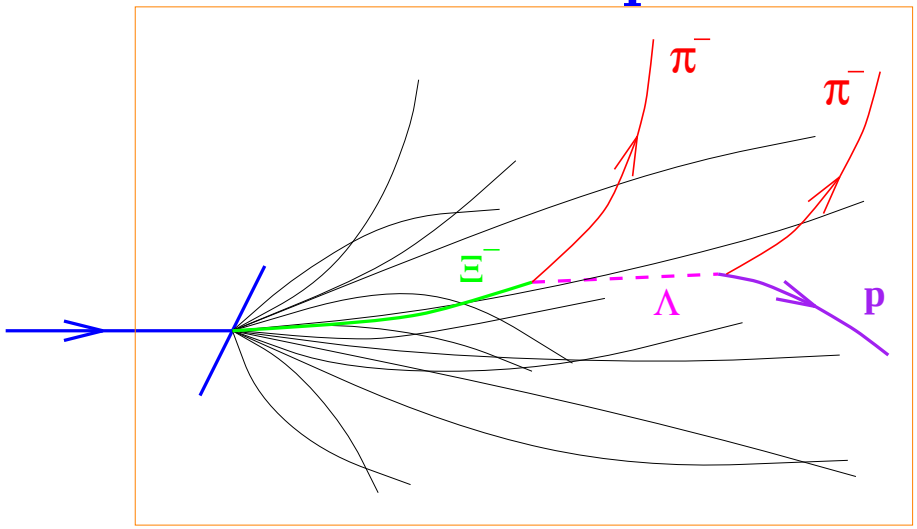

- **Production rates hence statistical significance is high;**

'CROSS-TALK' HADRON FORMATION MECHANISM IN QGP

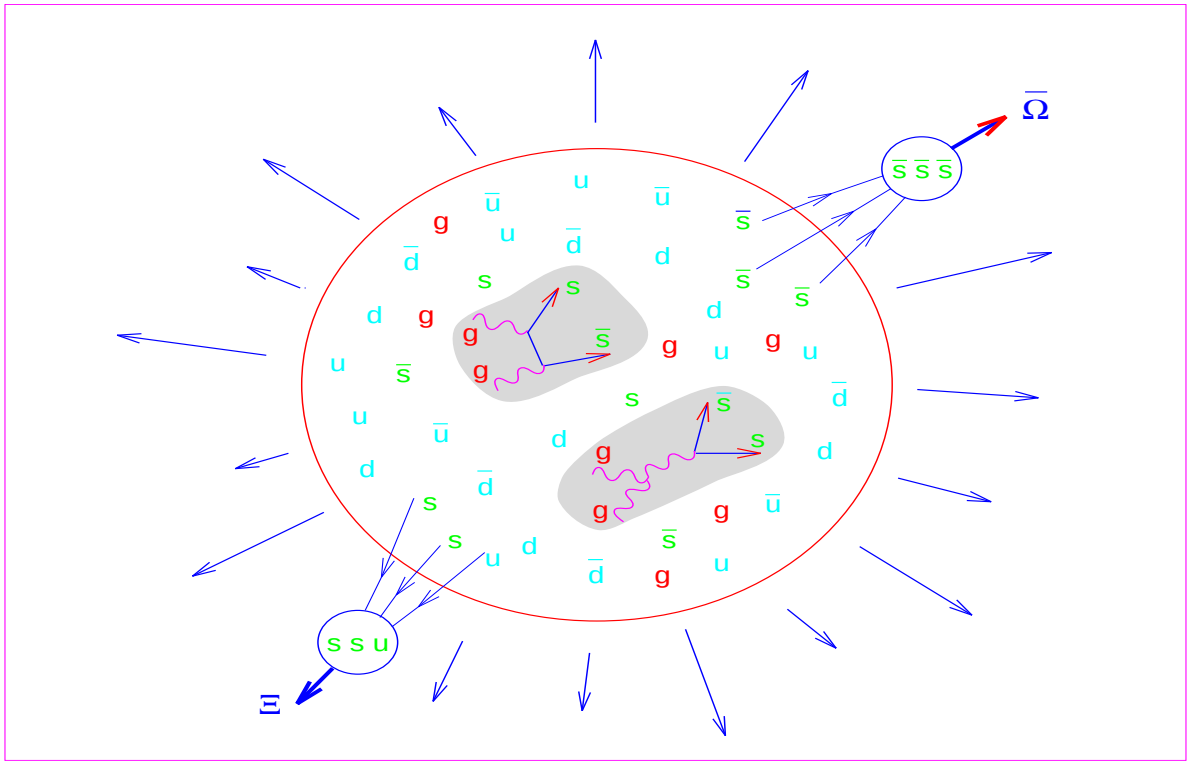

In quark-gluon plasma we have a reservoir of strange and anti-quarks. Hence formation of complex rarely produced multi strange (anti)particles possible which are difficult to make otherwise – requires 'cross talk' between quarks made in different microscopic reactions = deconfinement. We study strange antibaryons which have small background from direct N–N reactions.

THEORETICAL CONSIDERATIONS

- **production of strangeness in gluon fusion** $\boxed{GG \to s\bar{s}}$ **strangeness linked to gluons from QGP;**

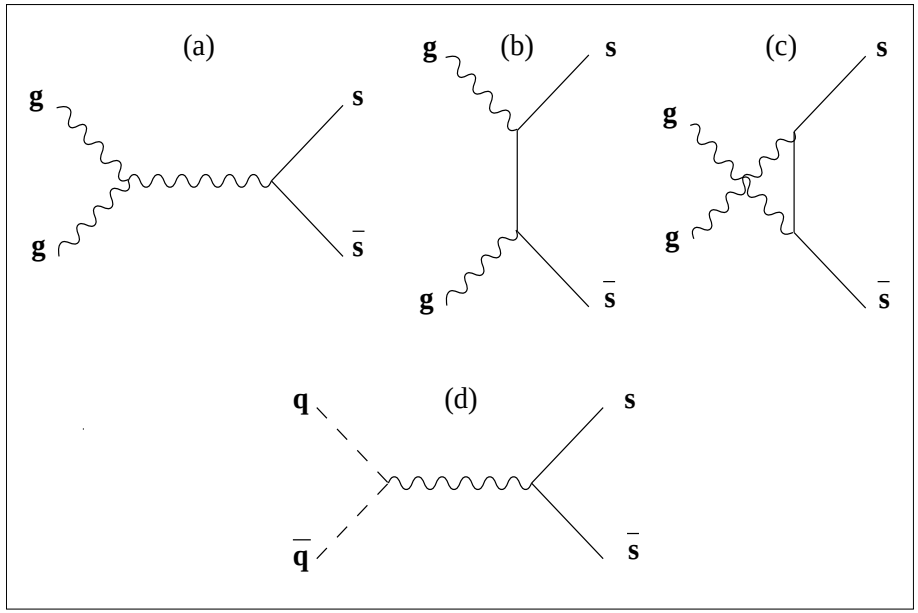

- **coincidence of scales:**

$$\boxed{m_s \simeq T_c} \to \boxed{\tau_s \simeq \tau_{\rm QGP}} \to$$

strangeness a clock for reaction

- **Often** $\boxed{\bar{s} > \bar{q}} \to$
strange antibaryon enhancement and
at RHIC also (anti)hyperon dominance of (anti)baryons.

Strangeness as Deconfinement Signatures

1. TOTAL Strangeness YIELD: s**strangeness/**b**baryon** **depends primarily on initial conditions and evolution dynamics**

(how long the system is at which T)

$\gamma_{\rm s}^{\rm QGP}$**: is QGP near chemical equilibrium?**

$$\gamma_{\rm s,q}^{\rm QGP} = \left.\frac{n_{\rm s,q}(t,T(t))}{n_{\rm s,q}(\infty,T(t))}\right|_{\rm QGP} \to 1?$$

---

2. Strangeness overpopulation at QGP BREAK-UP:

QGP phase space is squeezed into a smaller number of HG phase space cells: $\gamma_{\rm s}^{HG} \simeq 3\gamma_{\rm s}^{\rm QGP}$

---

3. TO BE SENSITIVE WE NEED ALSO TO CONSIDER $\gamma_q^{\rm HG} > 1$

over population of pion phase space is ENTROPY enhancement

---

4. STRANGENESS MOBILITY IN QGP IMPLIES

s–$\bar{s}$ **phase space symmetry, within baryon rich (SPS) environment**

IMPRINTED ON HADRONS AT HADRONIZATION

λ_s **= strange quark fugacity**

Kinetic description of strangeness production

The generic angle averaged cross sections for (heavy) flavor s, $\bar{s}$ production processes $g+g \to s+\bar{s}$ and $q+\bar{q} \to s+\bar{s}$, are:

$$\bar{\sigma}_{gg\to s\bar{s}}(s) = \frac{2\pi\alpha_{\rm s}^2}{3s}\left[\left(1+\frac{4m_{\rm s}^2}{s}+\frac{m_{\rm s}^4}{s^2}\right)\tanh^{-1}W(s) - \left(\frac{7}{8}+\frac{31m_{\rm s}^2}{8s}\right)W(s)\right],$$

$$\bar{\sigma}_{q\bar{q}\to s\bar{s}}(s) = \frac{8\pi\alpha_{\rm s}^2}{27s}\left(1+\frac{2m_{\rm s}^2}{s}\right)W(s). \qquad W(s)=\sqrt{1-4m_{\rm s}^2/s}$$

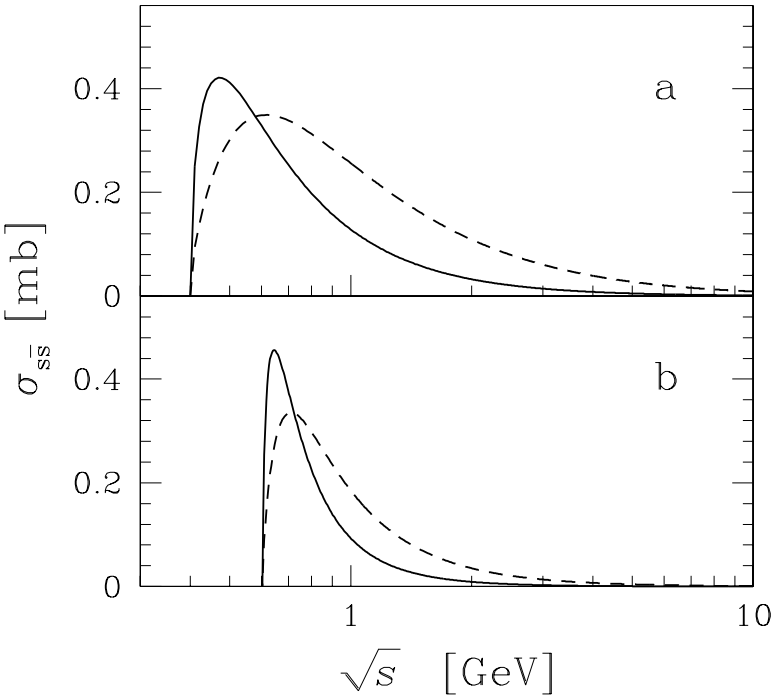

QGP Strangeness production cross sections:
Solid lines $q\bar{q} \to s\bar{s}$**; dashed lines** $gg \to s\bar{s}$**.**

a) TOP for fixed $\alpha_s = 0.6$**,** $m_{\rm s} = 200\,$**MeV;**
b) BOTTOM: for running $\alpha_s(\sqrt{s})$ **and** $m_{\rm s}(\sqrt{s})$**,**

with $\alpha_{s(M_Z)} = 0.118$**.** $m_s(M_Z) = 90 \pm 20\%$ **MeV,**
$m_s(1\,\mathbf{GeV}) \simeq 2.1 m_s(M_Z) \simeq 200\,\mathbf{MeV}$**.**

Thermal average of reactions

Kinetic (momentum) equilibration is faster than chemical, use thermal particle distributions $f(\vec{p}_1, T)$ to obtain average rate:

$$\langle \sigma v_{\rm rel} \rangle_T \equiv \frac{\int d^3p_1 \int d^3p_2 \sigma_{12} v_{12} f(\vec{p}_1, T) f(\vec{p}_2, T)}{\int d^3p_1 \int d^3p_2 f(\vec{p}_1, T) f(\vec{p}_2, T)} \,.$$

Invariant reaction rate in medium:

$$A^{gg\to s\bar{s}} = \frac{1}{2}\rho_g^2(t)\,\langle \sigma v\rangle_T^{gg\to s\bar{s}}\,, \quad A^{q\bar{q}\to s\bar{s}} = \rho_q(t)\rho_{\bar{q}}(t)\langle \sigma v\rangle_T^{q\bar{q}\to s\bar{s}}\,, \quad A^{s\bar{s}\to gg,q\bar{q}} = \rho_s(t)\,\rho_{\bar{\rm s}}(t)\,\langle \sigma v\rangle_T^{s\bar{s}\to gg,q\bar{q}}.$$

$1/(1+\delta_{1,2})$ introduced for two gluon processescompensates the double-counting of identical particle pairs, arising since we are summing independently both reacting particles.

This rate enters the momentum-integrated Boltzmann equation which can be written in form of current conservation with a source term

$$\partial_\mu j_s^\mu \equiv \frac{\partial \rho_s}{\partial t} + \frac{\partial \vec{v}\rho_s}{\partial \vec{x}} = A^{gg\to s\bar{s}} + A^{q\bar{q}\to s\bar{s}} - A^{s\bar{s}\to gg,q\bar{q}}$$

Strangeness density time evolution

in local restframe ($\vec{v}$) we have :

$$\frac{d\rho_s}{dt} = \frac{d\rho_{\bar{s}}}{dt} = \frac{1}{2}\rho_g^2(t)\,\langle\sigma v\rangle_T^{gg\to s\bar{s}} + \rho_q(t)\rho_{\bar{q}}(t)\langle\sigma v\rangle_T^{q\bar{q}\to s\bar{s}} - \rho_s(t)\,\rho_{\bar{s}}(t)\,\langle\sigma v\rangle_T^{s\bar{s}\to gg,q\bar{q}}$$

Evolution for s and $\bar{s}$ identical, which allows to set $\rho_s(t) = \rho_{\bar{s}}(t)$.
Use detailed balance to simplify

$$\frac{d\rho_s}{dt} = A\left(1 - \frac{\rho_s^2(t)}{\rho_s^2(\infty)}\right), \qquad A = A^{gg\to s\bar{s}} + A^{q\bar{q}\to s\bar{s}}$$

The generic solution at fixed T ($\rho \propto \tanh$) implies that in all general cases there is an exponential approach to chemical equilibrium

$$\frac{\rho_s(t)}{\rho_s^\infty} \to 1 - e^{-t/\tau_s}$$

with the characteristic time constant τ_s:

$$\tau_s \equiv \frac{1}{2}\frac{\rho_s(\infty)}{(A^{gg\to s\bar{s}} + A^{q\bar{q}\to s\bar{s}} + \ldots)}$$

$$A^{12\to 34} \equiv \frac{1}{1+\delta_{1,2}}\rho_1^\infty\rho_2^\infty\langle\sigma_s v_{12}\rangle_T^{12\to 34}\,.$$

Characteristic time constant and γ_s-evolution

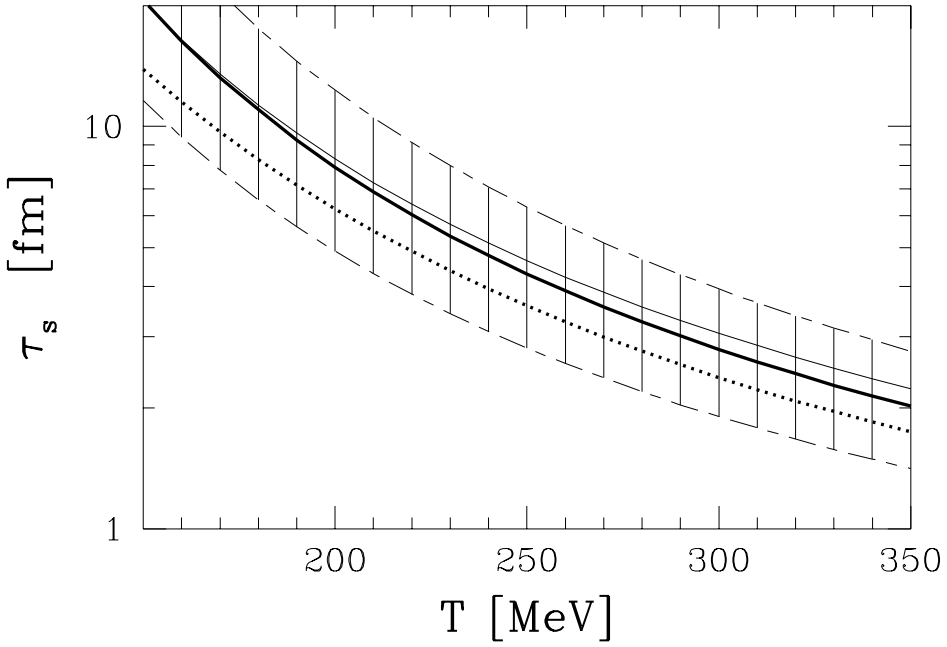

$\sigma^{\to s\bar{s}}_{\rm QCD}$ **gives** τ_s **similar to lifespan of the plasma phase!**
Strange quark pair production dominated by gluon fusion: $G+G\to s\bar{s}$**, also some (10%)** $q\bar{q}\to s\bar{s}$**, present; this is due to gluon collision rate.**
ENTROPY CONSERVING expansion i.e. at SPS T^3V **=Const. (not yet long. scaling):**

$$2\tau_s\frac{dT}{dt}\left(\frac{d\gamma_s}{dT}+\frac{\gamma_s}{T}z\frac{K_1(z)}{K_2(z)}\right)=1-{\gamma_s}^2\,,\quad \gamma_s(t)\equiv n_s(t)/n_s^\infty\,,\quad z=\frac{m_s}{T}\,,\quad K_i:\text{Besself.}$$

Once γ_s **known,** $\langle\rho_s(t)\rangle=\langle\bar{\rho}_s(t)\rangle=\int dx^3\rho_s^\infty(T(t,x))\gamma_s(T(t,x),\dot{T}(t,x))$;
evolution till $t\to t_f$**,but effectively production stops for** $T<180$ **MeV.**

What about charm? $m_s \to m_c$

We expect that thermal charm production is of relevance only for $T \to m_c(1\,\mathbf{GeV}) \simeq 1.5\,\mathbf{GeV}$, probably not accessible.

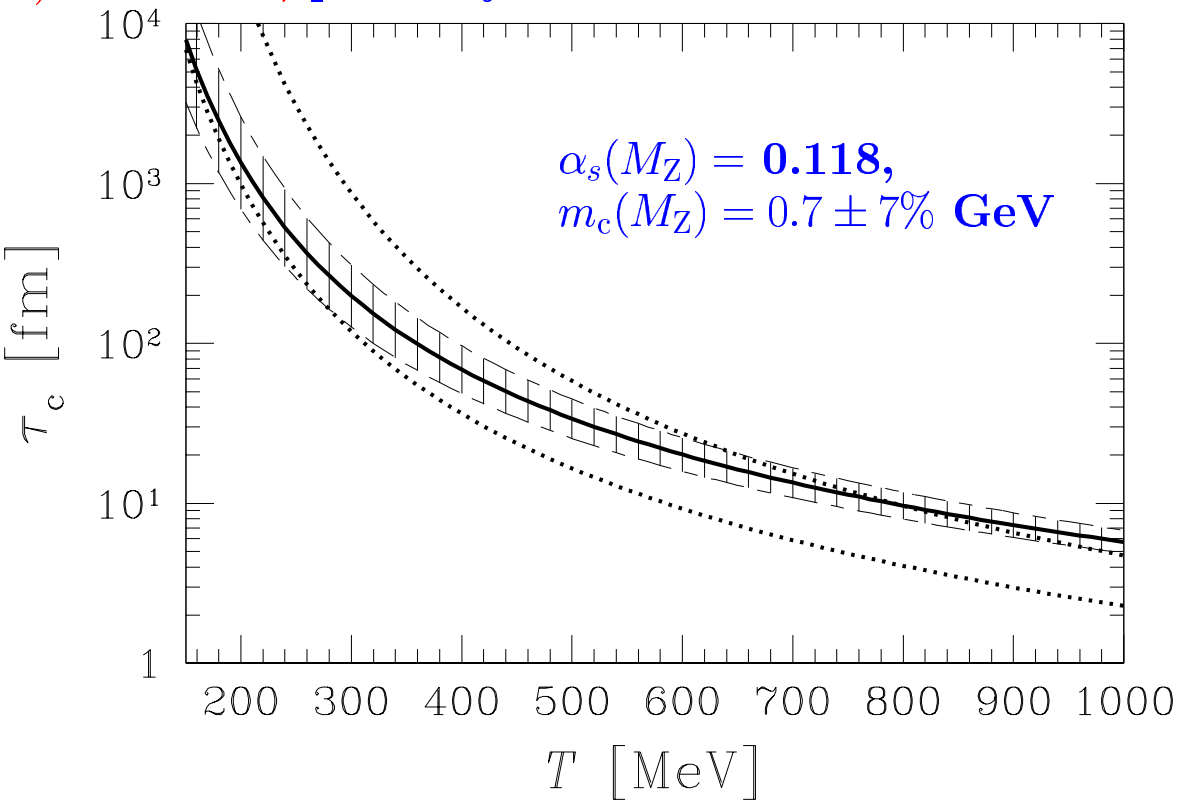

Lower dotted line: for fixed $m_c = 0.9\,\mathbf{GeV}$, $\alpha_s = 0.35$;
upper doted line: for fixed $m_c = 1.5\,\mathbf{GeV}$, $\alpha_s = 0.4$.
Equilibrium density for $\rho_c^\infty(m_c \simeq 1.5\,\mathbf{GeV})$.

Charm is produced relatively abundantly in first parton collisions. Benchmark: 10 $c\bar{c}$ pairs in central Au–Au at RHIC-200. This yield is greater than the expected equilibrium yield at hadronization of QGP.

EXPECTED STRANGENESS YIELD IN QGP and $\gamma_{\rm s}^{\rm QGP}/\gamma_{\rm q}^{\rm QGP}$

$$\frac{\rho_{\rm s}}{\rho_{\rm b}}=\frac{s}{q/3}=\frac{\gamma_{\rm s}^{\rm QGP}\frac{3}{\pi^2}T^3(m_{\rm s}/T)^2K_2(m_{\rm s}/T)}{\gamma_{\rm q}^{\rm QGP}\frac{2}{3}\left(\mu_{\rm q}T^2+\mu_{\rm q}^3/\pi^2\right)},\rightarrow\frac{s}{b}\simeq\frac{\gamma_{\rm s}^{\rm QGP}}{\gamma_{\rm q}^{\rm QGP}}\frac{0.7}{\ln\lambda_{\rm q}+(\ln\lambda_{\rm q})^3/\pi^2}.$$

assumption: $\mathcal{O}(\alpha_s)$ **interaction effects cancel out between** b,s

We consider $m_{\rm s}=200$ **MeV and hadronization** $T=150$ **MeV,**

.

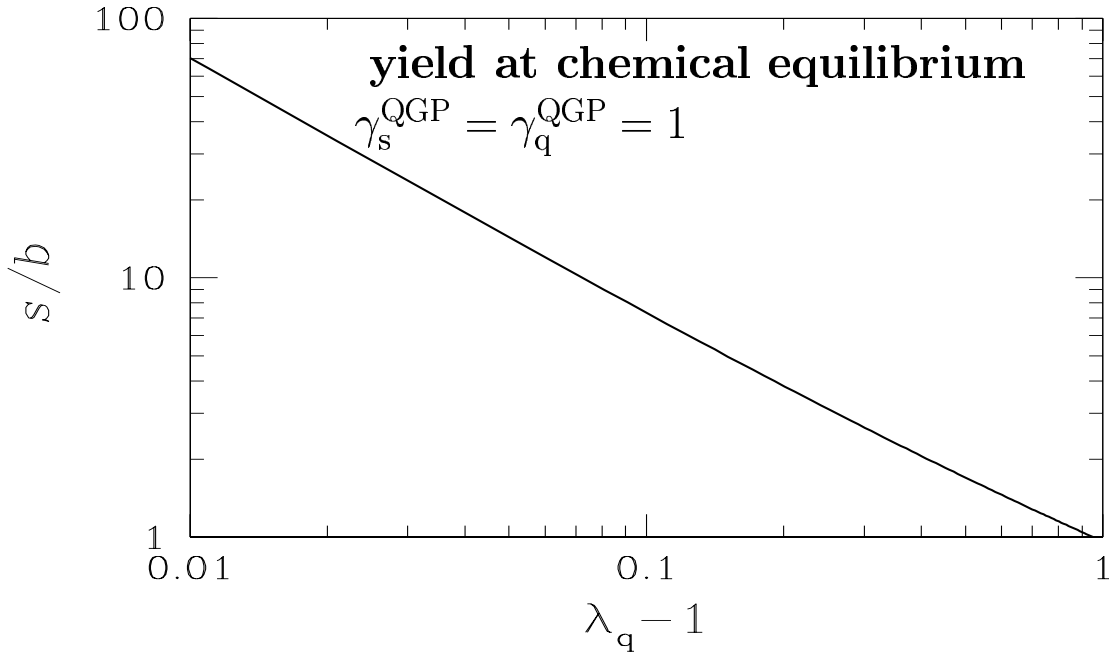

We read off:

for SPS with λ_q**=1.5–1.6, expect** $s/b\simeq 1.5$**, observe 0.7–0.8 i.e. 50% saturation**

for RHIC-130 with λ_q**=1.08–1.09, expect** $s/b\simeq 9$ **as observed, nearly full chemical equilibrium in QGP (oversaturation in HG)**

Retrospective: Strangeness Discoveries

MULTISTRANGE HYPERON ENHANCEMENT

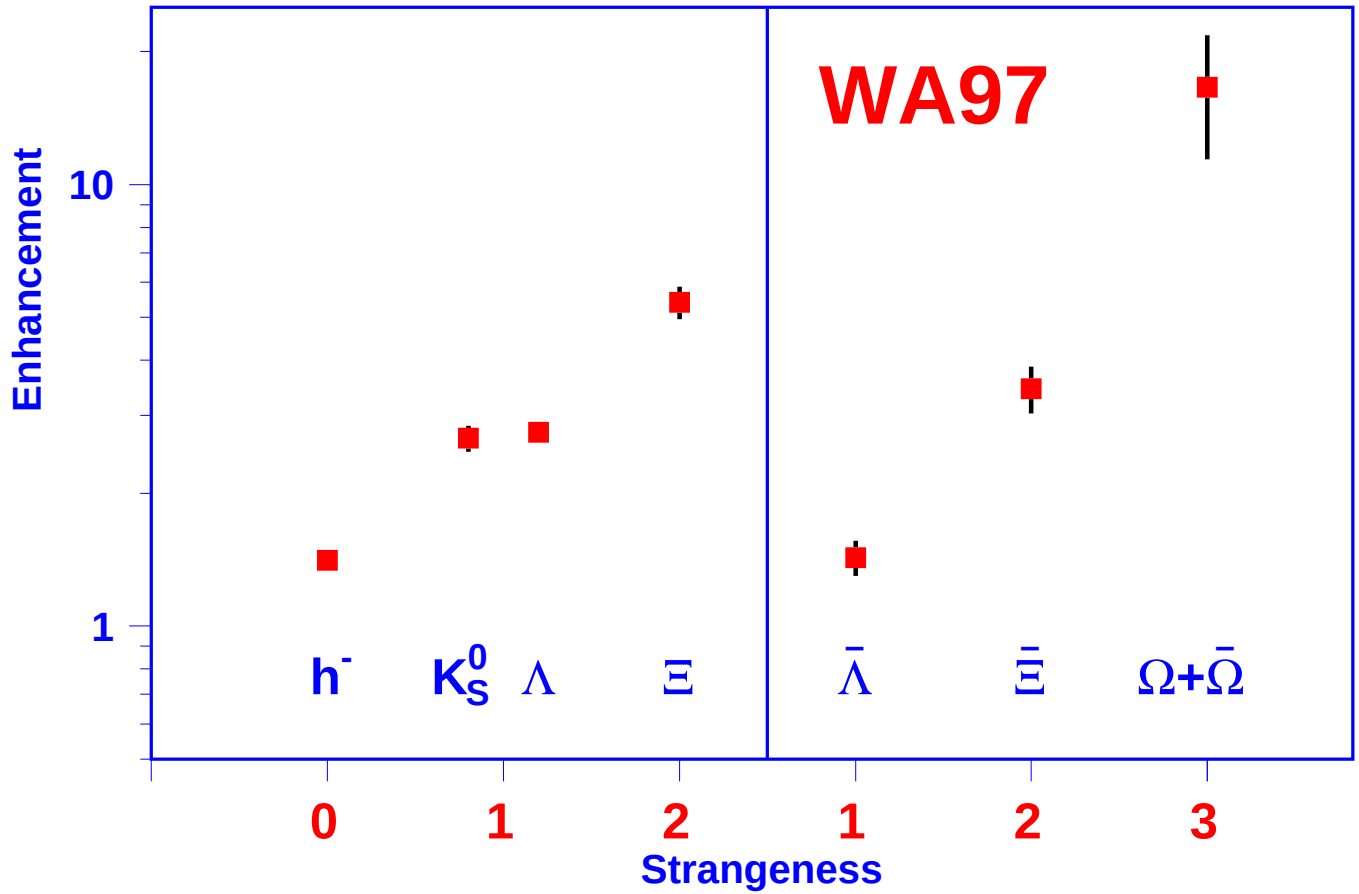

Results of WA97/NA57 collaboration. Enhancement GROWS with a) strangeness b) antiquark content as predicted. Enhancement is defined with respect toyield in p–Be collisions, scaled up with the number of 'wounded' nucleons.

Antibaryon excess at central CM rapidity

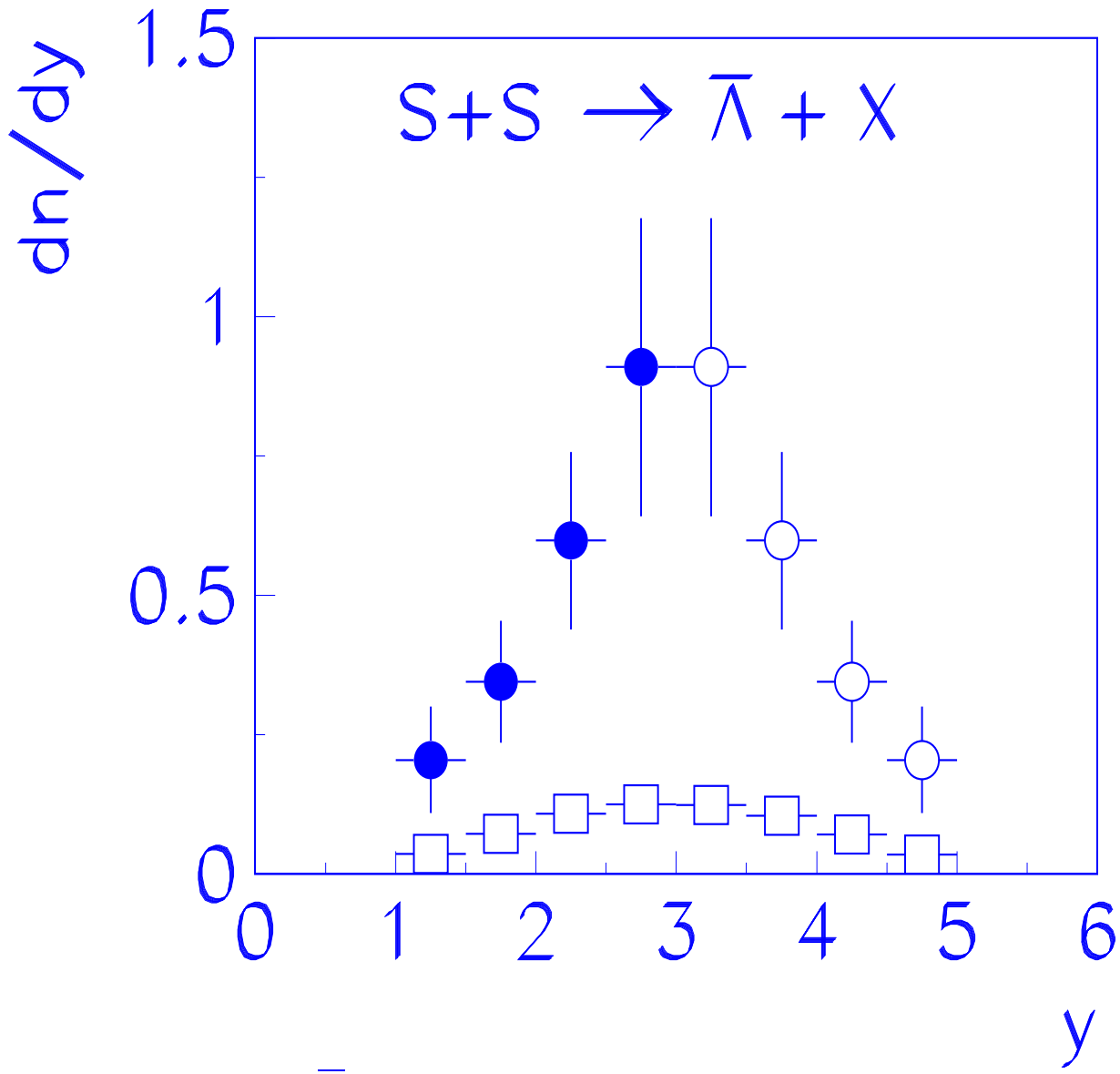

NA35II EXCESS $\bar{\Lambda}$ emitted from a central well localized source.
Background (squares) from multiplicity scaled NN reactions

MORE EFFECTIVE CONVERSION OF ENERGY INTO STRANGE MATTER

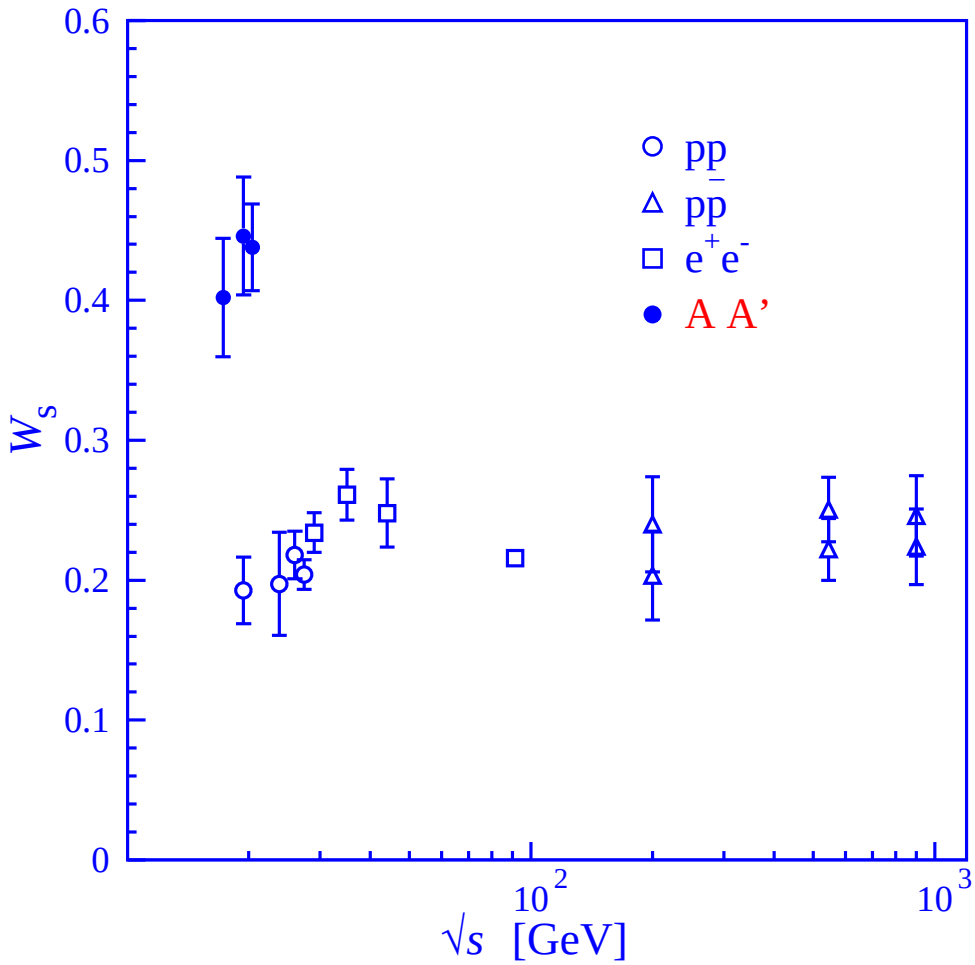

Enhancement of strangeness pair production compared to light quarks due to onset of thermal glue fusion processes – seen most clearly in Wróblewski ratio in which only newly made s- and q-pairs are counted:

$$W = \frac{2\langle s\bar{s}\rangle}{\langle d\bar{d} + u\bar{u}\rangle}$$

High $m_\perp$ slope universality

Discovered in S-induced collisions, very pronounced in Pb-Pb Interactions.

Why is the slope of baryons and antibaryons precisely the same?

Why is the slope of different particles in same m_t range the same?

Analysis+Hypothesis 1991: QGP quarks coalescing in SUDDEN hadronization

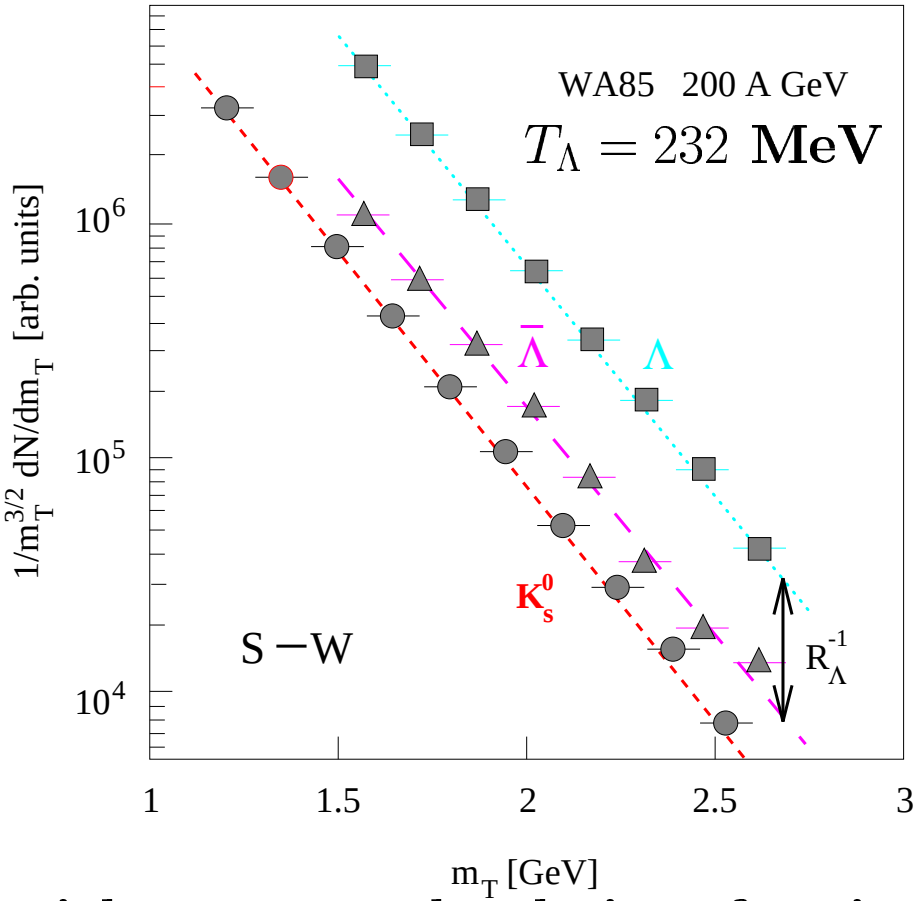

This allows to study ratios of particles measured only in a fraction of phase space

WA97	$T_\perp^{\rm Pb}$ [MeV]
$T^{\rm K^0}$	230 ± 2
T^{Λ}	289 ± 3
$T^{\overline{\Lambda}}$	287 ± 4
T^{Ξ}	286 ± 9
$T^{\overline{\Xi}}$	284 ± 17
$T^{\Omega+\overline{\Omega}}$	251 ± 19

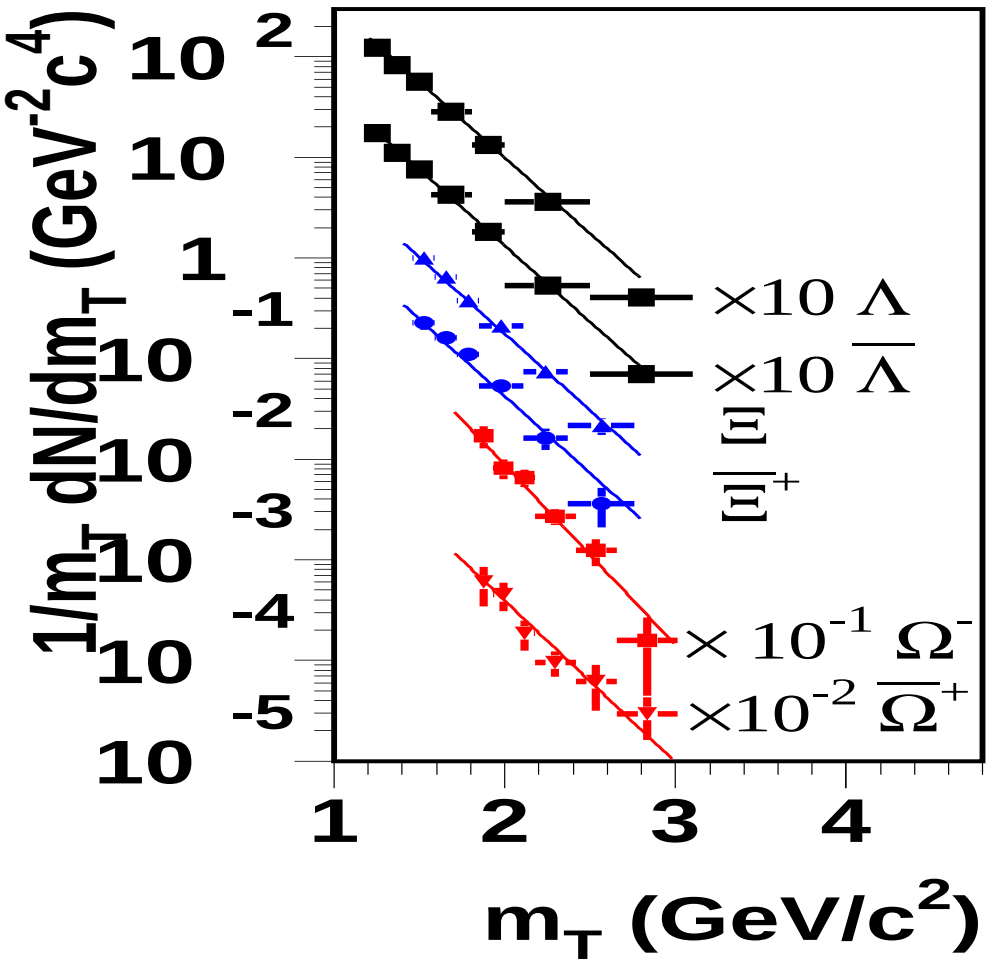

Λ within 1% of $\overline{\Lambda}$

Kaon – hyperon difference:
EXPLOSIVE FLOW effect
Difference between $\Omega + \overline{\Omega}$:
presence of an excess of low $p_\perp$ particles
we will return to study this in spectral analysis

FIRST (XI-)RESULTS FROM RHIC:

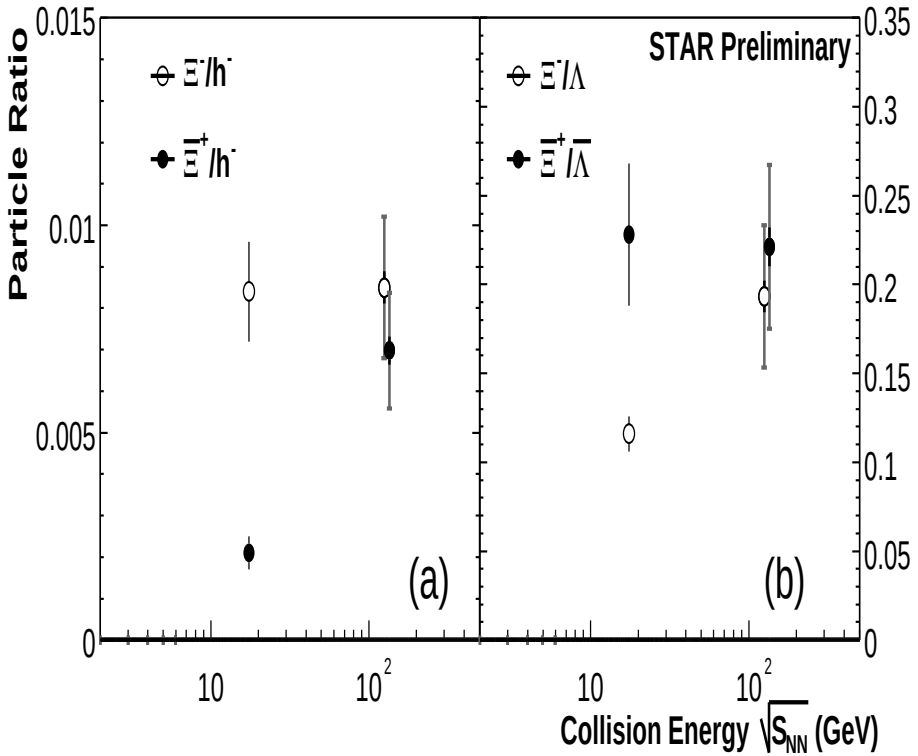

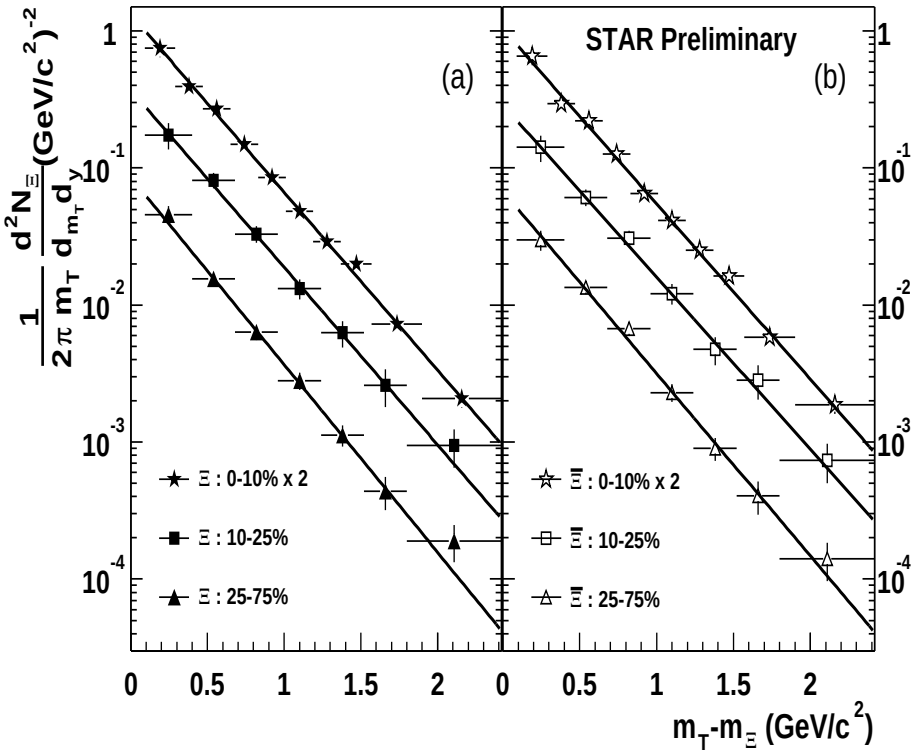

PARTICLE SLOPES IMPLY SUDDEN HADRONIZATION

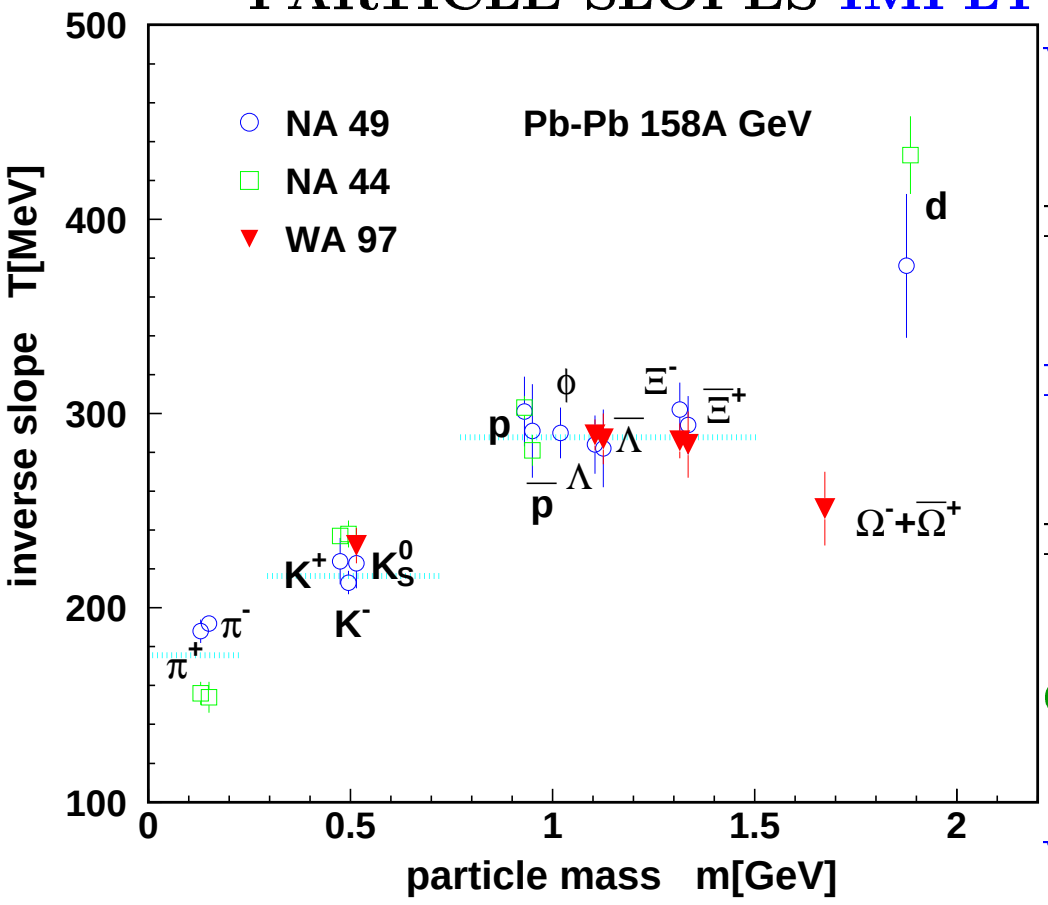

Why are the slopes rising in value?
→ **EXPLOSIVE FLOW** $v > 0.5c$

Figure reflects similar range p_T thus a very different m_T range

Diff. mass HYPERONS: SLOPES include resonance decays

Deuterons from final state interactions, disregard!

Omegas remain enigmatic and thus most interesting

Why is slope of baryons and antibaryons precisely the same?

EVAPORATION: inverse slope T related to $T_{\rm tf}$ the intrinsic temperature of the source which explodes with local flow velocity $v_{\rm tf}$:

$$T \simeq \frac{1+\vec{n}\cdot\vec{v}_{\rm tf}}{\sqrt{1-\vec{v}_{\rm tf}^2}}T_{\rm tf} \to \sqrt{\frac{1+v_{\rm tf}}{1-v_{\rm tf}}}T_{\rm tf}.$$

Caution – does not apply in the same fashion to all particles, precision rarely better than ±10%.

QGP PHASE $\Longrightarrow$ HADRON PHASE SPACE

EXPERIMENTAL SIGNATURE: Symmetry in $m_\perp$ spectra of strange baryons with antibaryons $\rightarrow$ production ('evaporation') into vacuum by a common (deconfined) source.

No hadronic 'phase'!
No 'mixed phase' either!
Direct emission of free-streaming hadrons from exploding QGP

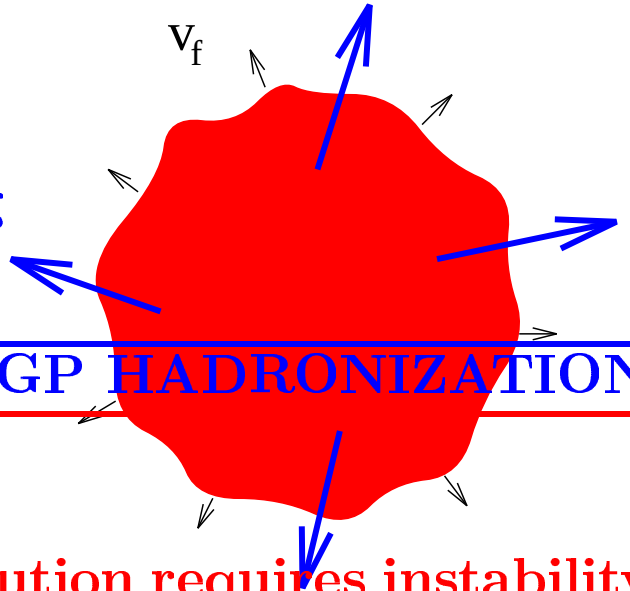

Orient analysis toward SUDDEN QGP HADRONIZATION reaction

NO slow transformation
contradiction to experiment – resolution requires instability in time evolution which leads $\rightarrow$ phase NONEQUILIBRIUM

Primary hypothesis of STATISTICAL HADRONIZATION

We assume that within a 'family', particle yields with same valance quark content are thermally equilibrated, e.g. the relative yield of $\Delta(1230)$ and N completely controlled by the ratio m/T:

$$\frac{n_\Delta}{n_N} = \frac{g_\Delta (m_\Delta T)^{3/2} e^{-m_\Delta/T}}{g_N (m_N T)^{3/2} e^{-m_N/T}}$$

Resonances often as important as gound state in counting of produced particles. Yields of particles are obtained summing over all resonances (recall Hagedorn's exponentially growing spectrum!) and compared with experiment in order to check if in principle this approach is valid.

OBJECTIVE: Physical properties of the source at hadronization
NEED the phase space of hadronic particles in great precision.
REFINED FERMI HADRONIZATION MODEL

$T_{\rm f}$	Local rest frame chemical freeze-out temperature
v_h,$v_{\rm f}$	Hadronization, Local flow speed of emitting source
$\lambda_{\rm s}$, $\lambda_{\rm q}$	Chemical fugacities describe conserved quantum number
$\gamma_{\rm s}$, $\gamma_{\rm q}$	Phase space occupancies describe quark pair yield

We imply that locally thermal equilibrium can be established.
However, chemical equilibrium is NOT assumed in complete way

HOW DOES THE MODEL WORK?

PARTICLE ABUNDANCES

$$\pi(q\bar{q}) \sim \gamma_q^2 \qquad N(qqq) \sim \gamma_q^3\lambda_q^3; \qquad \overline{N}(\bar{q}\bar{q}\bar{q}) \sim \gamma_q^3\lambda_q^{-3}$$

QUANTUM STATISTICS

$$\frac{N_\pi}{V} = g_\pi \int \frac{d^3p}{(2\pi)^3} \frac{1}{\gamma_q^{-2} e^{\sqrt{m_\pi^2+p^2}/T} - 1}, \qquad \gamma_q^2 < e^{m_\pi/T} \simeq (1.6)^2$$

$$\frac{N}{V} = g_N \int \frac{d^3p}{(2\pi)^3} \frac{1}{1+\gamma_q^{-3}\lambda_q^{-3}e^{E/T}} \qquad \frac{\overline{N}}{V} = g_N \int \frac{d^3p}{(2\pi)^3} \frac{1}{1+\gamma_q^{-3}\lambda_q^{+3}e^{E/T}}$$

$$\mu_N^{\rm eff} = 3T(\ln\lambda_q + \ln\gamma_q); \qquad \mu_{\overline{N}}^{\rm eff} = -3T(\ln\lambda_q - \ln\gamma_q)$$

The thermal emitted particles production yield dN_i within the time dt from a locally at rest surface element dS:

$$dN_i = \frac{dSd^3p}{(2\pi)^3} A_i v_i dt\,.$$

$v_i = dz/dt$ is the particle velocity normal to the surface element dS.

In a thermal quark-gluon source, phase space factor A_i is:

$$A_i = g_i\lambda_i\gamma_i e^{-E_i/T}\,, \qquad \lambda_i = \prod_{j\in i}\lambda_j\,, \quad \gamma_i = \prod_{j\in i}\gamma_j\,, \quad E_i = \sum_{j\in i} E_j\,,$$

in Boltzmann limit

$$R_\Lambda = \left.\frac{\overline{\Lambda}}{\Lambda}\right|_{m_\perp} = \frac{\overline{\Lambda}+\overline{\Sigma}^0+\overline{\Sigma}^*+\cdots}{\Lambda+\Sigma^0+\Sigma^*+\cdots} = \frac{\bar{s}\bar{q}\bar{q}}{sqq} = \lambda_{\rm s}^{-2}\lambda_{\rm q}^{-4} = e^{2\mu_{\rm S}/T}e^{-2\mu_b/T}\,.$$

$$R_\Xi = \left.\frac{\overline{\Xi^-}}{\Xi^-}\right|_{m_\perp} = \frac{\overline{\Xi^-}+\overline{\Xi^*}+\cdots}{\Xi^-+\Xi^*+\cdots} = \frac{\bar{s}\bar{s}\bar{q}}{ssq} = \lambda_{\rm s}^{-4}\lambda_{\rm q}^{-2} = e^{4\mu_{\rm S}/T}e^{-2\mu_b/T}\,.$$

This ratio is reliable, there is practically nothing that can influence it, constrains chemical potentials/fugacities strongly.

$$\left.\frac{\Xi^-(dss)}{\Lambda(dds)}\right|_{m_\perp} = \frac{g_\Xi\gamma_d\gamma_s^2\lambda_d\lambda_s^2}{g_\Lambda\gamma_d^2\gamma_s\lambda_d^2\lambda_s}\,.$$

g_i **are the spin statistical factors of the states considered.**

Judicial choice of compatible particle ratios reduces dependence on EXPLOSIVE flow,

For full phase space flow does not influence the observed yields. We allow fro flow in numerical studies

WHAT DO WE KNOW ABOUT PARAMETERS?

Assume exploding QGP-phase

1. **For given E/b, Equation of State relates the 5 parameters of state:**

   $$T_f,\ \lambda_q,\ \gamma_q,\ \lambda_s,\ \gamma_s$$

2. **Kinetic theory of strangeness production relates:**

   $$v_f,\ T_f \text{ and } \gamma_s$$

3. **Strangeness conservation in the source:**

   $$\langle s-\overline{s}\rangle = 0 \longrightarrow \lambda_s(T,\lambda_q;\gamma_s)$$

   for QGP: in S–Pb and at RHIC $\lambda_s = 1$

4. **Entropy/Baryon in source (QGP) $\leq$ in Final hadron** $\longrightarrow$ $\gamma_q \simeq 1.6$

   Explain below, also: Glue $\rightarrow q\bar{q}$ **adds quark pairs**

5. **Flow dynamics (e.g. Hydrodynamic): for bulk of matter** $v_f \simeq 1/\sqrt{(3)}$

WHY $\gamma_q \simeq 1.6$? **A striking feature of the data analysis is the maximization of entropy density in pion gas.** $E_\pi = \sqrt{m_\pi^2 + p^2}$

$$S_{\rm B,F} = \int \frac{d^3p\, d^3x}{(2\pi\hbar)^3} \left[\pm(1\pm f)\ln(1\pm f) - f\ln f\right], \qquad f_\pi(E) = \frac{1}{\gamma_q^{-2} e^{E_\pi/T} - 1}.$$

Pion gas properties: N**-particle,** E**-energy,** S**-entropy,** V**-volume as function of** γ_q**.**

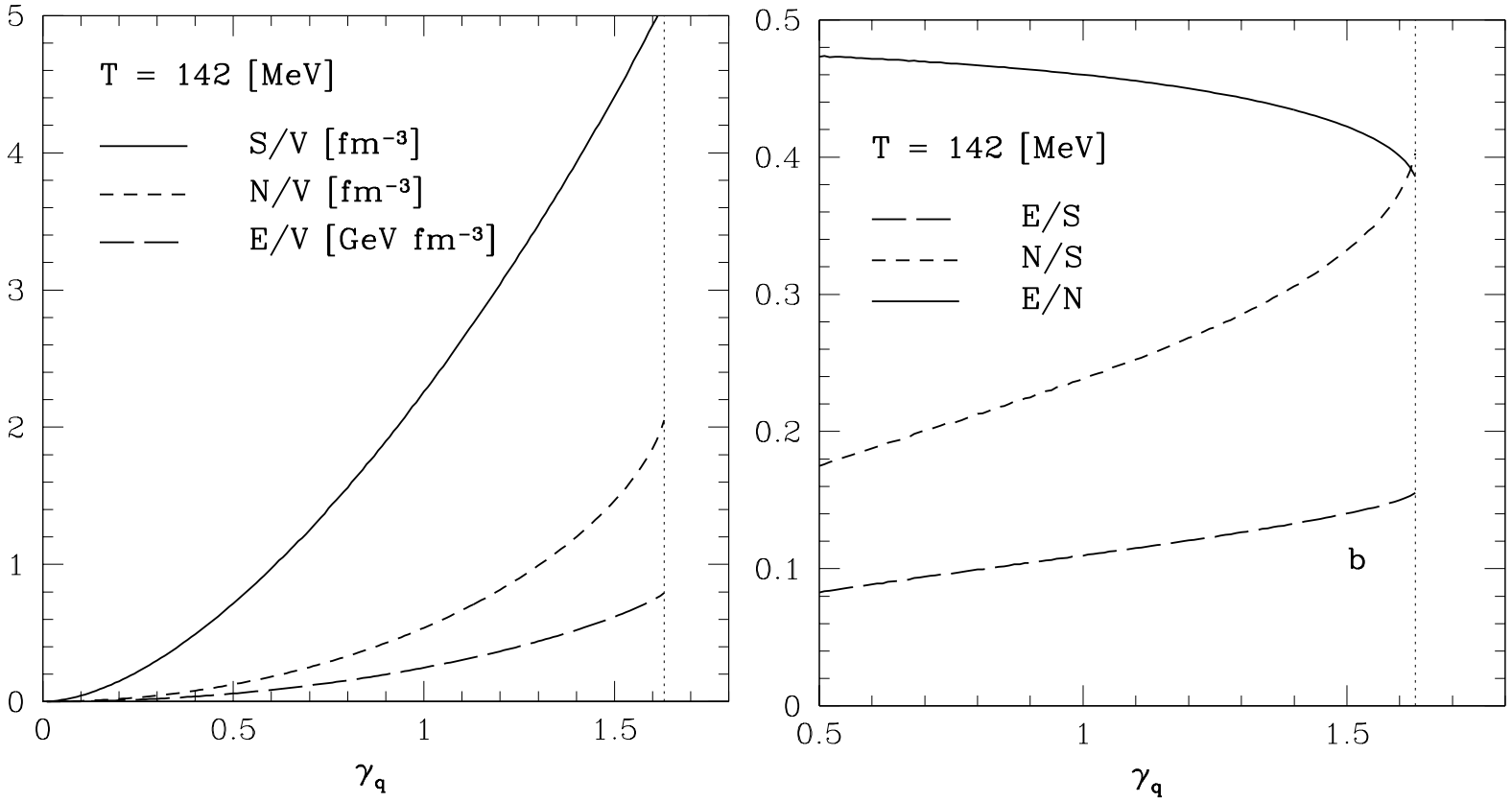

CONCLUSION: excess of QGP entropy pumped into pions

EXAMPLE: Pb–Pb ANALYSIS Fermi-2000 Model

Pb–Pb 158A GeV WA97 (top) and NA49 (bottom) S'2000 revised data

References

[1] **I. Králik, WA97,** *Nucl. Phys.* **A 638,115, (1998).**

[2] **G.J. Odyniec, NA49,** *J. Phys.* **G 23, 1827 (1997).**

[3] **F. Pühlhofer, NA49,** *Nucl. Phys.* **A 638, 431,(1998).**

[4] **C. Bormann, NA49,** *J. Phys.* **G 23, 1817 (1997).**

[5] **S.V. Afanasiev, NA49,** *Phys. Lett.* **B 491 59 (2000).**

[6] **G.J. Odyniec,** *Nucl. Phys.* **A 638, 135, (1998).**

[7] **D. Röhrig, NA49, in EPS-HEP Conf. Jerusalem, Aug. 1997.**

[8] **P.G. Jones, NA49,** *Nucl. Phys.* **A 610, 188c (1996).**

[9] **H. Appelshäuser** *et al.*, **NA49,** *Phys. Rev. Lett.* **82, 2471 (1999).**

Ratios	Ref.	Exp. Data	$\mathrm{Pb}\vert_v^{\mathrm{S},\gamma_q}$	$\mathrm{Pb}\vert_v^{\gamma_q}$
Ξ/Λ	[1]	0.099 ± 0.008	0.098	0.096
$\bar{\Xi}/\bar{\Lambda}$	[1]	0.203 ± 0.024	0.199	0.201
$\bar{\Lambda}/\Lambda$	[1]	0.124 ± 0.013	0.122	0.121
$\bar{\Xi}/\Xi$	[1]	0.255 ± 0.025	0.248	0.253
$\frac{(\Xi+\bar{\Xi})}{(\Lambda+\bar{\Lambda})}$	[2]	0.13 ± 0.03	0.111	0.110
~~K_s^0/ϕ~~	~~[3]~~	~~11.9 ± 1.5~~	13.0	13.4
ϕ/π^-	[5]	0.0125 ± 0.0018	0.0127	0.0124
K^+/K^-	[4]	1.80 ± 0.10	1.757	1.790
$p/\bar{p}$	[6]	$18.1 \pm 4.$	16.00	16.50
~~$\bar{\Lambda}/\bar{p}$~~	~~[7]~~	~~$3. \pm 1.$~~	0.53	0.54
K^-/π^-		0.082 ± 0.012	0.81	0.080
K_s^0/B	[8]	0.183 ± 0.027	0.188	0.192
h^-/B	[9]	1.97 ± 0.1	1.782	1.829
χ^2_{T}			2.25	1.36
$N;p;r$			10;3;2	10;4;2
$\chi^2_{\mathrm{T}}/\mathrm{dof}$	LESS	than	0.25	0.15

Chemical and Physical Properties for Pb–Pb (S'2000 data) and for S–Au/W/Pb

	$\mathbf{Pb}\vert_v^{\mathrm{s},\gamma_q}$	$\mathbf{Pb}\vert_v^{\gamma_q}$	$\mathbf{S}\vert_v$
$\chi^2_{\mathrm{T}};\ N;p;r$	**1.48; 11; 3; 2**	**0.76; 11; 4; 2**	**6.2; 16; 6; 6**
T_f [MeV]	151 ± 3	147 ± 5.5	144 ± 2
v_c	0.57 ± 0.05	0.52 ± 0.09	0.49 ± 0.02
λ_q	1.618 ± 0.026	1.625 ± 0.025	1.51 ± 0.02
λ_s	1.101^*	1.093 ± 0.02	1.00 ± 0.02
γ_q	$\gamma_q^{c*} = e^{m_\pi/2T_f}$=1.59	$\gamma_q^{c*} = e^{m_\pi/2T_f}$=1.62	1.41 ± 0.08
γ_s/γ_q	1.04 ± 0.05	1.05 ± 0.06	0.69 ± 0.03
E_f^{in}/S_f	0.163 ± 0.01	0.158 ± 0.01	0.186 ± 0.01
s_f/b	0.68 ± 0.05	0.69 ± 0.05	0.73 ± 0.05
$(\bar{s}_f - s_f)/b$	0^*	0.05 ± 0.05	0.17 ± 0.05

Fireball Properties and Parameters of Fits to RHIC-130 results

	100% $\Xi \to Y$ 40% $Y \to N$	40% $\Xi \to Y$ 40% $Y \to N$	40% $\Xi \to Y$ 40% $Y \to N$
T	140.1 ± 1.1	142.3 ± 1.2	164.3 ± 2.2
$\gamma_q^{\rm HG}$	1.64*	1.63*	1*
λ_q	1.070 ± 0.008	1.0685 ± 0.008	1.065 ± 0.008
μ_b [MeV]	28.4	28.3	31.0
$\gamma_s^{\rm HG}/\gamma_q^{\rm HG}$	1.54 ± 0.04	1.54 ± 0.0.04	1*
λ_s	1.0136*	1.0216*	1.0196*
$\mu_{\rm S}$ [MeV]	6.1	6.4	7.1
s/b	9.75	9.7	7.2
E/b [GeV]	35.0	34.6	34.8
S/b	234.8	230.5	245.7
E/S [MeV]	148.9	150.9	141.5
χ^2/dof	7.1/(19 − 3)	19/(19 − 3)	177.2/(19 − 2)

VERY large χ^2 originates in the inability to account for ratios of baryons and antibaryons for the chemical equilibrium assumption.

Specific strangeness content 9 times greater than at SPS.

Fireball energy content: internal thermal energy content $E/b \simeq 35$ GeV is 7+ times greater compared to top SPS result.

Laboratory energy contains kinetic energy associated with longitudinal and transverse flow of fireball matter. The energy of each particle is 'boosted' with the factor $\gamma_\perp^v \cosh y_\parallel$. Longitudinal flow $\Delta y = \pm 1.9$ (PHOBOS), on average we get $\int dy_\parallel \cosh y_\parallel / \int dy_\parallel \to \sinh(1.92)/1.9 = 1.7$. The transverse flow estimated with with $v_\perp = c/\sqrt{3} \to \gamma_\perp^v = 1.2$.

$$\gamma_\perp^v \langle \cosh y_\parallel \rangle = 2 \simeq \frac{65\,\mathbf{GeV}}{35\,\mathbf{GeV}}\,.$$

Richness of experimental results is still increasing....

	Data	100% $\Xi \to Y$ 40% $Y \to N$	40% $\Xi \to Y$ 40% $Y \to N$	40% $\Xi \to Y$ 40% $Y \to N$
$\bar{p}/p$	0.71 ± 0.06	0.672(0.4)	0.678(0.3)	0.689(0.1)
$\overline{\Lambda}_\Xi/\Lambda_\Xi$	0.71 ± 0.04	0.759(1.0)	0.748(0.9)	0.757(1.4)
$\overline{\Xi}/\Xi$	0.83 ± 0.08	0.794(0.2)	0.804(0.1)	0.816(0.0)
K^-/K^+	0.87 ± 0.07	0.925(0.6)	0.924(0.6)	0.934(0.8)
$K^-/\pi^\pm$	0.15 ± 0.02†	0.159(0.2)	0.161(0.3)	0.150(0.0)
$K^+/\pi^\pm$	0.17 ± 0.02†	0.172(0.0)	0.174(0.1)	0.161(0.2)
Λ_Ξ/h^-	0.059 ± 0.004†	0.057(0.3)	0.050(5.1)	0.045(11.9)
$\overline{\Lambda}_\Xi/h^-$	0.042 ± 0.004†	0.043(0.0)	0.037(1.3)	0.034(3.8)
Λ_Ξ/p	0.90 ± 0.12	0.832(0.3)	0.691(3.0)	0.491(11.6)
$\overline{\Lambda}_\Xi/\bar{p}$	0.93 ± 0.19	0.929(0.0)	0.763(0.8)	0.539(4.2)
$\pi^\pm/p_\Lambda$	9.5 ± 2	9.4(0.0)	9.2(0.5)	7.6(22.8)
$\pi^\pm/\bar{p}_\Lambda$	13.4 ± 2.5	13.7(0.1)	13.4(0.0)	10.9(7.9)
Ξ^-/π	0.0088±0.0008†	0.0096(1.0)	0.0103(3.6)	0.0067(7.1)
Ξ^-/h^-	0.0085±0.0015	0.0079(0.1)	0.0084(0.0)	0.0054(4.3)
$\overline{\Xi^-}/h^-$	0.0070±0.001	0.0063(0.5)	0.0068(0.1)	0.0044(6.7)
Ξ^-/Λ	0.193±0.009	0.195(0.1)	0.196(0.1)	0.132(45.2)
$\overline{\Xi^-}/\overline{\Lambda}$	0.221±0.011	0.213(0.6)	0.214(0.4)	0.144(48.7)
Ω/Ξ^-		0.205	0.21	0.18
$\overline{\Omega}/\overline{\Xi^-}$		0.22	0.23	0.20
$\overline{\Omega}/\Omega$	0.95±0.1	0.87(0.7)	0.88(0.5)	0.89(0.4)
$\bar{p}/h^-$		0.046	0.049	0.063
ϕ/K^-	0.15±0.03	0.178(0.9)	0.185(1.3)	0.146(0.0)
χ^2/dof		7.1/(19 − 3)	19/(19 − 3)	177.2/(19 − 2)

Fits of central-rapidity hadron ratios at $\sqrt{s_{\rm NN}} = 130$ GeV.

Columns: ratio considered, data value with reference, the non-equilibrium fit with 100% $\Xi \to Y$ cascading ($f_\Xi = 1$) and 40% $Y \to N$ ($f_\Lambda = 0.4$), the non-equilibrium fit with 40% $\Xi \to Y$ and 40% $Y \to N$, and in the last column, the chemical equilibrium fit with 40% cascading . The superscript * indicates quantities fixed by constrains and related considerations. The superscript † indicates the error is dominated by theoretical considerations. Subscripts Ξ, Λ mean that these values include weak cascading. In parenthesis we show the contribution of the particular result to the total χ^2.

Absolute Chemical Equilibrium EXCLUDED at RHIC

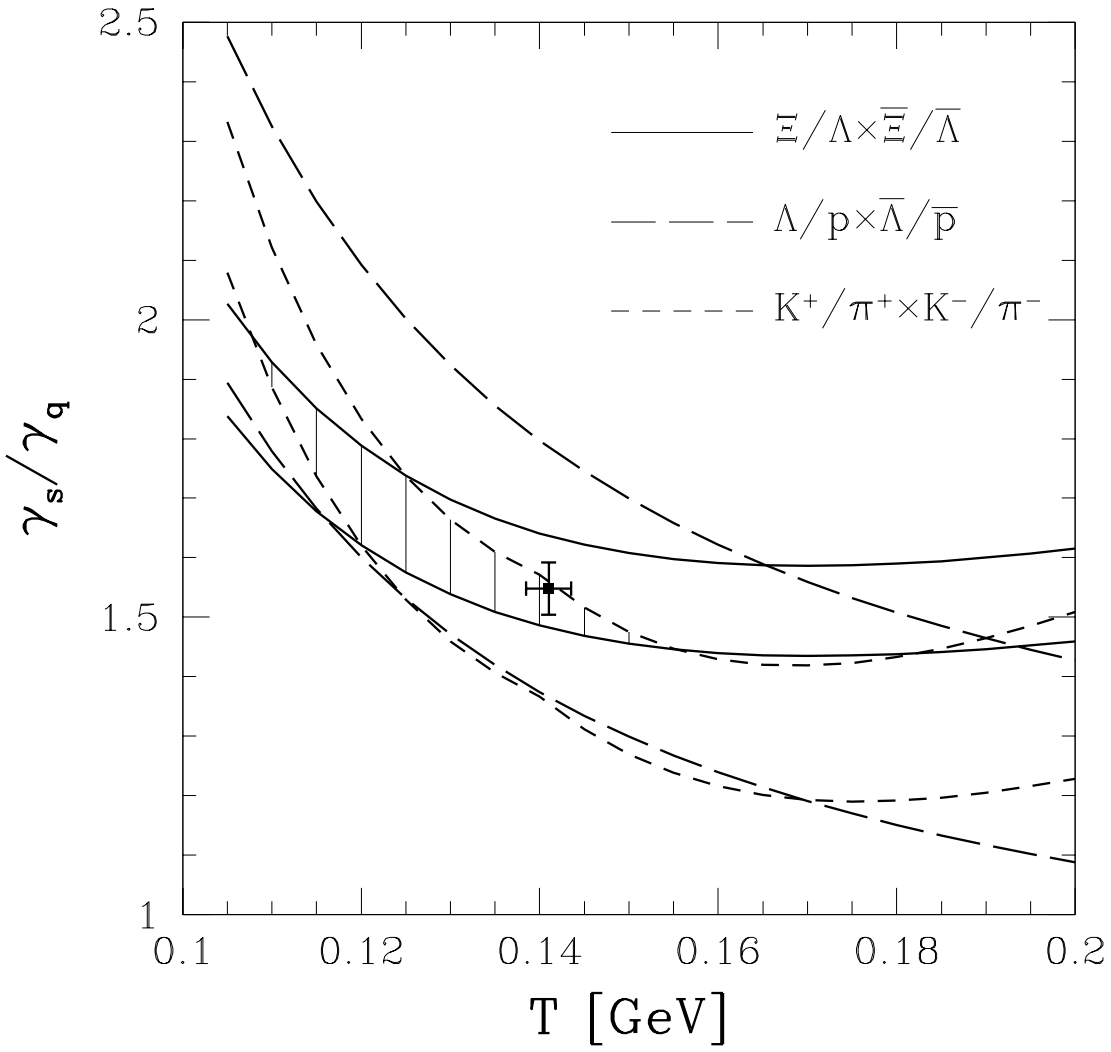

We show here products of particle ratios in which all chemical factors but the ratio of final state phase space occupancies cancel.

Equilibrium fit would need to be at the bottom of figure. Excluded STRONGLY by high yields of double strange CASCADES.

We show the current best fit to all data.

Note that best fit we have (next page) is for $\gamma_q \simeq 1.6$ (max in entropy) and a very large value $\gamma_s \simeq 2.5$, as would be expected from phase space arguments comparing QGP and HG phases.

$m_\perp$ spectra **Hadron $m_\perp$-spectra are result of flow and thermal motion and are strongly influenced by resonance decays. The Flow-Boltzmann distribution we adapt with two velocities, one local temperature:**

$$\frac{d^2N}{dm_T dy} \propto \left(1 - \frac{\vec{v}_f^{-1}\cdot\vec{p}}{E}\right) \gamma\, m_T \cosh y\, e^{-\gamma\frac{E}{T}\left(1-\frac{\vec{v}\cdot\vec{p}}{E}\right)}\,, \quad \gamma = 1/\sqrt{1-v^2}$$

Resonance 2-body decay contribution:

$$\frac{dN_X}{dm_\perp} = \frac{dN_X}{dm_\perp}|_{\rm direct} + \sum_{\forall R\to X+2+\ldots} \frac{dN_X}{dm_\perp}|_{R\to X+2+\ldots}\,, \frac{dN_X}{dm_\perp^2 dy} = \frac{g_r b}{4\pi p^*}\int_{Y_-}^{Y_+} dY \int_{M_{T-}}^{M_{T+}} dM_T^2\, J\, \frac{d^2N_R}{dM_T^2 dY}\,.$$

$$J = \frac{M}{\sqrt{P_T^2 p_T^2 - \{M E^* - M_T m_T \cosh\Delta Y\}^2}}\,, \Delta Y = Y - y\,, E^* = (M^2 - m^2 - m_2^2)/2M\,,$$

$$p^* = \sqrt{E^{*2} - m^2}$$

$$Y_\pm = y \pm \sinh^{-1}\left(\frac{p^*}{m_T}\right)\,, \quad M_{T\pm} = M\frac{E^* m_T \cosh\Delta Y \pm p_T\sqrt{p^{*2} - m_T^2\sinh^2\Delta Y}}{m_T^2\sinh^2\Delta Y + m^2}$$

EXAMPLE: Λ and $\overline{\Lambda} - m_\perp$ SPS SPECTRA

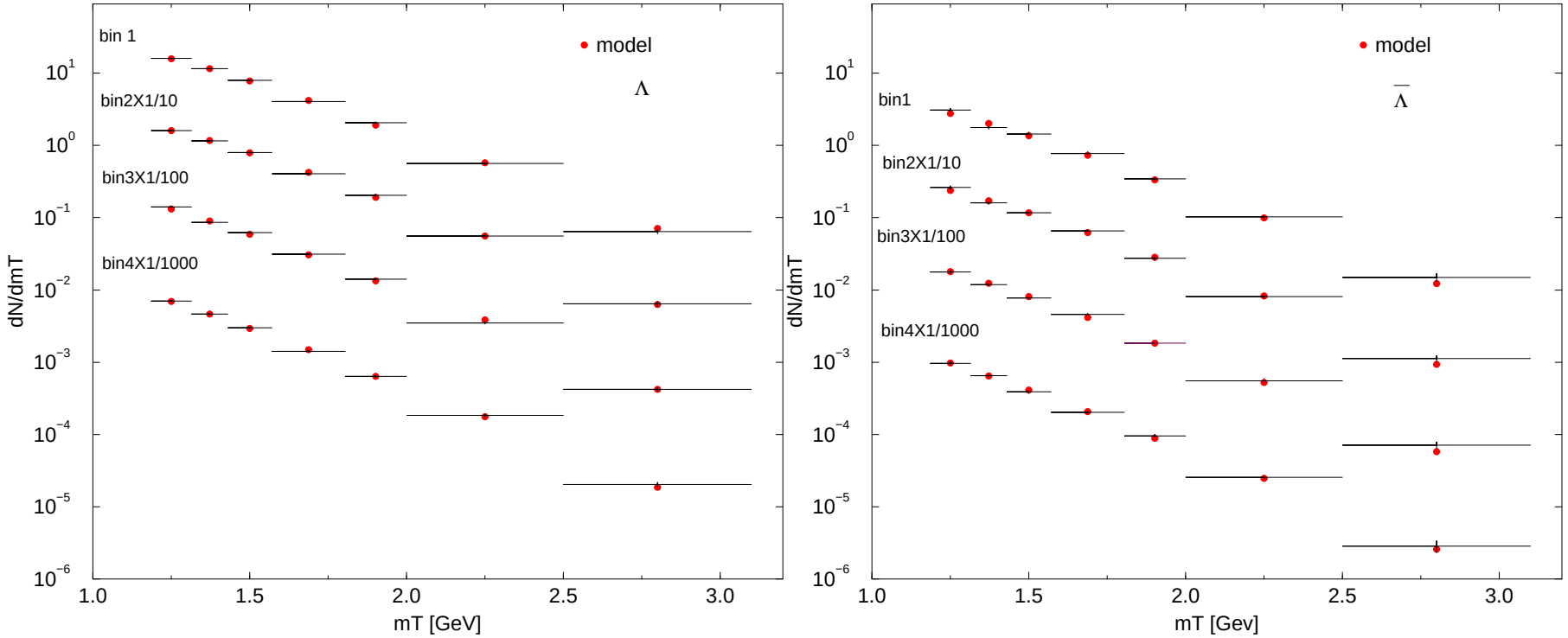

Thermal analysis m_T spectra: Λ (left) and $\overline{\Lambda}$ (right) for 4 different centralities.
'dots' theoretical values; HISTOGRAM: WA97 data in different centrality bins.

NCE FOR SUDDEN BREAKUP: CHEMICAL AND THERMAL FREEZE-OUT T, v AGREE

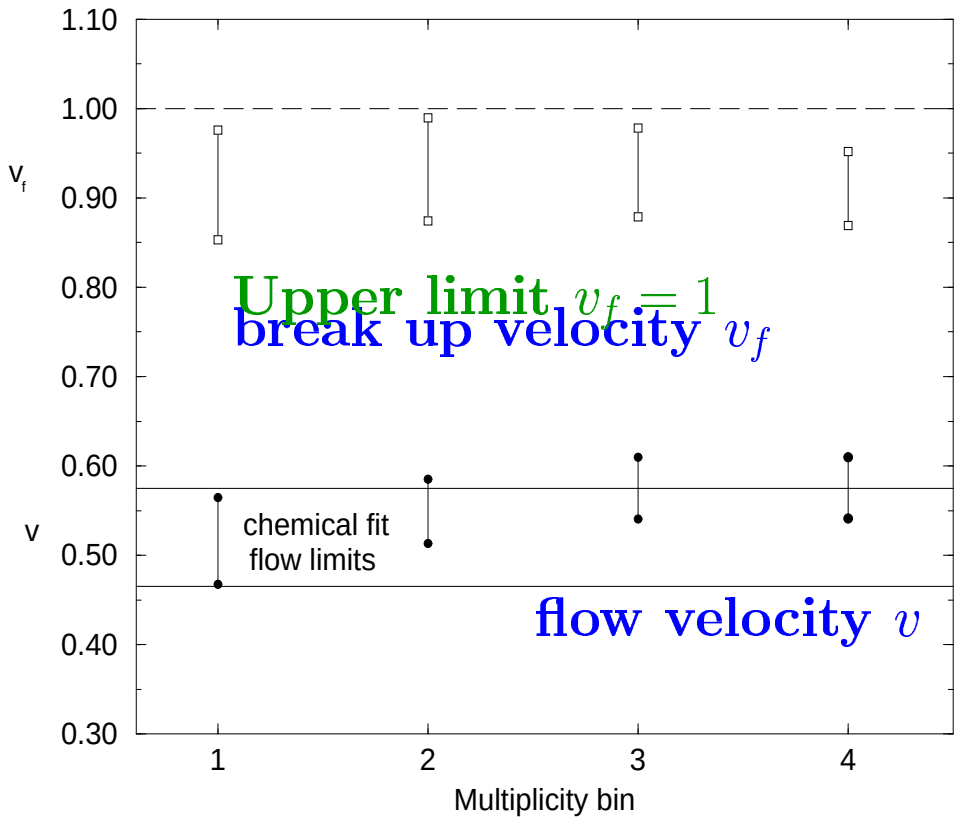

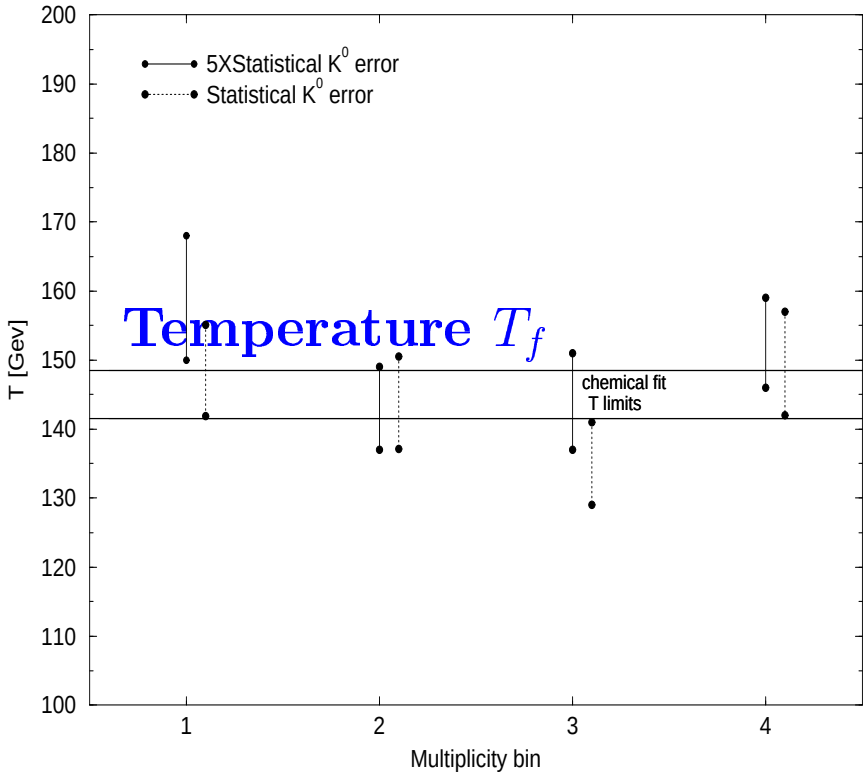

5 different collision centrality bins. We note flow velocity increase (within errors) with increasing size (centrality). Aside of this, there is no indication of a significant or systematic change of T, v, v_f with centrality, e.g. new state of matter is formed in all 4 centrality bins ($A > 100$). It will be interesting to see if the low centrality $A \simeq 50$ studied by experiment WA57 will show different freeze-out properties.

Quark Universe

Our objective here is to study the Universe in the hadronic phase, in the range $300 < T < 5$ MeV in which the nearly free gas of quarks and gluons hadronizes and natimatter rich Universe annihilates into the final particle content as seen today.

Hadronization Point in the Universe

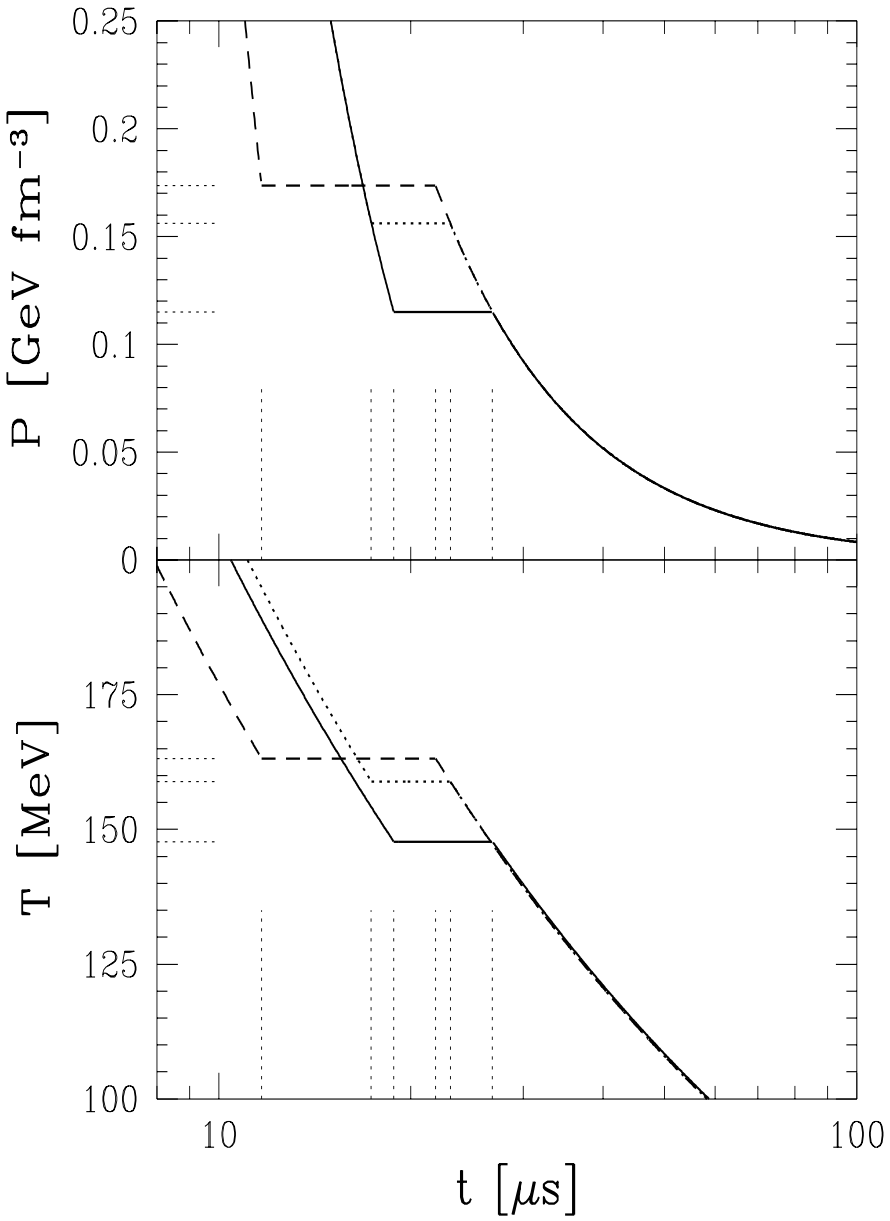

TIME CONSTANT:

$$\tau_{\rm U} = \sqrt{\frac{3c^2}{32\pi G\mathcal{B}}} = 36\sqrt{\frac{\mathcal{B}_0}{\mathcal{B}}}\,\mu\mathbf{s},$$

$$\mathcal{B}_0 = 0.19\,\frac{\mathbf{GeV}}{\mathbf{fm}^3} = (195\,\mathbf{MeV})^4.$$

Pressure (upper) and temperature (lower part) in the Universe, as function of time, in the vicinity of the phase transition from the deconfined phase to the confined phase. Solid lines, $\mathcal{B}^{1/4} = 195$ MeV; dotted lines, $\mathcal{B}^{1/4} = 170$ MeV (lower part) and $\mathcal{B}^{1/4} = 220$ MeV (upper part) all for $\alpha_{\rm s} = 0.6$.

TRACING μ IN THE UNIVERSE

Recent advances in the understanding of equations of state of QGP allow precise exploration of the conditions in which matter (protons, neutrons) formed. Neutrino oscillations essential!

INPUT: $\eta \equiv n_{\rm B}/n_\gamma = 5.5 \pm 1.5 \times 10^{-10}$

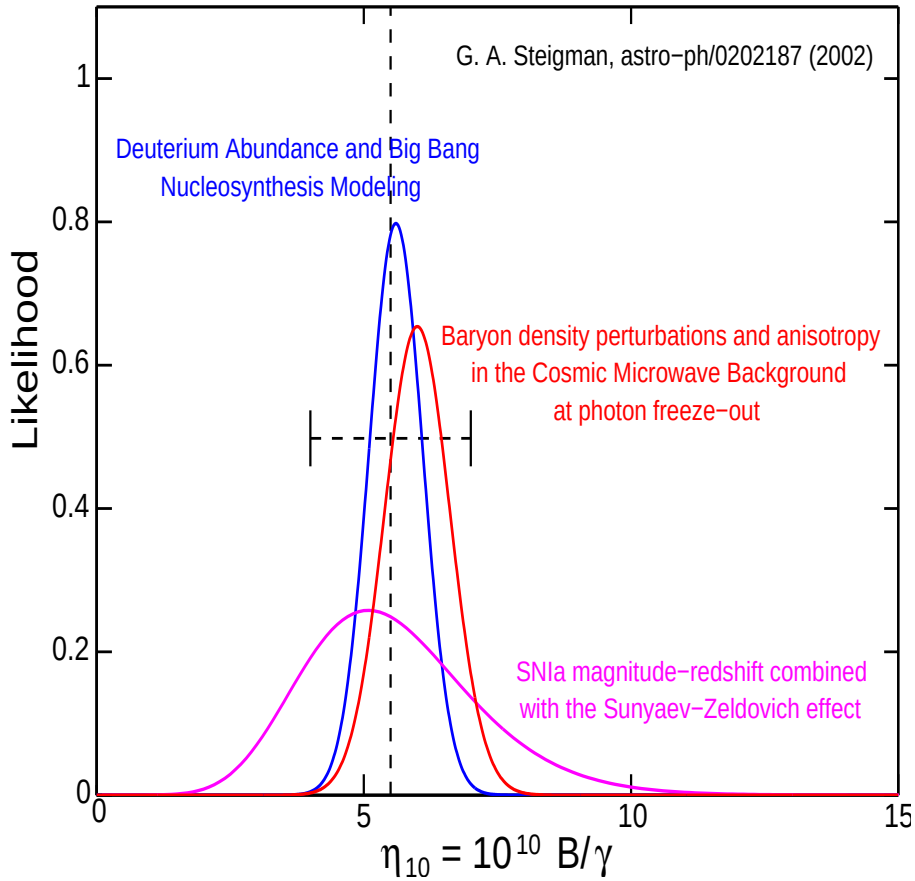

Objective

1) Describe in quantitative terms the chemical composition of the Unvierse at hadronization:

$$T \simeq 160\,{\rm MeV} \qquad t \simeq 40 \mu s,$$

2) Understand the quark-hadron phase transformation dynamics, baryon number distillation;

3) Describe the composition of the Universe during evolution towards the condition of neutrino decoupling

$$T \simeq 1\,{\rm MeV} \qquad t \simeq 10\,s$$

Chemical potentials

- **Photons in chemical equilibrium, assume the Planck distribution, implying a zero photon chemical potential; i.e., $\mu_\gamma = 0$.**
- **Because reactions such as $f + \bar{f} \rightleftharpoons 2\gamma$ are allowed, where f and $\bar{f}$ are a fermion – antifermion pair, we immediately see that $\mu_f = -\mu_{\bar{f}}$ whenever chemical and thermal equilibrium have been attained.**
- **More generally for any reaction $\nu_i A_i = 0$, where ν_i are the reaction equation coefficients of the chemical species A_i, chemical equilibrium occurs when $\nu_i \mu_i = 0$, which follows from a minimization of the Gibbs free energy.**
- **Weak interaction reactions assure:**

$$\mu_e - \mu_{\nu_e} = \mu_\mu - \mu_{\nu_\mu} = \mu_\tau - \mu_{\nu_\tau} \equiv \Delta\mu_l, \qquad \mu_u = \mu_d - \Delta\mu_l, \qquad \mu_s = \mu_d \ ,$$

- **The experimentally-favored "large mixing angle" solution is correct, the neutrino oscillations $\nu_e \rightleftharpoons \nu_\mu \rightleftharpoons \nu_\tau$ imply that:**

$$\mu_{\nu_e} = \mu_{\nu_\mu} = \mu_{\nu_\tau} \equiv \mu_\nu,$$

  and the mixing is occurring fast in 'dense' matter.

- **There are three chemical potentials which are 'free' and we choose to follow the following: μ_d, μ_e, and μ_ν.**

- **Quark chemical potentials can be used also in the hadron phase, e.g. $\Sigma^0\,(uds)$ has chemical potential $\mu_{\Sigma^0} = \mu_u + \mu_d + \mu_s$**

- **The baryochemical potential is:**

$$\mu_b = \frac{1}{2}(\mu_p + \mu_n) = \frac{3}{2}(\mu_d + \mu_u) = 3\mu_d - \frac{3}{2}\Delta\mu_l = 3\mu_d - \frac{3}{2}(\mu_e - \mu_\nu).$$

Chemical Conditions

Three chemical potentials obtained solving the three available constraints:

i. *Charge neutrality* $(Q = 0)$ **is required to eliminate Coulomb energy. This implies that:**

$$n_Q \equiv \sum_i Q_i \, n_i(\mu_i, T) = 0,$$

where Q_i and n_i are the charge and number density of species i.

ii. *Net lepton number equals net baryon number* $(L = B)$ **is required in baryogenesis:**

$$n_L - n_B \equiv \sum_i (L_i - B_i) \, n_i(\mu_i, T) = 0,$$

iii. *Constant in time entropy-per-baryon* (S/B) **i.e. the Universe evolves adiabatically,**

$$\frac{\sigma}{n_B} \equiv \frac{\sum_i \sigma_i(\mu_i, T)}{\sum_i B_i \, n_i(\mu_i, T)} = 4.5^{+1.4}_{-1.1} \times 10^{10}$$

TRACING μ_d IN THE UNIVERSE

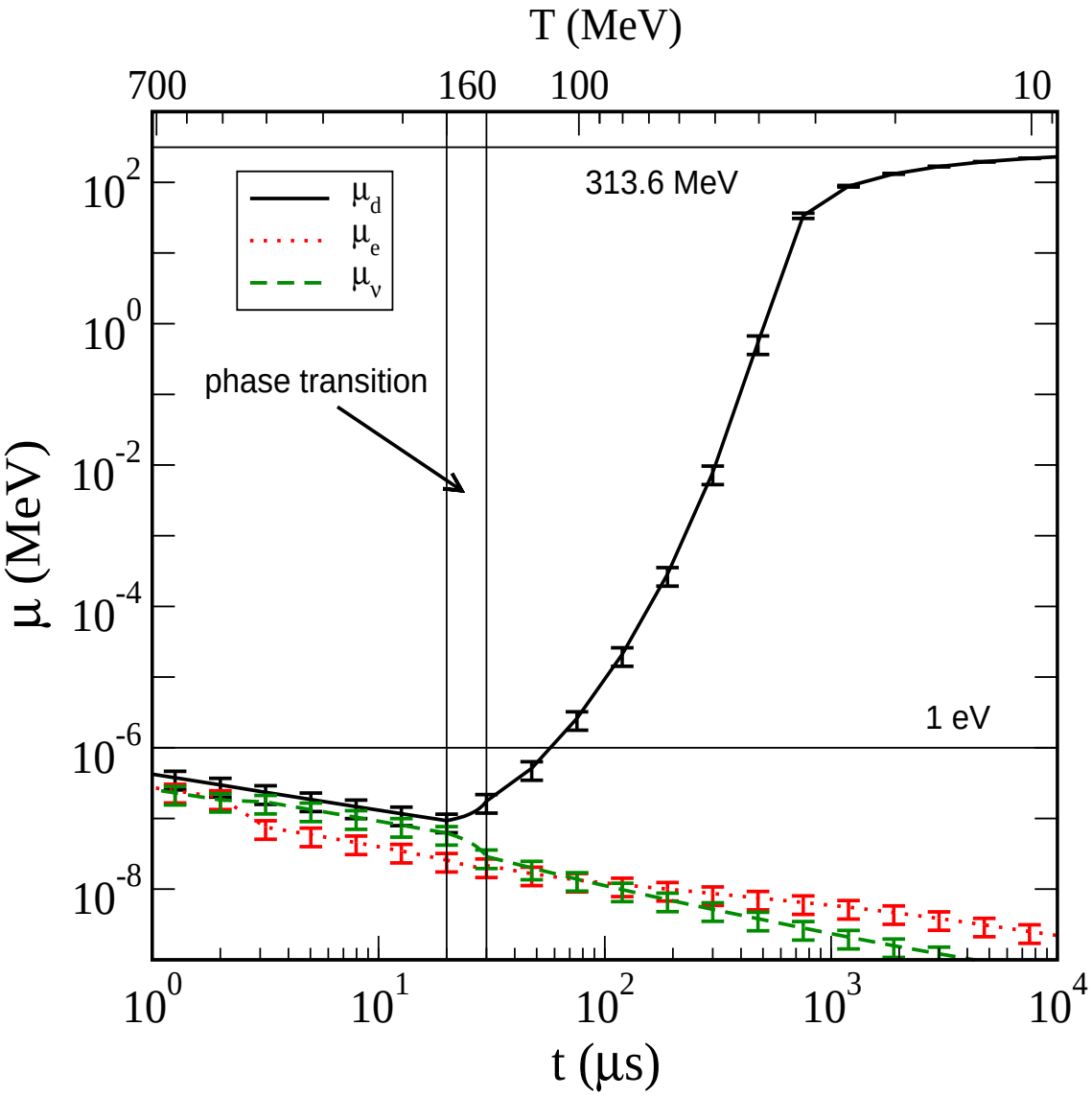

Minimum $\mu_b = 0.33^{+0.11}_{-0.08}$ eV.

μ_b relevant at final hadron $(\pi, \overline{N})$ freeze-out.

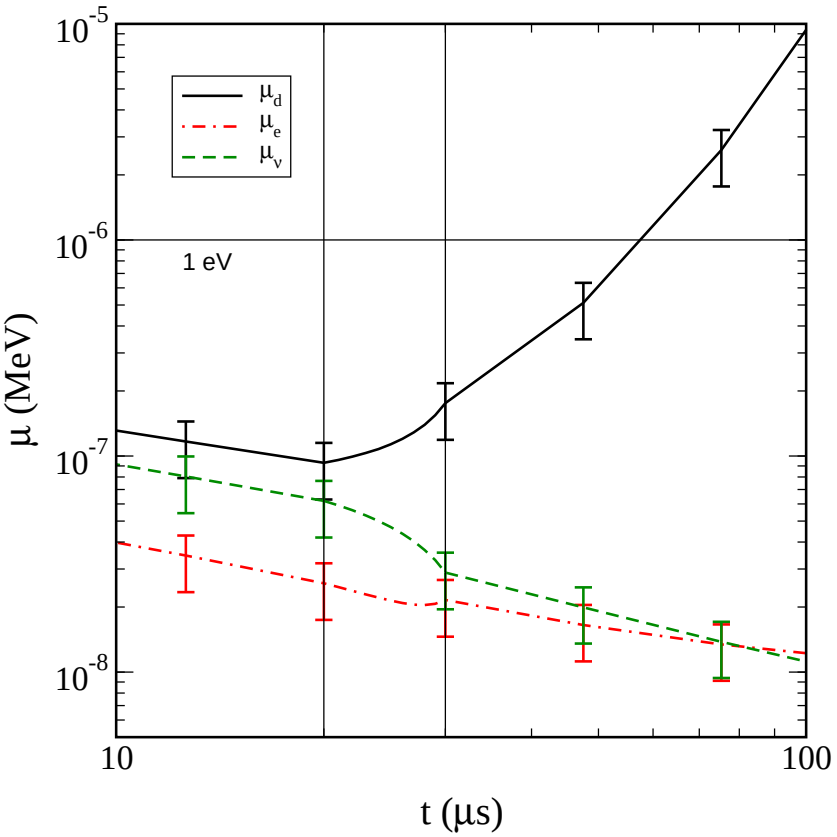

Mixed Phase

Many properties of the Universe jump as one compares QGP with Hadron Phase. Thus we introduce the mixed hadron-quak phase and parameterize the partition function during the phase transformation as

$$\ln Z_{\rm tot} = f_{\rm HG} \ln Z_{\rm HG} + (1 - f_{\rm HG}) \ln Z_{\rm QGP}$$

$f_{\rm HG}$ represents the fraction of total phase space occupied by the HG phase.

The three constraints are accordingly modified, e.g.:

$$Q = 0 = n_Q^{\rm QGP} V_{\rm QGP} + n_Q^{\rm HG} V_{\rm HG} = V_{\rm tot} \Big[(1 - f_{\rm HG}) n_Q^{\rm QGP} + f_{\rm HG} n_Q^{\rm HG} \Big[$$

where the total volume $V_{\rm tot}$ is irrelevant to the solution. Analogous expressions can be derived for $L - B$ and S/B constraints.

We assume that mixed phase exists $10\,\mu s$ and that $f_{\rm HG}$ changes linearly in time. Actual values wil require dynamic nucleation transport theory description.

Charge and baryon number distillation

Initially at $f_{\rm HG} = 0$ all matter in QGP phase, as hadronization progresses with $f_{\rm HG} \to 1$ the baryon component in hadronic gas reaches 100%.

The constraint to a charge neutral universe conserves charge in both fractions. Charge in each fraction can be finite.

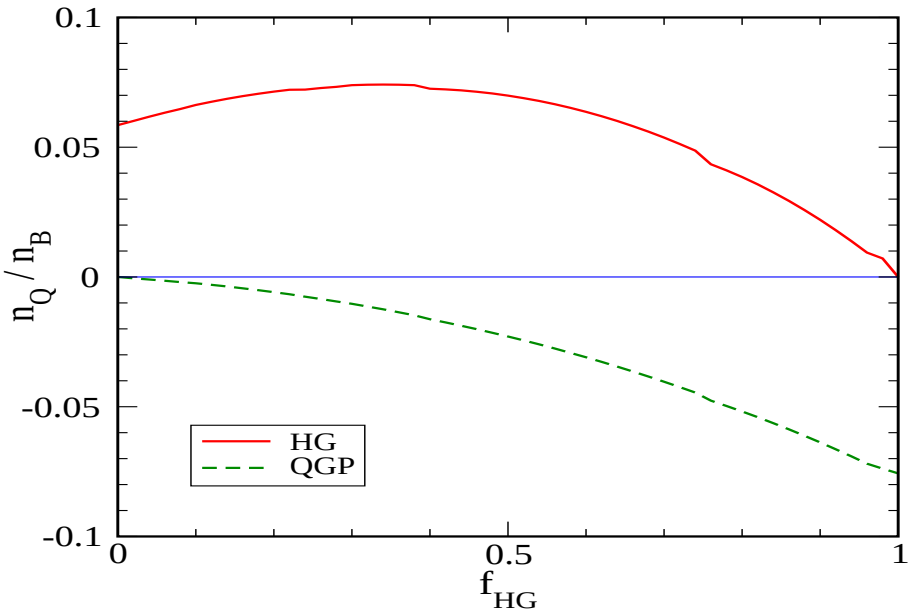

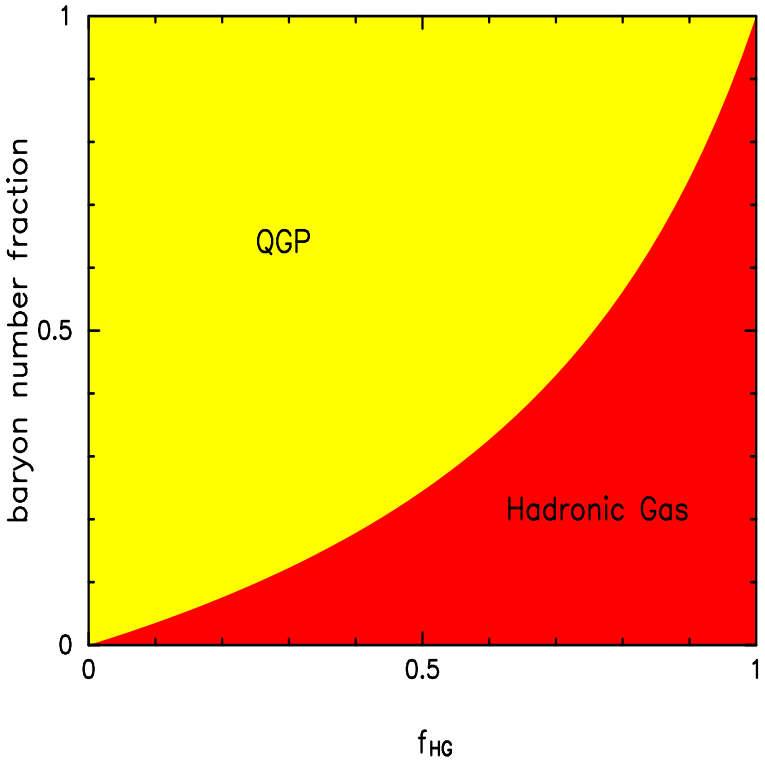

Even a small charge seperation introduces a finite non-zero Coulom potential and this amplifies the existnet baryon asymmetry. This mechanism noticed by Witten in his 1984 paper, and exploited by A. Olinto for generation of magnetic fields.

Hadronic Universe Particle Densities

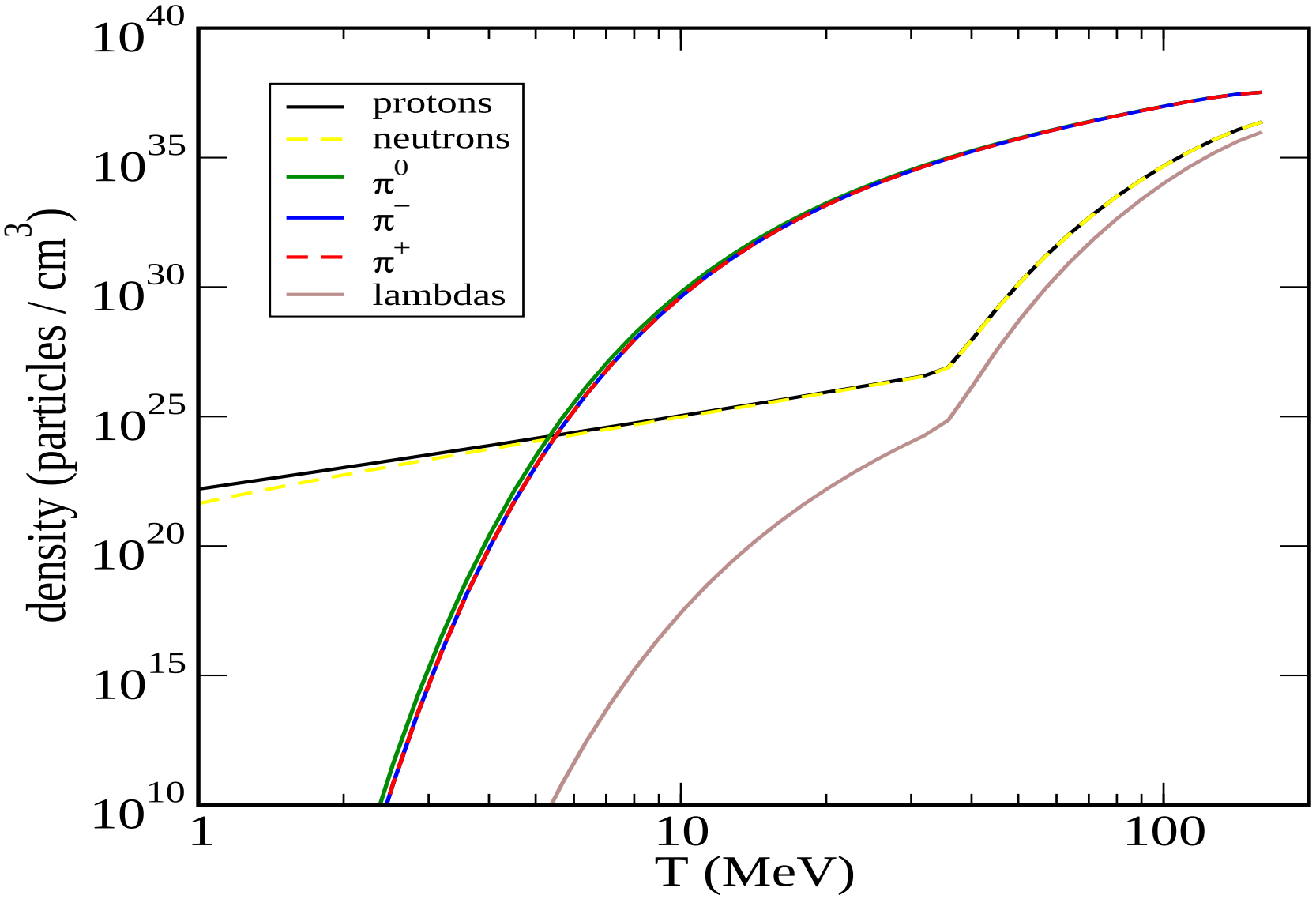

Energy in luminous hadronic Universe

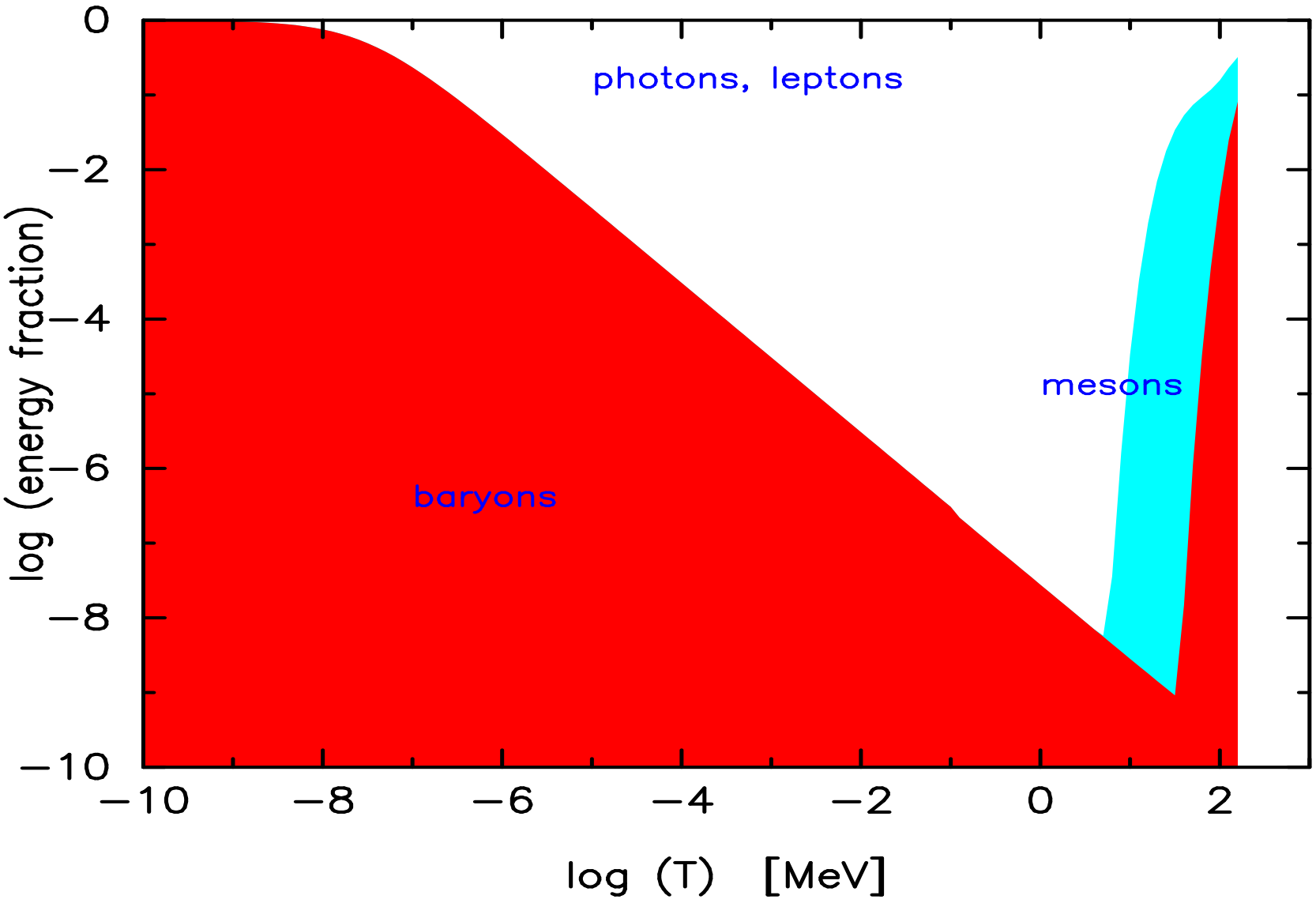

Other source of baryon asymmetry

What if the CPT is broken, the finite baryon number is supported by resulting particle-antiparticle mass asymmetry. In PDG the limit on mass differences is at the level of many eV. This is larger than the baryochemical potential required to sustain the asymmetry near phase transfromation. We explore this assuming that quark-anti-quark mass difference possible, is expresed as hadron mass difference and we found:

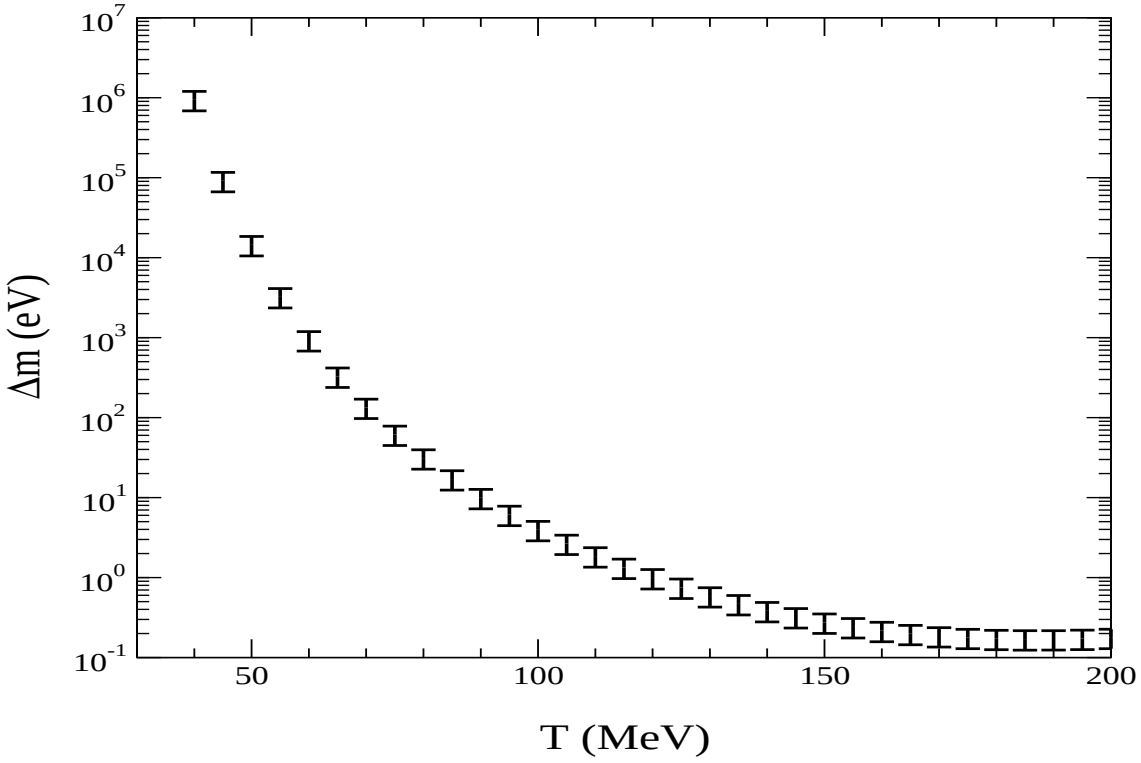

We found a better CPT limit on $m - \overline{m}$

We define the K_L and K_S states in the standard formalism (see e.g. Perkins):

$$K_L = \frac{1}{\sqrt{2+2\epsilon^2}}\left[(1+\epsilon)K^0 + (1-\epsilon)\bar{K^0}\right] \ , \ K_S = \frac{1}{\sqrt{2+2\epsilon^2}}\left[(1-\epsilon)K^0 - (1+\epsilon)\bar{K^0}\right] \ ,$$

where $K^0 = |d\bar{s}\rangle$, $\bar{K^0} = |\bar{d}s\rangle$, and $\epsilon = 2.07 \pm 0.28 \times 10^{-3}$ is the direct CP violation parameter.

We express the (assumed) CPT-violating mass difference between quarks and antiquarks as:

$$m_{s,\bar{s}} = m_s^0 \pm \frac{\delta m_s}{2} \qquad m_{d,\bar{d}} = m_d^0 \pm \frac{\delta m_d}{2} \ ,$$

where the signs of δm_s and δm_d are undetermined. The mass difference between K_L and K_S becomes:

$$\Delta m = \Delta m_w \ + \ 2\,\epsilon f\,\left[(m_{\bar{s}} - m_s) - (m_{\bar{d}} - m_d)\right]$$

where Δm_w is the second order WI mass difference which explains the known mass differnce in K_S–K_L, $\Delta m \equiv m_{K_L} - m_{K_S} = 3.463 \pm 0.010 \times 10^{-6}$ eV. $f \simeq 1$ expresses the response of Kaon mass to a small change in quark masses.

This means:

$$|(m_{\bar{s}} - m_s) - (m_{\bar{d}} - m_d)| \ \ll \ \frac{\Delta m}{2\epsilon f} \ \approx \ 10^{-3}\,\mathrm{eV}\ .$$

We find that the current upper limit to the mass difference between quarks and antiquarks in the d and s flavors is $\ll 10^{-3}\,\mathrm{eV}$ if the magnitude of the CPT violation is uncorrelated across flavors. In this case, the relative precision with which the strange quark mass difference is determined appears to be by far the most precise such value presently known:

$$\left|\frac{m_s - m_{\bar{s}}}{m_s + m_{\bar{s}}}\right| \ll 10^{-11}\,,$$

providing a strong constraint for any CPT model considered. Also, we excluded the possibility that the quark mass differnce is associated with baryon asymmetry in the early Universe.

FINAL REMARKS

At CERN-SPS and BNL-RHIC laboratory study of quark-gluon plasma

the stuff from the early Univere

Strangeness: a fingerprint of a new state of matter

In lab: SUPERCOOLED QGP FIREBALL BREAKS-UP SUDDENLY

(which has a great influence on observables)

We begin to transfer the 'know-how' from the study of nuclear collisions to the study of the early Universe

---